

# Strain-based optimization of human tissue-engineered small diameter blood vessels

**Citation for published version (APA):**

Stekelenburg, M. (2006). *Strain-based optimization of human tissue-engineered small diameter blood vessels*. [Phd Thesis 1 (Research TU/e / Graduation TU/e), Biomedical Engineering]. Technische Universiteit Eindhoven. <https://doi.org/10.6100/IR610210>

**DOI:**

[10.6100/IR610210](https://doi.org/10.6100/IR610210)

**Document status and date:**

Published: 01/01/2006

**Document Version:**

Publisher's PDF, also known as Version of Record (includes final page, issue and volume numbers)

**Please check the document version of this publication:**

- A submitted manuscript is the version of the article upon submission and before peer-review. There can be important differences between the submitted version and the official published version of record. People interested in the research are advised to contact the author for the final version of the publication, or visit the DOI to the publisher's website.
- The final author version and the galley proof are versions of the publication after peer review.
- The final published version features the final layout of the paper including the volume, issue and page numbers.

[Link to publication](#)

**General rights**

Copyright and moral rights for the publications made accessible in the public portal are retained by the authors and/or other copyright owners and it is a condition of accessing publications that users recognise and abide by the legal requirements associated with these rights.

- Users may download and print one copy of any publication from the public portal for the purpose of private study or research.
- You may not further distribute the material or use it for any profit-making activity or commercial gain
- You may freely distribute the URL identifying the publication in the public portal.

If the publication is distributed under the terms of Article 25fa of the Dutch Copyright Act, indicated by the "Taverne" license above, please follow below link for the End User Agreement:

[www.tue.nl/taverne](http://www.tue.nl/taverne)

**Take down policy**

If you believe that this document breaches copyright please contact us at:

[openaccess@tue.nl](mailto:openaccess@tue.nl)

providing details and we will investigate your claim.

# **Strain-based optimization of human tissue-engineered small diameter blood vessels**

A catalogue record is available from the Library Eindhoven University of Technology

ISBN-10: 90-386-2728-9

ISBN-13: 978-90-386-2728-1

Cover design: Maria Stekelenburg / Michelle Tjelpa

Printed by Universiteitsdrukkerij TU Eindhoven, Eindhoven, The Netherlands.

The financial support of “Stichting Hart- en Vaatziekten, Maastricht” is gratefully acknowledged.

# **Strain-based optimization of human tissue-engineered small diameter blood vessels**

## Proefschrift

ter verkrijging van de graad van doctor aan de  
Technische Universiteit Eindhoven, op gezag van de  
Rector Magnificus, prof.dr.ir. C.J. van Duijn, voor een  
commissie aangewezen door het College voor  
Promoties in het openbaar te verdedigen  
op woensdag 28 juni 2006 om 16.00 uur

door

**Maria Stekelenburg**

geboren te Raamsdonksveer



Dit proefschrift is goedgekeurd door de promotoren:

prof.dr. L.H.E.H. Snoeckx  
en  
prof.dr.ir. F.P.T. Baaijens

Copromotor:  
dr.ir. M.C.M. Rutten

*- de eenvoud van de tweevoud -*



# Contents

<b>Summary</b>	xi
<b>1 General introduction</b>	<b>1</b>
1.1. Introduction	2
1.2. Coronary arteries	2
1.3. Mechanical properties of coronary arteries	4
1.4. Coronary artery disease and bypass grafting	5
1.5. Vascular tissue engineering	6
1.6. Aim of this thesis	7
1.7. Outline of this thesis	7
<b>2 Scaffolds and tubular constructs</b>	<b>9</b>
2.1 Introduction	10
2.2 Scaffolds in vascular tissue engineering	10
2.3 Materials & Methods	13
2.3.1 <i>Electrospun constructs</i>	14
2.3.2 <i>PGA tubular constructs</i>	15
2.3.3 <i>Scanning Electron Microscopy</i>	16
2.3.4 <i>Mechanical testing</i>	16
2.3.5 <i>Cells and cell seeding</i>	16
2.3.6 <i>Evaluation of cell infiltration and tissue formation</i>	18
2.4 Results	18
2.4.1 <i>Tubular constructs</i>	18
2.4.2 <i>Mechanical properties</i>	19
2.4.3 <i>Seeding test PCL constructs</i>	20
2.4.4 <i>PGA constructs</i>	20
2.5 Discussion	20
2.6 Acknowledgements	22
<b>3 Characterization of tissue-engineered blood vessels</b>	<b>23</b>
3.1 Introduction	24
3.1.1 <i>Tissue analyses</i>	24
3.1.2 <i>Mechanical testing</i>	25
3.2 Materials & Methods	27
3.2.1 <i>Materials</i>	27
3.2.2 <i>Constructs / 4 week static culture</i>	28
3.2.3 <i>Histology</i>	28
3.2.4 <i>Mechanical testing</i>	29
3.2.5 <i>Biochemical assays</i>	30
3.2.6 <i>Statistics</i>	31
3.3 Results	31
3.3.1 <i>Histology</i>	31

3.3.2	<i>Mechanical properties</i> .....	32
3.3.3	<i>Biochemical assays</i> .....	35
3.4	Discussion.....	36
<b>4</b>	<b>Axially strained tissue-engineered blood vessels</b>	<b>39</b>
4.1	Introduction.....	40
4.2	Materials and Methods.....	41
4.2.1	<i>Tubular constructs</i> .....	41
4.2.2	<i>Bioreactor design</i> .....	41
4.2.3	<i>Cells / Seeding procedure</i> .....	42
4.2.4	<i>Culture and mechanical conditioning</i> .....	42
4.2.5	<i>Evaluation of tissue formation</i> .....	43
4.2.6	<i>Statistics</i> .....	44
4.3	Results.....	45
4.3.1	<i>Macroscopic appearance</i> .....	45
4.3.2	<i>Histology</i> .....	45
4.3.3	<i>Quantitative evaluation of tissue formation</i> .....	46
4.3.4	<i>Mechanical testing</i> .....	47
4.4	Discussion.....	48
<b>5</b>	<b>Circumferentially strained tissue-engineered blood vessels</b>	<b>51</b>
5.1.	Introduction.....	52
5.2.	Materials and Methods.....	53
5.2.1	<i>Tubular constructs</i> .....	53
5.2.2	<i>Cells / Seeding procedure</i> .....	53
5.2.3	<i>Bioreactor design</i> .....	53
5.2.4	<i>Measurement of strain and pressure</i> .....	55
5.2.5	<i>Culture and mechanical conditioning</i> .....	55
5.2.6	<i>Evaluation of tissue formation</i> .....	55
5.2.7	<i>Statistics</i> .....	57
5.3.	Results.....	58
5.3.1	<i>Quantification of circumferential strain</i> .....	58
5.3.2	<i>Histology</i> .....	59
5.3.3	<i>Quantitative evaluation of tissue formation</i> .....	61
5.3.4	<i>Mechanical testing</i> .....	61
5.2.5	<i>Burst pressure</i> .....	63
5.4.	Discussion.....	65
5.5.	Acknowledgements.....	68
<b>6</b>	<b>Comparison between tissue-engineered blood vessels and native equivalents</b>	<b>69</b>
6.1.	Introduction.....	70
6.2.	Materials & Methods.....	70
6.2.1	<i>Tissue engineered blood vessels</i> .....	70
6.2.2	<i>Human and porcine native blood vessels</i> .....	71
6.2.3	<i>Histology</i> .....	71
6.2.4	<i>Biochemical assays</i> .....	71

6.2.5	<i>Mechanical testing</i> .....	72
6.2.6	<i>Statistics</i> .....	72
6.3.	Results .....	72
6.3.1	<i>Histology</i> .....	72
6.2.2	<i>Quantitative evaluation of tissue formation</i> .....	73
6.2.3	<i>Mechanical testing</i> .....	74
6.4.	Discussion .....	77
<b>7 Endothelial cells</b>		<b>81</b>
7.1.	Introduction .....	82
7.2.	Materials&Methods .....	83
7.2.1	<i>Cell culture</i> .....	83
7.2.2	<i>Bioreactor/seeding device</i> .....	83
7.2.3	<i>Constructs and cell seeding</i> .....	84
7.2.4	<i>Evaluation of EC seeding</i> .....	85
7.3.	Results .....	86
7.4.	Discussion .....	88
7.5.	Acknowledgements .....	90
<b>8 General discussion</b>		<b>91</b>
8.1.	Introduction .....	92
8.2.	Tissue-engineered constructs .....	92
8.2.1	<i>Tissue development</i> .....	93
8.2.2	<i>Mechanical properties</i> .....	94
8.3.	Future research .....	95
8.3.1	<i>Mechanical testing</i> .....	95
8.3.2	<i>Elasticity / Compliance</i> .....	96
8.3.3	<i>Endothelial cells</i> .....	97
8.3.4	<i>Animal studies</i> .....	97
8.3.5	<i>Cell sources</i> .....	98
8.2.3	<i>Clinical implantation</i> .....	99
<b>References</b>		<b>101</b>
<b>Samenvatting</b>		<b>111</b>
<b>Dankwoord</b>		<b>113</b>
<b>Curriculum Vitae</b>		<b>115</b>



# Summary

Coronary arteries originate from the root of the aorta and supply blood to the heart. These arteries can become stiffer and narrowed due to the buildup of atherosclerotic plaque in the inner vessel layers. As the plaque increases in size, the lumen of the coronary arteries decreases and less blood can flow through them. Eventually, coronary artery disease (CAD) can lead to chest pain or a myocardial infarction. Treatment for this disease includes medicines, minimally invasive interventional procedures such as angioplasty and stent implantation, and coronary artery bypass grafting (CABG). Today most CABG operations are performed using combinations of the autologous left internal mammary artery and the saphenous vein. These grafts, especially the latter, perform suboptimal. In addition, a relative large part of all patients do not have suitable veins or arteries, caused by disease of the replacement vessel itself, usage in previous surgeries, the need for multiple bypasses or a combination of all these factors. Therefore, other types of vascular grafts have been proposed to replace the native substitute. Synthetic grafts, such as ePTFE and Dacron, perform well at diameters  $>6\text{mm}$ , but are not suitable for small-diameter ( $<4\text{mm}$ ) applications, i.e. the area of application of CABG. Therefore another source of these vascular grafts is needed, which might be provided by tissue engineered (TE) small diameter blood vessels.

In vascular tissue engineering a combination of cells, engineering materials, and suitable biochemical and mechanical factors is used to culture living vascular grafts. Basically, the technique uses the patient's own cells in combination with a scaffold, i.e. a cell carrier. Mechanical and/or chemical conditioning protocols are applied to stimulate the tissue formation during an in-vitro culture period. In general, an ideal vascular graft should at least meet the following functional criteria: it should possess sufficient tensile strength to provide mechanical support, contain an adequate elastic component to provide recoil and a wall structure that prevents aneurysm formation. In addition, it should have a confluent endothelium to prevent thrombosis and to provide full functionality to the blood vessel. The present thesis focuses mainly on the first criterion, i.e., increasing the mechanical strength of TE blood vessels. This is achieved by subjecting tubular constructs to strain-based conditioning protocols. The final goal was to culture strong blood vessels from human cells harvested from saphenous veins. Several scaffold concepts were evaluated for their capacity to enable tissue culture and for their mechanical properties. Starting point was a P4HB coated PGA scaffold. It was investigated whether an additional inner or outer electrospun PCL layer enhanced the mechanical properties in terms of construct strength and elasticity. As the PGA/P4HB scaffold already proved its potential in TE heart valves, in a first approach TE blood vessels based on solely this scaffold material were cultured. In these tubular constructs human saphenous vein myofibroblasts were seeded in combination with a fibrin gel. This gel enabled easy cell seeding and improved the tissue formation. Strain-based conditioning consisted of static and dynamic straining protocols in both axial and circumferential direction. For this, two separate bioreactors were developed, one that allowed static and/or dynamic axial straining of tubular constructs and a second one that combined static axial with dynamic circumferential straining. Compared to static



non-strained controls, static axial strain, which built up as a consequence of counteracting the compaction of the tissue in axial direction, resulted in enhanced tissue formation and mechanical properties in the TE tubular constructs. It was found that the mechanical properties were better developed in axial than in circumferential direction. The additional effect of dynamic strain in axial direction was limited or even negative. The mechanical properties in circumferential direction, more critical for the mechanical behavior of a vessel than those in axial direction, improved significantly when the tubular constructs were subjected to an additional dynamic strain in circumferential direction. After 4 weeks of in-vitro culture, the combination of static axial strain with dynamic circumferential strain resulted in the strongest TE blood vessels. These vessels could withstand a pressure up to 900mmHg, which demonstrated that the presented TE blood vessels were stronger compared to other TE vessels cultured under similar conditions, as reported in literature.

In the present thesis, the properties of the TE constructs were also compared to those of native equivalents, i.e. from human saphenous veins, human left internal mammary arteries and porcine coronary arteries. In general, the amounts of DNA and extracellular matrix in the TE constructs were, to a certain extent, comparable to those of native vessels. However, in terms of structural organization, native vessels were better developed and organized. The mechanical properties in the physiological relevant range, at least those assessed by tensile testing, were remarkably similar in TE constructs and native arteries. In contrast, the ultimate strength of the native vessels was much higher than that of the TE constructs. However, at time of implantation, the structural and mechanical properties of the TE vessels do not need to be identical to those of a native artery as the TE constructs are composed of viable tissue with the potential to remodel, repair, and grow in the in-vivo environment.

Besides mechanical strength, which was the main focus of this thesis, TE blood vessels should also be elastic, compliant and possess a functional endothelium. Further mechanical testing should elucidate the need for improvement of the elasticity and compliance of the TE vessels. Endothelial cell seeding experiments on the TE constructs were performed and demonstrated that the ECs attached to the tissue engineered constructs. Further investigation is, however, necessary to achieve a confluent and functional EC layer. Only when these mechanical issues and the critical role of the endothelium are sufficiently solved, research on implantation into animal models might elucidate the potential of the presented constructs.

In conclusion, small diameter TE blood vessels as presented in this thesis showed good tissue development and are strong enough, justifying future research including animal models. Prior to implantation in these models, matters on the elasticity and compliance of the vessels have to be addressed through more elaborated mechanical testing protocols. In addition, the constructs should possess a functional endothelium.

# 1

## General introduction

## 1.1. Introduction

Large numbers of patients suffer from disorders in the vascular system, resulting in a clear clinical need for functional arterial replacements. Autologous vessels are the standard for small diameter grafts, however, many patients not have a vessel suitable for use because of vascular disease, previous harvest or need for multiple bypasses. In addition, these grafts, especially the widely applied autologous venous grafts, do not perform optimally. Synthetic materials that are successful for large-diameter grafts fail when applied to small-diameter applications like the coronary artery. As a result, tissue engineering has emerged as a promising approach to address the shortcomings of current therapies. Vascular tissue engineering involves the culture of functional small-diameter grafts by using an autologous cell source combined with a natural or synthetic scaffold and by subjecting these tubular constructs to chemical and/or mechanical stimulation. To increase the strength of human tissue-engineered (TE) blood vessels, which is the focus of this thesis, several approaches are possible regarding cell sources, scaffolds and conditioning protocols. The approach that is applied in the present thesis includes a combination of scaffold materials and strain-based mechanical conditioning. To enable the definition of design criteria for TE blood vessels, this first chapter describes the function, anatomy and mechanical properties of coronary arteries. It further discusses the need and demands for functional bypass grafts and the possibilities of vascular tissue engineering.

## 1.2. Coronary arteries

Coronary arteries supply blood to the heart. These arteries originate from the root of the aorta in the sinuses of Valsalva and are divided into the right and left coronary arteries (Fig. 1.1a). Although the anatomy of the coronary system is subject to individual variation, the right coronary artery (RCA) generally supplies the right ventricle and atrium, while the left coronary artery (LCA) supplies the intraventricular septum, and the left ventricle and atrium. Both arteries course over the heart, branching into

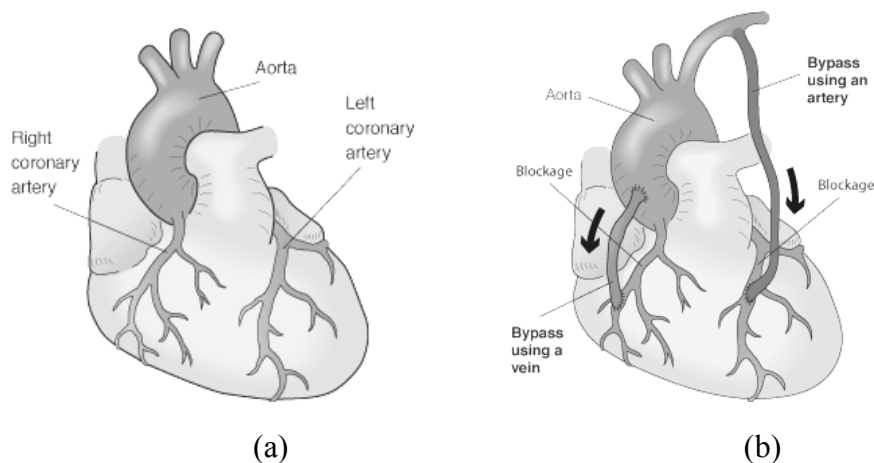


Figure 1.1: *Heart and coronary circulation (a), coronary bypass grafting (b).* Source [www.besttreatments.co.uk](http://www.besttreatments.co.uk)

segments that penetrate into the tissue, and dividing into capillary networks. In all other vascular beds, blood flow roughly parallels the pressure profile in the aorta, rising in systole and falling in diastole. However, in the coronary circulation, flow is somewhat paradoxical: although the heart is the source of its own perfusion pressure, myocardial contraction effectively compresses its own vascular supply. Therefore, the profile of blood flow through the coronary arteries depends on both the perfusion pressure in the aorta and the extravascular compression provided by the contracting ventricle. During early diastole, the blood flow in the LCA rises to extremely high levels, in the order of 300-400ml/min. In the RCA, the peak blood flow is approximately 50-60ml/min (Boron, 2003). The location on the contracting and relaxing heart imposes a cyclic axial strain on the coronary arteries up to 10-15%. The circumferential strain due to the pulsatile flow is in the order of 4-10% (Zilla, 1999). In addition, the blood flow imposes a shear stress on the vessel wall, which equals approximately 0.7Pa in human coronary arteries (Doriot, 2000).

The vessel wall of a coronary artery consists of different structural layers (Fig 1.2). An inner lining of endothelium provides non-thrombogenicity and is involved in various physiological processes, such as hemostasis maintenance, vasomotor tone regulation, inflammatory and immunological regulation. The media layer includes elastin fibers and smooth muscle cells that are oriented circumferentially and regulate the contractile properties of the blood vessel. The media layer is separated from the inner endothelium layer by a dense elastic membrane. The outer layer consists of connective tissue. The vessel wall includes the elastic components elastin and collagen that determine the mechanical behavior of the blood vessel, as described in the next section.

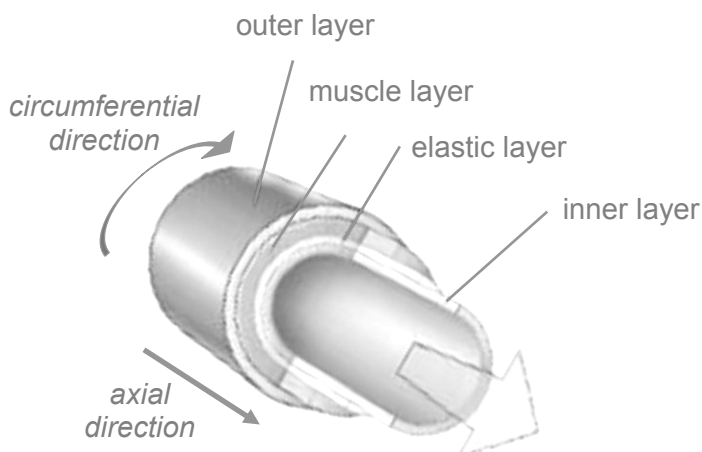


Figure 1.2: Layered structure of an artery. Arrows define the axial and circumferential direction.

### 1.3. Mechanical behavior of coronary arteries

Blood vessels bear two distinct mechanical characteristics, being elasticity and strength. The stiffness of a blood vessel is mainly determined by its collagen content, whereas elastin acts as a recoil protein that stretches and pulls the vessel back to its original

diameter after loading. Elastin prevents vascular dilatation that would be caused by creep of collagen due to the pressures of in-vivo blood flow. The degree of contribution of elastin and collagen is not only determined by the amounts of these proteins, but also by the orientation of the fibers and the degree of crosslinking between individual fibers. The separate contributions of elastin and collagen fibers can be best quantified by “chemical dissection” (Boron, 2003). After selective digestion of the elastin fibers with elastase, which unmasks the behavior of collagen fibers, the stress-strain relationship in the vessel wall is very steep (Fig. 1.4). After selective digestion of collagen fibers with formic acid, which unmasks the behavior of elastic fibers, the stress-strain curve is fairly flat. In a normal vessel, however, the combined behavior of collagen and elastin is not simply the sum of both. At low strains the collagen structure is folded. Therefore, at low strains, only the elastic fibers elongate while the collagen ‘unfolds’. Increasing strain recruits collagen fibers resulting in a steeper slope of the stress-strain curve (Boron, 2003). The ultimate stress that a blood vessel can bear is related to its burst pressure, which is a measure generally used to quantify the strength of a blood vessel. The burst pressure of a human coronary artery is in the order of 2000mmHg (L’Heureux, 2006). Vascular compliance describes the ability of a vessel to expand and contract passively with changes in pressure. The compliance, which is defined as the ratio of the change in volume and pressure, is variable according to the range of strain in which it is determined, as can be derived from Fig. 1.4. Indeed, the slope of the stress-strain curve increases at higher strains due to the heterogeneity of the elastic material of the vascular wall, as described above. Distinct differences in compliance exist between arteries and veins. At low pressures, the compliance of a vein is about 10 to 20-times larger than that of an artery. Therefore, veins can accommodate large changes in blood volume with only a small change in pressure. However, at higher pressures and volumes, venous compliance becomes similar to arterial compliance.

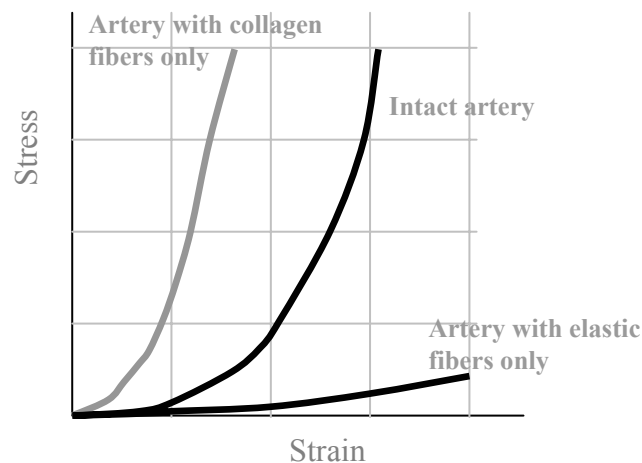


Figure 1.4: *Separated contribution of elastin and collagen to the mechanical behavior of blood vessels, adapted from Boron (2003)*

#### 1.4. Coronary artery disease and bypass grafting

Coronary artery disease (CAD) occurs when the coronary arteries become stiffer and narrowed due to a buildup of atherosclerotic plaque in the inner vessel walls. As the plaque increases in size, the lumen of the artery decreases and less blood can flow through. Eventually, even under resting conditions, blood flow to the heart muscle is reduced, and, because blood carries much-needed oxygen, the heart muscle does not receive the required amount of oxygen. CAD can lead to chest pain or a myocardial infarction. Treatments for this disease include medication, minimally invasive interventional procedures such as angioplasty and stent implantation, and coronary artery bypass grafting (CABG). Coronary angioplasty is based upon removing the stenosis by a catheter-based intervention. In CABG, arteries or veins from other areas in the body are used to bypass the obstructed coronary arteries (Fig. 1.1b). In the Netherlands, approximately 10,000 patients per year undergo CABG (data from 1999). These bypasses were originally performed using saphenous veins. This vein is running on the inside of the leg from the ankle to the groin. There is a deep venous system that drains about 90% of the blood from the legs back to the heart. The saphenous vein is part of the superficial system that normally drains about 10% of the total amount of blood. The saphenous vein can therefore be removed without adversely affecting the leg. A major drawback of venous grafts is that, after grafting, major remodeling occurs, leading to reocclusion of the vessel. In the first year the occlusion rate is between 15% and 26%. By 10 years, one-third of vein grafts are occluded, and of those patent, half show marked arteriosclerotic changes (Raja, 2004). In the 1970's and 1980's, cardiothoracic surgeons discovered that an artery from the inside of the chest wall, the internal thoracic artery, also called the internal mammary artery, can be used instead of vein and that this type of bypass was less prone to reocclusion than saphenous vein grafts. Today most CABG operations are performed using combinations of this artery and the saphenous vein. In addition to the above shortcomings of currently used grafts, removal of a functional vessel from its location in the body is suboptimal. In case of usage of the saphenous vein, the reported prevalence of leg wound complications after coronary artery bypass grafting is 2% to 24% (Goldsboroug, 1999). Furthermore, in a fairly large number of patients, other problems are present like disease of the replacement vessel itself, usage in previous surgeries or the need for multiple bypasses. Therefore, many types of vascular grafts have been proposed to replace the native substitute (Canver, 1995; Rashid, 2004). These include fresh or cryopreserved allografts, xenografts, decellularised tissues, and synthetic grafts, all of which have their own advantages and disadvantages, as reviewed by several investigators (Leon, 2003; Rashid, 2004; Vara, 2004; Edelman, 1999; Matsuda, 2004; Xue, 2003; Kasisi, 2005; Sarraf, 2003; Teebken, 2002; Isenberg, 2006). The two standard grafts for vascular reconstruction are based on expanded polytetrafluoroethylene (ePTFE) and Dacron (polyethylene terephthalate fibre). It has been shown that both perform well at diameters > 6mm, but neither material has been suitable for small-diameter (<4mm) applications, such as required for CABG. Various modifications have been applied to improve the outcome of these synthetic grafts (Sifalian, 2002). However, little or only marginal clinical improvements have been achieved. Therefore, as a relative new approach, living

tissue-engineered (TE) small diameter blood vessels might obviate many of the above problems associated with the use of autologous and prosthetic grafts.

## 1.5. Vascular tissue engineering

In tissue engineering a combination of cells, engineering materials, and suitable biochemical and mechanical factors is used to culture constructs that improve or replace biological functions (Fig. 1.3). It uses the patient's own cells in combination with a scaffold, i.e. a cell carrier. Mechanical and/or chemical conditioning protocols are applied to stimulate the tissue formation during culture. Tissue engineering applied in the field of cardiovascular research involves the culture of heart valves and small diameter blood vessels. Important characteristics of TE vascular grafts include: viable tissue, remodeling capacity according to functional needs and ability to grow when placed in children. A functional TE vascular graft should at least meet the following criteria: it should possess tensile strength to provide mechanical support and an elastic component to provide recoil and prevent aneurysm formation. In addition, it should have a confluent endothelium to prevent thrombosis and to provide full functionality to the blood vessel. The present thesis mainly focuses on the first requirement, i.e. mechanical strength. The demands regarding strength, e.g. in terms of burst pressure, are not well defined. TE blood vessels should at least withstand physiological pressure. In addition, they should withstand surgical handling at implantation. It can be postulated that TE blood vessels should at least withstand pressures up to 500mmHg. The strength of TE blood vessels is determined by the scaffold and the developing tissue. Most commonly used scaffolds in vascular tissue engineering include biodegradable synthetic polymers. This approach is based on the idea that over time the scaffold degrades, while the mechanical properties of the developing tissue increase. The formation of tissue can be stimulated by subjecting the construct to mechanical stimuli. One of the most promising scaffold materials is polyglycolic acid (PGA), a rapidly degrading polymer. As such, the application of mechanical strain to PGA based constructs seeded with animal cells resulted in strong TE blood vessels (Niklason, 1999; Hoerstrup, 2001). Strong TE blood vessels based on human cells, however, were only obtained after long culture times up to 3 months (L'Heureux, 1998). In addition, these TE vessels were seeded with umbilical-cord-derived cells, which is impractical for growing autologous vessels for patients. In a shorter culture time, i.e. 7-8 weeks, relative strong TE vessels were cultured from human saphenous vein myofibroblasts (Klinger, 2006). However, these cells were genetically modified using a transfection that increased the replicative capacity of the fibroblasts. Constructs seeded with unmodified cells resulted in very weak TE blood vessels. In our laboratories, Mol and co-workers (2006) did succeed in culturing strong TE constructs, i.e. heart valve leaflets, based on unmodified human saphenous vein myofibroblasts in a relative short culture period of 4 weeks. These



Figure 1.3: *Tissue engineering concept including cells, scaffold, conditioning protocols and implantation.*

investigators extended the PGA scaffold with a poly-4-hydroxybutyrate (P4HB) coating and a fibrin gel. In addition, the seeded constructs were subjected to a strain-based conditioning protocol. It is therefore hypothesized that, with the above combination of scaffold materials and cells, in combination with strain-based mechanical conditioning, it is possible to culture strong human TE blood vessels in a relative short culture period.

## **1.6. Aim of this thesis**

The aim of this study is to culture TE blood vessels with human cells. These vessels should, in terms of strength, be suitable for implantation. To improve the strength of the TE blood vessels, mechanical conditioning is performed in a strain-based manner.

## **1.7. Outline of this thesis**

Chapter 2 focuses on various types of scaffolds used in tissue engineering and, more specifically, in the field of vascular tissue engineering. Several scaffold concepts are proposed based on proven applications and mechanical properties. Tubular constructs based on P4HB coated PGA and/or electrospun PCL are tested for production process, cell seeding and mechanical behavior.

In chapter 3, we will describe the most promising scaffold concepts that are now seeded with human fibroblasts and cultured for 4 weeks. Based on the resulting tissue formation and scaffold properties, one concept has been selected for further optimization via mechanical conditioning. Chapter 4 will focus on the conditioning of TE vascular constructs in longitudinal (axial) direction. In chapter 5, static axial strain was combined with dynamic circumferential strain, which resulted in strong TE blood vessels. To evaluate the properties of these constructs, measurements on native human and porcine small diameter blood vessels are performed where a comparison was made in terms of biochemical tissue contents and mechanical behavior (Chapter 6). In addition to mechanical strength, TE grafts should also possess a confluent, functional endothelium to provide non-thrombogenicity. Therefore, chapter 7 discusses the application of endothelial cells onto TE constructs. It describes pilot studies on seeding these cells on the TE constructs in the bioreactor set-up. In chapter 8 all results are summarized and discussed. It further speculates on future applications and possible obstacles.





# 2

## Scaffolds and tubular constructs

## 2.1 Introduction

The mechanical properties of tissue-engineered (TE) blood vessels are determined by both the scaffold and the tissue that is formed during culture. The goal of the present study is to select a suitable scaffold for TE blood vessels. This scaffold can contribute for a short initial period, in case of a fast degrading scaffold, or for longer periods of time. In the present chapter we briefly review different scaffold materials. In addition, several production techniques of fiber-based scaffolds are discussed. These can be used to enhance the mechanical properties of the scaffold in terms of strength and elasticity. Based on proven scaffold concepts and on adequate mechanical properties, 5 types of tubular scaffolds are proposed, all of which are tested for production process, cell seeding and mechanical properties.

## 2.2 Scaffolds in vascular tissue engineering

Scaffolds used in tissue engineering serve as a (temporary) skeleton that supports the growing tissue and provides the desired shape of the construct until the cells produce their own extracellular matrix. Scaffolds for vascular TE should meet several criteria; in general the scaffold should be biocompatible, biodegradable and mechanically stable. Furthermore a high surface area-volume ratio is required, as well as an interconnected structure. For vascular constructs it should be producible in a tubular structure. The structure and function of the scaffold is influenced by the scaffold material and the production process.

### Scaffold materials

Two types of scaffolds can be distinguished, biological and synthetic. Biological scaffolds are derived from human or animal tissue. Collagen and decellularized veins or arteries are examples of such types of scaffolds. Type I collagen, a major component of most connective tissues, facilitates cell attachment and can support tissue growth. Due to its biological and physical properties, collagen has been widely used in tissue engineering. In 1986, Weinberg and Bell constructed the first complete TE biological vessel with collagen as the scaffold material (Weinberg, 1986). Bovine smooth muscle cells and fibroblasts were separately embedded in a collagen gel and used to form medial and adventitial layers, respectively. Endothelial cells were used to form a layer of endothelium on the luminal surface. However, the graft lacked adequate mechanical strength, even when Dacron meshes were used for reinforcement. The strongest constructs, which included 2 Dacron meshes, had a burst pressure of 323mmHg. Several groups adapted the collagen-based model of Weinberg and Bell to investigate aspects of cellular behavior and construct functionality (L'Heureux, 1993; Ziegler, 1994; Seliktar, 2000). Although these studies provided a superfluity of information, the poor mechanical properties have essentially limited this model to in-vitro investigations.

The decellularized biological scaffold was introduced to obtain a physiological matrix scaffold that resembles that of native blood vessels (Wilson, 1995). For this scaffold, the cells are removed using detergent and enzymatic extraction techniques, leaving an

acellular matrix that serves as a scaffold for autologous cells. The obvious advantage of this scaffold is that it is composed of extracellular matrix proteins typically found in the body. When derived from a vessel, the three-dimensional architecture is very similar to that of the original vessel it is replacing, thus conferring appropriate mechanical and physical properties. Cell infiltration and tissue remodeling is often limited in these scaffolds, although Simionescu (2006) recently reported promising results. Despite these encouraging results, there are concerns regarding the potential transmission of endogenous retroviruses or potentially infective proteins such as prions even when human vessel-derived substrates are used (Kallenbach, 2004).

Biodegradable synthetic scaffolds are synthesized from substances not found in nature. They degrade over a variable period of time, so ultimately they are no longer part of the graft. The two best-investigated biodegradable polymers are polyglycolic acid (PGA) and polylactic acid (PLA). PGA is a highly crystalline and hydrophilic polymer and was used to produce the first synthetic absorbable suture (Frazza, 1971). Within 2 to 4 weeks after implantation the suture loses its mechanical strength due to polymer hydrolysis. PLA is more hydrophobic than PGA because of the presence of an extra methyl group in the lactide molecule, which limits water uptake. This results in a lower hydrolysis rate. Both materials are FDA approved and therefore favorable materials for tissue engineering applications. PGA fiber-based matrices have proven to be useful in the engineering of many types of soft tissues (Shinoka, 1996; Niklason, 1999; Hoerstrup, 1998; Sodian, 2000). However, these matrices are subjected to contractile forces exerted by the adherent cells. As the mechanical properties of PGA decrease rapidly in culture, the matrices cannot withstand these forces and contract over time, resulting in a loss of the desired size and shape of the engineered tissues. To overcome this problem several research groups extended the PGA scaffold with co-polymers, coatings or other materials (Shum-Tim, 1999; Watanabe, 2001; Kim, 1998). Hoerstrup (2001), e.g., applied a poly-4-hydroxybutyrate (P4HB)-coating that improved the mechanical properties and allowed molding the scaffolds into complex three-dimensional shapes like heart valves.

Although scaffolds based on PGA look very promising, it might be necessary to further improve their mechanical properties, i.e. not only in terms of strength but also regarding elasticity and compliance. The PGA scaffold could be expanded by combining it with other porous structures of biodegradable polymers.

### **Production techniques**

Techniques that are used to produce porous scaffolds for tissue engineering include particle leaching, gas formation, high-pressure gas expansion, phase separation and emulsion freeze-drying methods (Mikos, 1994; Nam, 2000; Mooney, 1996; Harris, 1995; Whang, 1995). In case of polymer fiber-based scaffolds, conventional techniques include melt spinning, wet spinning, and dry spinning (Pavlov, 2004; Williamson, 2004). These techniques usually produce fibers with diameters in the range of 10-50 $\mu\text{m}$ . Several research groups, however, state that scaffolds should be physically analogous to native extracellular matrix and therefore should exist of nanoscaled fibers (Nair, 2004; Kidoaki, 2005). Electrospinning allows the generation of fibers with submicron diameters and is therefore widely applied in tissue engineering. It is a relatively simple, straightforward and cost-effective method, applicable to a large variety of materials. For

tissue engineering purposes, spun poly- $\epsilon$ -caprolactone (PCL) has been widely used because it lacks toxicity, has a low cost and degrades relatively slowly (Yoshimoto, 2003; Zhang, 2005; Khil, 2005).

A drawback of most electrospun scaffolds is the small pore size which results from the fine fiber structure. This hampers proper cell ingrowth and, as such, has limited the use of these scaffolds mostly to applications as 2-dimensional substrates. In such scaffolds, cells attach to the surface rather than inside the scaffold. Cell adhesion and proliferation on such electrospun scaffolds were investigated by several research groups (Mo, 2004; Zhang, 2005; Kwon, 2005; Xu, 2004). To overcome the problem of limited cell penetration and to allow the construction of a 3-dimensional electrospun construct, the pore size should be enlarged. Although this can be influenced by varying the spinning parameters (Deitzel, 2001; Mo, 2004), this effect is only limited. Recently, Kidoaki and co-workers (2005) introduced multilayering and mixing electrospinning techniques for the design of multi-component, structured scaffolds. To this end, among other things, segmented polyurethane (SPU) and polyethylene oxide (PEO) were combined. SPU and PEO were simultaneously electrospun as a mixed scaffold. PEO might be used as a leaching polymer as it is soluble in chloroform as well as in water. By doing so, a more open electrospun scaffold could be obtained by dissolving PEO through impregnation in water after the spinning process.

By using such mixed electrospinning techniques or by combining electrospun structures with, e.g., PGA, scaffolds could be produced that have, to a certain extent, controllable mechanical properties and allow adequate tissue development.

### **Seeding methods**

Aside from the scaffold material and structure, also the seeding method can affect the properties of TE tissue. Several seeding techniques are used in tissue engineering applications, being either static or dynamic in nature. Static seeding, the most commonly used procedure, is performed by injecting a concentrated cell suspension into the scaffold. Dynamic seeding procedures involve stirring or agitation of cells in suspension together with the scaffold. A drawback is that the physical forces created by these methods can destroy nascent cell-polymer interactions while static seeding often needs multiple seeding steps and is therefore a complex and time-consuming procedure.

As pointed out earlier, seeding electrospun scaffolds can be difficult because the pores are often too small. To overcome this problem, Yoshimoto and co-workers seeded electrospun scaffolds by pushing them onto a cell pellet (Yoshimoto, 2003). However, this seems not to be applicable to large and/or complex geometries like tubes or valves.

For more efficient and easy seeding, involving only a single seeding step, cells can be encapsulated in gels, for example collagen or fibrin gels. Ameer and co-workers (2002) described a seeding method in which fibrin - as a cell carrier - was combined with a biodegradable polymer fiber mesh. Mol and colleagues (2005) also used this method and reported successful cell seeding into PGA meshed coated with PCL. Aside from its easy applicability, seeding with the fibrin gel also resulted in limited loss of soluble collagen into the culture medium and a more mature extracellular matrix in a shorter period of time.

### Scaffold concepts

Considering the above described scaffold materials and production techniques, several types of tubular scaffolds are proposed and investigated in this study. The choice of the scaffold concepts was based on tissue development in combination with controllable mechanical properties. The first was proven in, e.g., scaffolds produced from P4HB coated PGA (Mol 2006), while the latter was demonstrated in e.g., electrospun PCL (Khil, 2005; Bolgen, 2005). Therefore the scaffolds described in the present study are based on these two materials. In total five scaffold concepts are proposed, a schematic representation of which is given in Fig 2.1. The first two consisted of solely electrospun PCL. Besides a pure electrospun PCL scaffold (Fig. 2.1a), PCL was spun in combination with PEO. This spun PEO was washed out in water after the spinning process, leaving a more open electrospun PCL(PEO) structure (Fig. 2.1b). The other three concepts basically consisted of P4HB-coated PGA. One type consisted of pure PGA coated with P4HB (Fig. 2.1c). As the PGA/P4HB construct rapidly loses its mechanical properties, as was shown in the present study, the PGA construct was extended with a thin layer of electrospun PCL at the inner wall of the construct (Fig. 2.1d). This PCL extension might serve as an inner elastic layer, as TE vessels often lack such a layer in the initial culture period. Another approach to enhance the mechanical strength of a PGA scaffold was to apply an outer layer of electrospun PCL, which might serve as a support stocking (Fig. 2.1e).

All tubular constructs were analyzed for ease of production and cell seeding as well as for their mechanical properties, assessed by tensile testing.

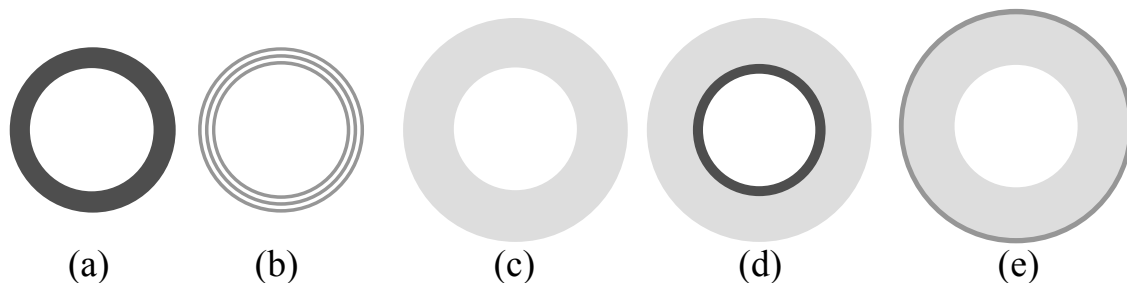


Figure 2.1: Schematic representation of the 5 tubular scaffold structures; cross-section of pure electrospun PCL (a), PCL(PEO) (b), PGA/P4HB (c) and PGA/P4HB with an inner (d) or outer (e) layer of electrospun PCL. The grayscale indicates the density/pore size of the scaffold, darker being a dense structure with relative small pores (i.e. electrospun PCL), light areas refer to a more open structure (e.g. PGA).

## 2.3 Materials & Methods

### Materials

Poly( $\epsilon$ -caprolactone) (PCL) and polyethylene oxide (PEO), with an average molecular weight of 80 and 600 kDa, respectively, were dissolved in 99.9% HPLC-grade

chloroform at a concentration of 17.5 and 4% w/v, respectively (Sigma, Aldrich, USA). Polyglycolic acid (PGA) sheets (thickness 1.0mm; specific gravity 69 mg/cm<sup>3</sup>; Cellon, Luxemburg) were coated with a thin layer of 1% w/v poly-4-hydroxybutyrate (P4HB) (Symetis Inc., Switzerland) dissolved in tetrahydrofuran (THF).

### 2.3.1 Electrospun constructs

The electrospinning setup is shown in Fig 2.2. A 10ml polypropylene syringe was filled with a PCL or PEO solution and placed in an infusion pump (Harvard apparatus). This pump fed the polymer solution via PTFE tubing into a 23G needle with a flow rate of 30 $\mu$ l/min. A voltage of 15kV was applied to the needle using a high-voltage power supply (Wallis Worthing, UK). A polymer jet was ejected from the needle tip towards the grounded, rotating and translating, mandrel located 15cm below the tip. The rotational frequency was 1 Hz while the translation speed was 4cm/s.

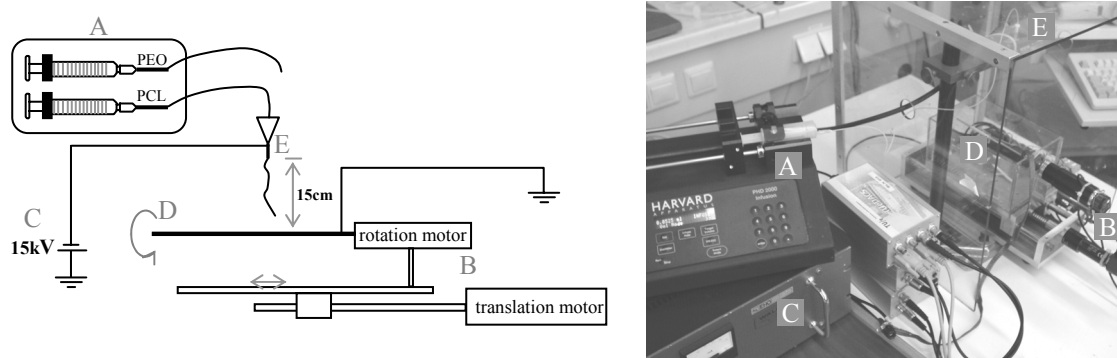


Figure 2.2: *Electrospinning set-up with a syringe pump (A), a translation/rotation motor (B), a high power voltage (C), a rotating rod (D) and needle (E) through which the polymer solution is fed.*

Pure PCL electrospun tubes were obtained by spinning 250 $\mu$ l of the polymer solution on a rotating and translating mandrel with a diameter of 3mm. Typical tubular constructs had an inner diameter of 3mm and a wall thickness of approximately 200 $\mu$ m. The PCL(PEO) tubes were produced by spinning PCL and PEO sequentially in alternating layers, starting with a layer of PCL, followed by PEO, PCL etc. The first layer consisted of 50 $\mu$ l PCL, followed by multiple layers of 100 $\mu$ l PEO and 25 $\mu$ l PCL, ending with a layer of PCL. This procedure was repeated until the total amount of electrospun PCL was equal to 250 $\mu$ l. These tubes were then gently shaken in water overnight so that the PEO was dissolved and washed out. Before immersion in water, the tubes were briefly immersed in 70% alcohol in order to pre-wet them. Subsequently the tubes were dried in a vacuum oven. The resulting constructs had an inner diameter of 3mm and a wall thickness of approximately 300-400 $\mu$ m.

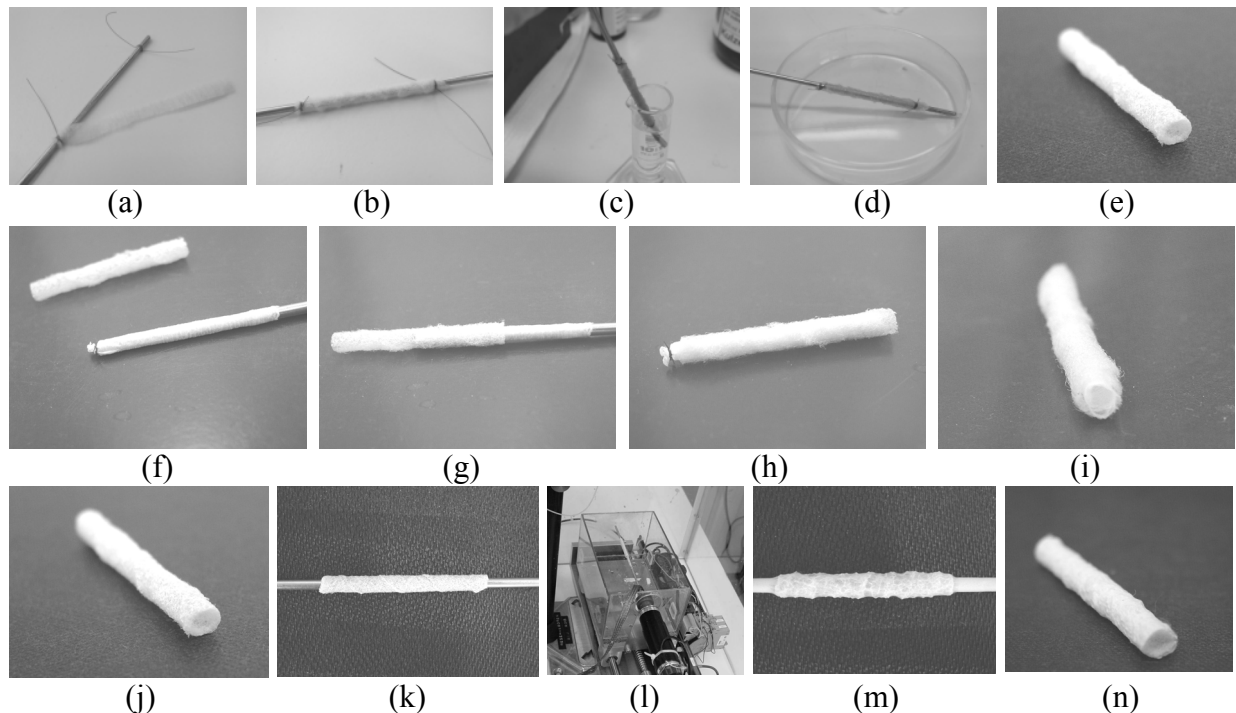


Figure 2.3: Production of PGA tubular constructs coated with P4HB (a-e), with inner (f-i) or outer (j-n) electrospun PCL layer

### 2.3.2 PGA tubular constructs

As reported by Niklason and co-workers (1999), PGA sheets for vascular tissue engineering can be sewn into tubes with PGA suture to form tubular scaffolds. In a slightly different approach, which might give a more uniform structure without sutures, a sheet of PGA can be wrapped around a rod followed by dip coating in a P4HB solution. As such, a PGA sheet of approximately 80x5x1mm was wrapped around a rod with a diameter of 3mm. Both ends were secured with a suture before dip-coating the tube in a 1w/v% P4HB (Fig 2.3a-e). The PGA sheet had to be carefully wrapped around the rod so that the turns were close together. After coating this resulted in a well connected, uniform tube (Fig 2.4a). When the turns were not close enough to each other (Fig 2.4b), the construct could easily tear apart, e.g., during attachment in a bioreactor or during a straining protocol. Too much overlap between the turns (Fig 2.4c) resulted in a non-uniform wall-thickness. After evaporation of the solvent, the tubular construct was removed from the rod. To remove solvent remnants, the scaffolds were dried under vacuum overnight.

For PGA scaffolds with an inner layer of electrospun PCL, the PCL tube was slipped over a rod and secured at the end with a suture (Fig 2.3f-i). Then the PGA/P4HB construct was slid over the PCL tube. The PGA/P4HB and PCL combination could then be removed from the rod. An, at first sight, easier method to first wrap the PGA around the PCL followed by the coating process was not feasible as the electrospun PCL dissolves in the solvent of the P4HB coating.

For PGA scaffolds with an outer PCL layer (Fig. 2.3j-n), the PGA/P4HB construct was first slid over the mandrel of the electrospinning device. Then a PCL solution was spun



on top of the rotating and translating mandrel. The layer thickness of the PCL could be varied and was chosen as a balance between mechanical properties and cell seeding, considering that a thick layer might improve mechanical properties but would also result in a dense outer layer complicating cell seeding.

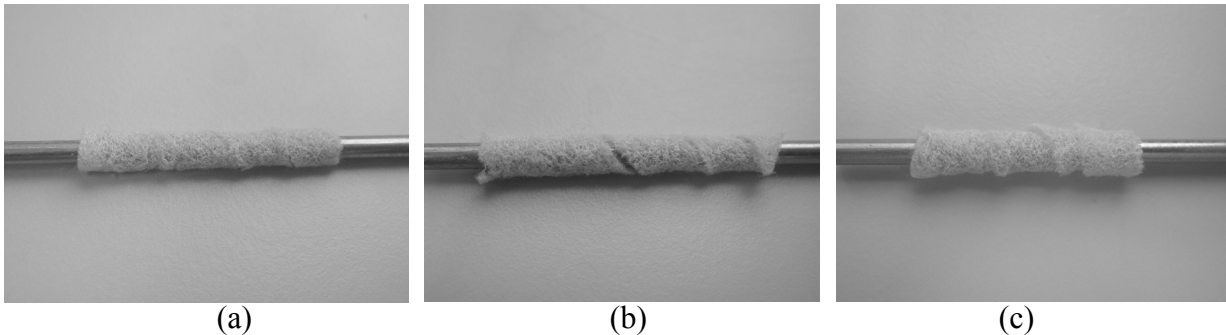


Figure 2.4: *Fabrication of a tubular constructs from a PGA sheet, shown in the correct way (a), with turns not close enough together (b), and with too much overlap between turns (c)*

### 2.3.3 Scanning Electron Microscopy

For visual characterization, the tubular scaffolds were sputter-coated with gold. The morphology of the scaffolds was evaluated using a scanning electron microscopy (SEM, Philips XL30ESEM-FEG, the Netherlands) at an accelerating voltage of 10kV. Each construct was visualized at the outer and inner surface, and at the cross section. The scaffolds were visually inspected for pore size and homogeneity.

### 2.3.4 Mechanical testing

The two basic scaffold materials, PGA coated with P4HB and pure electrospun PCL, were tested mechanically as a function of time by means of uniaxial tensile tests. These tests were performed using a tensile tester (custom-built, equipped with a load cell of 20N) at a constant strain rate of the initial length/min. A strip of PGA (100\*10\*1mm) was coated on one side with P4HB and filled with a fibrin gel. It was kept in culture medium in an incubator at 37°C. Uniaxial tensile tests on parts of this strip (3\*10\*1mm, n=3) were performed at day 1, 4, 7, and 11.

Pure electrospun PCL tubes were divided into 2 groups of 4 pieces each. The first group was mechanically tested at day 1. The other group was placed in culture medium for 4 weeks in an incubator, which equals the applied culture period of TE blood vessels, and then tested in the same way. The engineering stress was calculated as the force/initial surface. The resulting stress-strain curves were compared and a Young's modulus was calculated as the ratio of stress/strain taken at the linear region of the curve.

### 2.3.5 Cells and cell seeding

In this study two types of cells were used, 3T3 mouse fibroblasts and human myofibroblasts isolated from saphenous veins (HVSC). The mouse fibroblasts were

used for the cell infiltration studies as these cells are small and they proliferate fast. The HVSC were used for tissue culture studies as these cells show good in-vitro tissue generation (Schnell, 2001). In addition, these cells are easily obtainable and therefore suitable for human tissue engineering applications.

### **Mouse fibroblasts**

The cell infiltration properties of both types of electrospun PCL constructs were tested using 3T3 mouse fibroblasts. These cells were plated as monolayers and cultured to confluence in a 1:1 mixed medium solution of DMEM low glucose and HAM's F12 (BioWhittaker, Cambrex, the Netherlands), containing 10% fetal bovine serum (FBS) and 1% penicillin-streptomycin (Biochrom, VWR, the Netherlands). The cultures were maintained in a humidified incubator at 37°C and 5% CO<sub>2</sub>. When reaching 90% confluence, the fibroblasts were trypsinized and used for cell seeding.

### **Seeding test PCL scaffolds**

The tubular electrospun PCL constructs were sterilized, pre-wet in 70% alcohol and, without drying in between, rinsed in PBS and immersed in culture medium overnight. Fibroblasts were suspended in a sterile bovine thrombin solution with a concentration of 10 IU thrombin/ml medium (Sigma, USA). Subsequently the cells-thrombin solution was added to a sterile bovine fibrinogen solution (10mg actual protein/ml medium), in a 1:1 mixture. For each tube 100µl fibrin gel was used. After careful mixing, the gel was pipetted on a sterile glass surface. The medium was sucked out of the tubes and the tubes were rolled through the cell-fibrin solution to force the cells into the scaffold. To evaluate cell infiltration, the mouse fibroblasts were seeded with  $50 \times 10^6$  cells/ml in the scaffold, cultured for 1 week and analyzed by histology.

### **Human myofibroblasts**

Human myofibroblasts were harvested from the saphenous vein (HVSC) and expanded using regular culture methods (Schnell et al., 2001). The medium to culture these cells consisted of DMEM Advanced (Gibco, USA), supplemented with 10% FBS (Biochrom, Germany), 1% Glutamax (Gibco, USA) and 0.1% gentamycin (Biochrom, Germany). The medium for seeding and subsequent tissue culture, referred to as TE-medium, contained 0.3% gentamycin and additional L-ascorbic acid 2-phosphate (0.25 mg/ml, Sigma, USA) to stimulate extracellular matrix production (Hoerstrup, 1999).

### **Four week static culture**

To test the cell infiltration properties and tissue development in the tubular PGA constructs, HVSC were seeded and cultured for 4 weeks under static conditions. The PGA constructs were sterilized by soaking in 70% ethanol for 3 hours and subsequent drying in a LAF-cabinet. Then the constructs were washed in PBS and placed in TE-medium overnight. For seeding, fibrin gel was used as a cell carrier. The cells were suspended in a sterile thrombin solution (10 IU/ml medium; Sigma, USA) and then mixed with an equal amount of sterile fibrinogen solution (10mg actual protein / ml medium; Sigma, USA). The total solution ( $30-40 \times 10^6$  cells/ml) was mixed with a pipette until the starting point of the polymerization process of the gel. Then the cell-fibrin solution was immediately dripped onto the scaffold. The seeded constructs were placed

into culture flasks and the gel was allowed to polymerize in the incubator for 20 minutes. Afterwards the flasks were filled with 25ml of TE medium and placed in the incubator for the indicated time period. This medium was refreshed every 3 to 4 days.

**2.3.6 Evaluation of cell infiltration and tissue formation**

The cell infiltration and tissue formation was evaluated by histology. Respectively after 1 week, in case of the seeding test, or 4 weeks of culture, a ring of each construct was fixed in 4% phosphate-buffered formalin and embedded in Technovit (Kulzer, Klinipath, the Netherlands). Sections of 5µm thickness were cut and stained with toluidine blue and subsequently analyzed by light microscopy.

**2.4 Results**

**2.4.1 Tubular constructs**

Macroscopic photographs (top row) and SEM images of the various tubular scaffold types are shown in Fig. 2.5. The SEM micrographs show the structure of the outer and the inner surface and the cross-section of the scaffold. The latter well illustrates the layered structure. At the left of the figure the two PCL concepts are shown, the standard electrospun PCL scaffold (Fig. 2.5a) and the PCL(PEO) scaffold (Fig. 2.5b). The inside

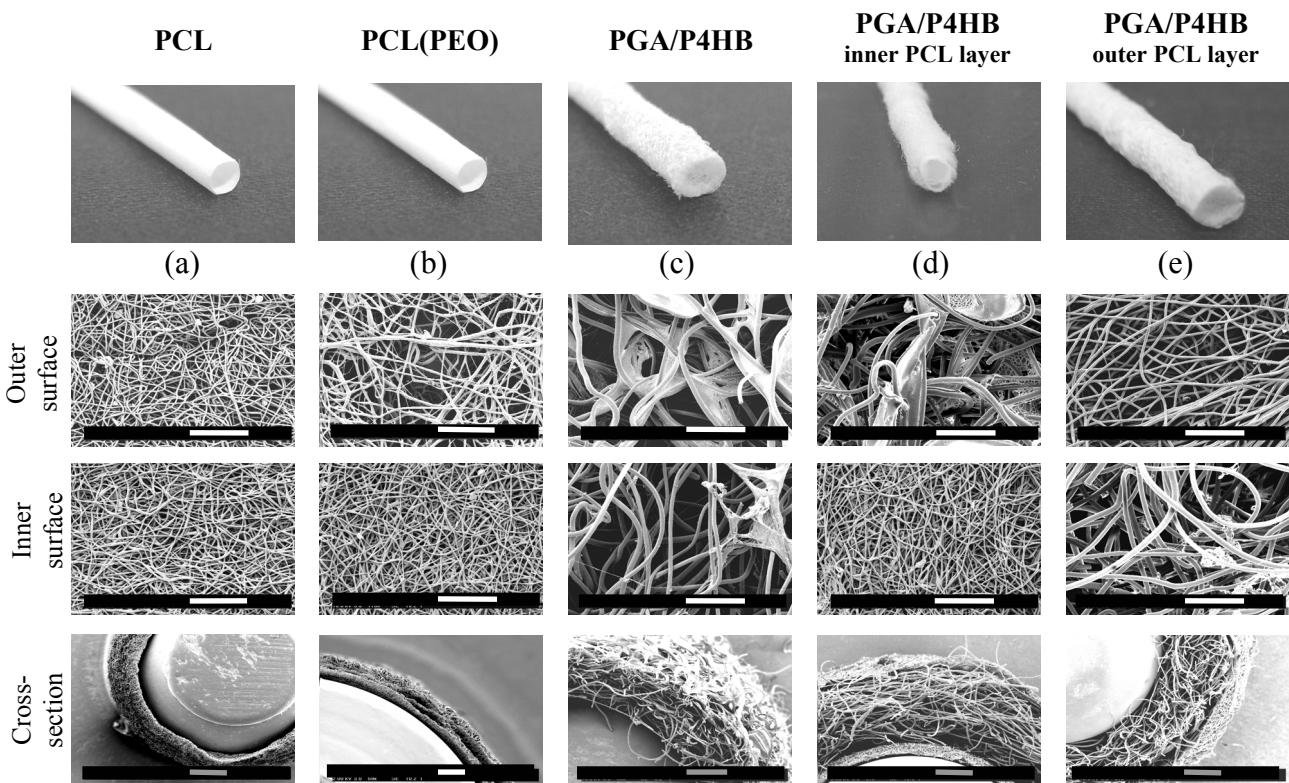


Figure 2.5: Photographs and SEM micrographs of the various tubular scaffolds showing the outer and inner surfaces and the cross sections. Note the apparent different structure of the electrospun PCL at the inner and outer side of the PGA (d,e). The white bars indicate 200µm, the grey bars indicate 500µm.

structure of both scaffolds is identical, i.e., a dense electrospun PCL layer with pore sizes between 5 and 25 $\mu\text{m}$ . This, however, is not the case at the outer surface. The PCL(PEO) scaffold has a more heterogeneous structure with larger pores, ranging from 5 to 150 $\mu\text{m}$ . This is caused by the fact that the thin PCL layers, except for the first one, were spun on top of a more irregular structure of the electrospun PEO. The cross-section clearly shows the layered structure of the PCL(PEO) scaffold.

At the right of Fig. 2.5 the 3 PGA scaffold concepts are presented. SEM pictures of the PGA/P4HB scaffolds (Fig. 2.5c) show that the P4HB coating is more pronounced at the outer surface than at the inner surface. This is also illustrated in the cross section image. Apparently, as the PGA was wrapped around a rod during the coating procedure, the P4HB coating did not penetrate into the whole scaffold, although it was completely immersed in the solution. The PGA/P4HB scaffold with inner PCL layer (Fig. 2.5d) has a dense electrospun PCL layer at the inner side and a P4HB-coated PGA surface at the outside. The cross-section shows the ratio between the layer thicknesses of the PCL and the PGA. The 5<sup>th</sup> concept (Fig. 2.5e) shows a distinctly more open electrospun PCL layer at the outside of the construct. As the PCL was electrospun on top of the relatively rough PGA surface, the formed PCL layer was not as dense as electrospun PCL spun on a normal, smooth mandrel. The inside of this construct shows the PGA surface with relatively little P4HB coating.

## 2.4.2 Mechanical properties

Both basic scaffold materials, PGA coated with P4HB and pure electrospun PCL, were mechanically tested. Fig. 2.6a shows stress-strain curves of the PGA/P4HB scaffold as a function of time, i.e. measured at 1, 4, 7 and 11 days after putting the scaffold in culture medium. It clearly shows that the mechanical properties started to decline drastically after 7 days. The averaged Young's moduli ( $E$ ) decreased from 0.34 to 0.28, 0.23 and 0.12MPa after 4, 7 and 11 days, respectively (insert Fig 2.6a). The stress-strain curves of the electrospun PCL constructs are shown in figure b. There were no significant differences between the curves at day 1 and 28. This result was expected, as the

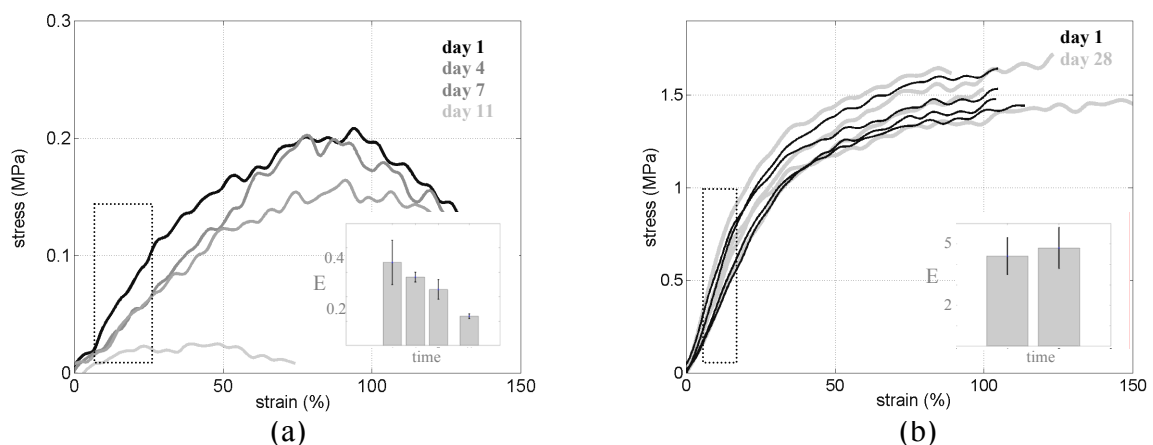


Figure 2.6: Stress-strain curves of PGA/P4HB (left) and electrospun PCL (right) measured at different time points. Notice the different y-axes. The inserts show the Young's moduli  $\pm$  sd, determined from the linear portion of the curves (dashed boxes), as a function of time, values are given in the text.

degradation of PCL takes much longer than 4 weeks. The averaged Young's modulus (E) of this material was 4.4 (t=0d) and 4.8 (t=28d) MPa (insert Fig. 2.6b).

### 2.4.3 Seeding test PCL scaffolds

Histological examination of the pure PCL scaffold seeded with mouse 3T3 fibroblasts after 1 week of culture, demonstrated that most cells were located on the outside of the scaffold (Fig. 2.7a-b). Only few cells were found inside the scaffold; the majority did not infiltrate into the electrospun PCL and therefore formed a dense layer on the outer surface only. The results for the PCL(PEO) scaffold are shown in Fig. 2.7c-d. A distinct layered structure is visible and cells are present throughout the whole construct. In other regions of this construct (data not shown) where the PCL layers were more compressed, cell infiltration was less pronounced.

### 2.4.4 PGA constructs

Figure 2.8 shows the histological evaluation of the PGA constructs (Fig. 2.8a,d), with an inner (Fig. 2.8b,e) and outer (Fig. 2.8c,f) electrospun PCL layer after a culture period of 4 weeks. Figure 2.8a, and in more detail figure 2.8b, shows a homogeneous distribution of cells throughout the scaffold. Fragmented scaffold remnants are visible in dark purple. In the PGA/P4HB construct with the inner PCL layer (Fig. 2.8b,e), most of the cells were found in the PGA/P4HB part. Cells proliferated into the relative dense PCL layer, but the cell distribution was not homogeneous throughout the constructs. A layer of cells was found at the luminal side of the tubular construct. The construct with the outer PCL layer (Fig. 2.8c,f) formed a more uniform entity. As already shown in Fig. 2.5, this electrospun layer was much more open compared to the PCL layer at the inside of the construct, allowing a homogeneous cell distribution in the PGA/P4HB and PCL part.

## 2.5 Discussion

In this study several tubular scaffold concepts were proposed as scaffolds for vascular tissue engineering. They consisted of P4HB coated PGA and/or electrospun PCL. PGA/P4HB scaffolds already proved their potential in tissue engineered heart valves (Mol, 2006). Electrospinning of biodegradable polymers, e.g., PCL, is a technique that is more and more used in the field of tissue engineering. PGA is a fast-degrading material, while PCL degrades much slower. Combining both scaffold types might lead to constructs with improved mechanical properties.

The present study demonstrated that electrospun PCL as an independent scaffold for vascular tissue engineering has serious drawbacks. However, as an extension to PGA/P4HB constructs, it might contribute to improved mechanical properties.

Our study clearly shows that the fiber-distribution in pure electrospun PCL scaffolds is too dense for proper cell infiltration. In contrast, the proposed PCL(PEO) scaffold is more open and showed improved cell penetration properties, although not homogeneous



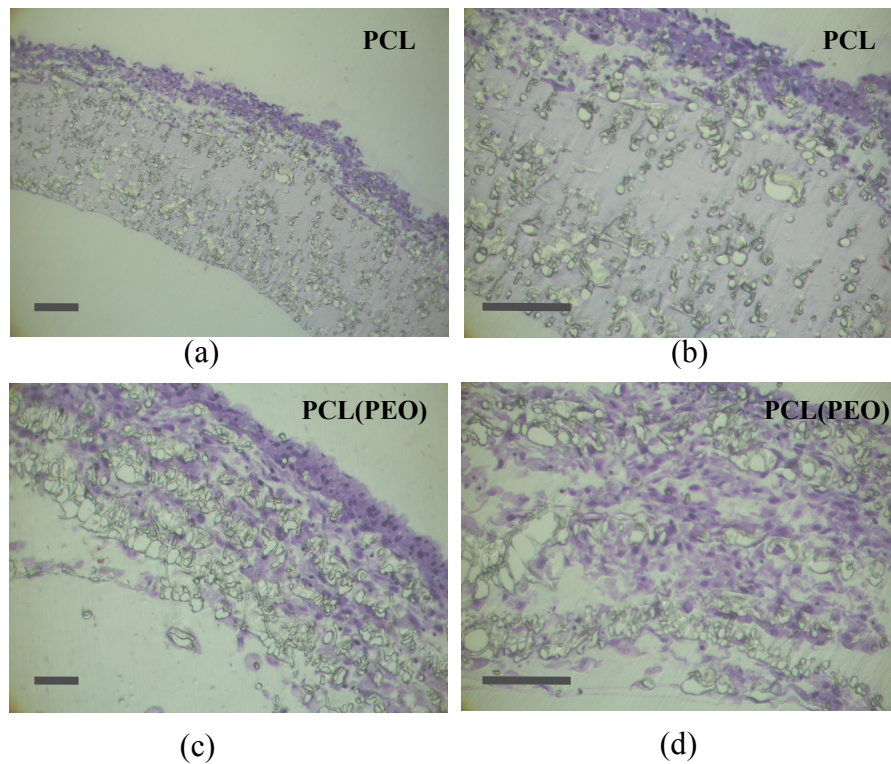


Figure 2.7: Toluidine blue stained sections of 3T3 seeded electrospun PCL (a,b) and PCL(PEO) (c,d) scaffolds, the bars indicate 50 $\mu$ m.

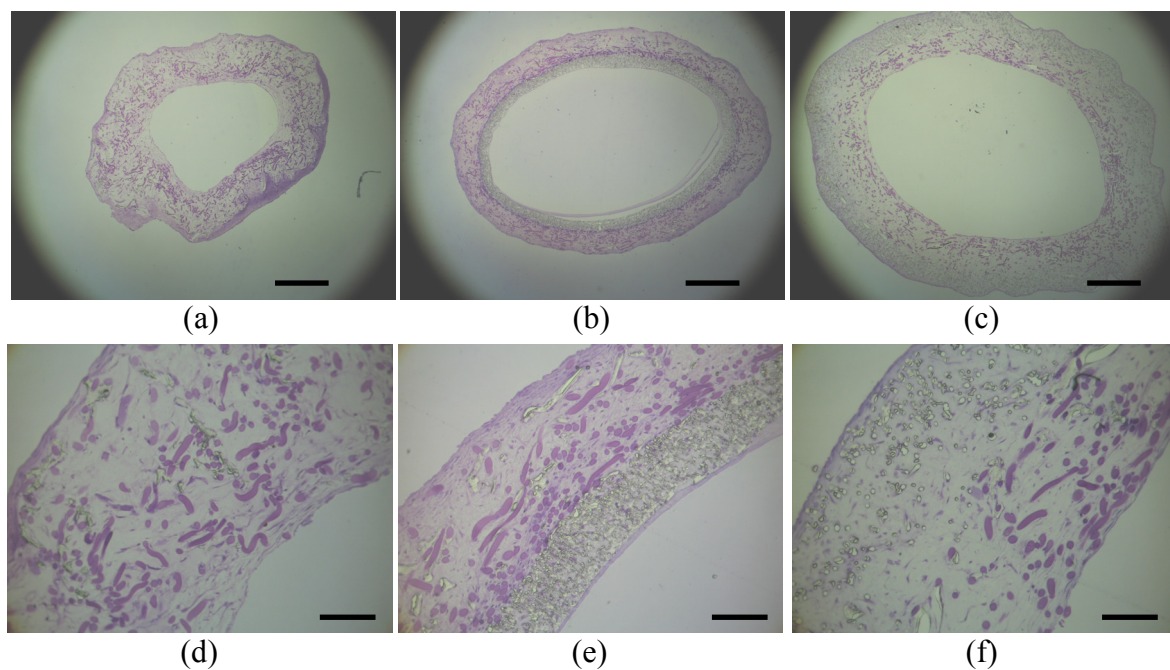


Figure 2.8: Toluidine blue staining of HVSC seeded PGA constructs (a), with inner (b) and outer (c) PCL layer after a 4 week culture period, detailed images are shown in d-f, the bars indicate 1mm (a-c) and 200 $\mu$ m (d-f).

throughout the whole construct. The production process of the PCL(PEO) tubes is, compared to the pure PCL constructs, a time-consuming and less reproducible process. This is partly caused by the fact that PEO is electrically charged and therefore more difficult to spin in a reproducible way. Furthermore, the PCL layers should be relatively thin to keep the construct structure open. Thus, many layers have to be spun when a wall thickness of several hundreds of micrometers has to be achieved. In addition, as PCL is hydrophobic, the seeding of these scaffolds could only be performed by forcing the cells into the constructs by rolling the tubes through the cell solution.

Considering these production and cell infiltration difficulties, the PCL(PEO) tubes seem less applicable in vascular tissue engineering compared to e.g. PGA constructs. However, electrospun PCL has good mechanical properties that do not decline as rapidly as those of PGA. It is therefore suggested that the combination of electrospun PCL and PGA scaffolds will be more promising. The more so because dynamic culture protocols (as described in chapter 4 and 5) generally start after one week of static culture, followed by several weeks of dynamic culture. As the mechanical integrity of the PGA/P4HB scaffold starts to decline drastically after 1 week, the freshly formed tissue should be able to withstand these dynamic conditions. An added layer of electrospun PCL might prolong the load bearing capacity of the scaffold material and allow a more gradual development of the tissue. This might be true especially for the proposed scaffold with an outer PCL layer as this compound construct showed a homogeneous cell distribution.

The application of electrospun polymers to enhance the mechanical properties of TE blood vessels was recently published by Stitzel and co-workers (2006). The starting point was not a biodegradable polymer but animal derived collagen and elastin. Poly(D,L-lactide-co-glycolide) (PLGA) was added to the spinning mixture, consisting of a blend of type I collagen and elastin, to improve the mechanical properties in terms of compliance and strength. By adding the polymer, the burst pressure and compliance of these constructs were similar to those in native vessels. However, cells that were seeded on the luminal and outer surface did not penetrate throughout the whole scaffold. In addition, although these types of constructs, i.e. based on collagen and elastin, contained the right amount of extracellular matrix, it was not produced by the cells themselves. Therefore it is questionable whether these kinds of constructs are capable of remodeling and growth. This study (Stitzel, 2006) did show that electrospun polymers can be used to improve the mechanical properties. Therefore, PGA/P4HB constructs, which showed homogeneous cell distributions, with or without electrospun PCL layers are further investigated. These constructs are seeded with human myofibroblasts and cultured for 4 weeks, as described in chapter 3. Mechanical properties of all constructs are assessed by uniaxial tensile tests.

## 2.6 Acknowledgements

We gratefully acknowledge Robert van Lith for his contributions to the electrospinning experiments.

# 3

## Characterization of tissue-engineered blood vessels



## 3.1 Introduction

To evaluate soft tissue-engineered (TE) constructs, the tissue properties have to be compared to those of native tissue. In literature these artificial constructs, whether vessels, valves or other engineered substitutes, are characterized in many different ways. To be able to compare different TE constructs with each other and with native tissue, it is important to identify and discuss the characterization methods. For this, a distinction can be made between tissue content analysis and measurements of mechanical properties. The first can be performed by e.g., histology or biochemical assays. The second by e.g., uniaxial or biaxial tensile tests, burst pressure or compliance measurements.

In this chapter the various characterization methods are discussed. In addition, static cultures of different tubular TE constructs are analyzed using part of these methods. On the basis of tissue development and mechanical properties, a scaffold concept is selected for future studies including mechanical conditioning protocols, as will be described in chapters 4 and 5.

### 3.1.1 Tissue analyses

Histology is a key approach to analyze the tissue formation of soft TE constructs. Hematoxylin-eosin (H&E) and Masson's trichrome stains are most commonly used. H&E staining, but also toluidine blue staining, reveals cells and general tissue morphology. Masson's trichrome staining reveals nuclei, cytoplasm, muscle and collagen. Also immunohistochemical staining can be used to visualize collagen. In addition, this technique can be used to visualize elastin (Williams and Wick, 2004), although Movat's pentachrome stains can also be used for this purpose (Ogle, 2002; Schenke, 2004). Furthermore, immunostaining can be used to demonstrate the presence of the smooth muscle cell (SMC)-specific proteins such as  $\alpha$ -smooth muscle actin ( $\alpha$ -SMA, Schmidt, 2005, Niklason, 2001; Williams, 2004).

To visualize the TE constructs in more detail, transmission electron microscopy (TEM) is used as well. In a study by Hoerstrup and co-workers (2002), TEM revealed tissue elements typical of viable, secretorally active myofibroblasts, such as actin/myosin filaments as well as collagen fibrils and elastin fiber networks. TEM was also applied to visualize SMCs that were distributed in lamellae, with interposed layers of collagen fibrils. Evidence of polymer phagocytosis by SMCs was presented by Niklason (2001).

While (immuno) histochemistry and TEM are effective to determine the morphological quality of TE vessels, biochemical assays can reveal the composition of the tissue in a quantitative way. Many investigators determined the amount of DNA as a marker for cell number, hydroxyproline as an indicator for collagen content, and/or glycoaminoglycans (GAG), which are responsible for the compressibility of the tissue (Mol, 2004; Williams, 2004). The amount of soluble collagen in culture medium can be determined using the SirCOL<sup>TM</sup> assay (Mol, 2004).

Another way to analyze TE tissue is to evaluate its biological functionality, e.g., the contractile function (Niklason, 2001). The vasoreactivity of fibrin-based TE was investigated by Swartz (2005). Boccafoschi (2005) tested the biological performance of collagen-based scaffolds by blood performance using clotting time measurements, platelet adhesion tests and thrombelastography, which is the only test that evaluates the entire dynamics of clot formation. The thrombogenicity index informs about the dynamics of blood coagulation as well as the strength of the final clot.

### 3.1.2 Mechanical testing

#### Tensile tests

The determination of mechanical properties is very important in the characterization of TE blood vessels as these properties, beside other factors, strongly determine the success of implantation as a vascular graft. Uniaxial tensile testing is one of the most common methods to assess these properties. For this, blood vessel constructs can be tested as longitudinal strips (Opitz, 2002; Clerin, 2003) or as circumferential ring samples (Berglund, 2004; Swartz, 2005). Properties in longitudinal direction are measured by clamping the strip sample and straining it until break while measuring the required force. In case of the circumferential stretch tests, two wires or pins are inserted through the lumen of a vessel segment, to which increasing tension is applied.

Tensile tests, combined with the construct dimensions, result in stress-strain curves. The stress can be defined as an engineering stress, equaling the measured force divided by the initial cross-sectional area, or as a Cauchy stress, defined as the force divided by the deformed cross-sectional area. Both definitions are used in literature. When incompressibility is assumed, the relation between both stress measures in a uniaxial tensile test is given by:

$$\sigma_{\text{Cauchy}} = \lambda \sigma_{\text{engineering}} \quad (3.1)$$

where  $\lambda$  is equal to the stretch, defined as  $l/l_0$ , i.e., the sample length at a given time divided by the initial length. In the course of this thesis, the stress is defined as the engineering stress, unless otherwise stated. The strain is defined as  $(l-l_0)/l_0$  (\*100%). In literature, also the true strain is used, defined as the natural log of the ratio of the stretch. Quantities that are extracted from the stress-strain curves are the Young's modulus  $E$ , defined as the slope of the linear portion of the curve, the ultimate tensile strength (UTS) and the elongation at break. These measures, however, do not include all the information that is held in a stress-strain curve. The Young's modulus is extracted from the linear portion of the curve at relatively high strain levels. In this region the behavior is dominated by the collagen in the vessel which, *in vivo*, prevents vessel rupture and provides the majority of the tensile support at superphysiological pressures. Elastin, another important matrix component, acts in the physiological range and provides, *in vivo*, the necessary resilience to recover from deformations associated with pulsatile flow. Information about this behavior can be recovered from the shape of the stress-strain curves at low stresses, i.e. the physiological working range of the vessel. By supplying only measures like  $E$  and UTS (Schmidt, 2005; Opitz, 2004), without showing the actual curves, this information is lost.

In addition to uniaxial tensile testing, Berglund and co-workers (2004) used stepwise stress relaxation tests to elucidate the viscoelastic behavior of TE vascular grafts. Using this approach, it was demonstrated that the viscoelastic properties of collagen-based constructs improved with the addition of an elastin scaffold. In another study by these investigators (Berglund, 2005), collagen-based constructs were combined with 2 types of acellular supports. Creep and relaxation tests showed that constructs with an untreated dehydrated collagen support exhibited viscoelastic properties that were close to those of native arteries. Ogle and co-workers (2002) also investigated the mechanical properties in greater detail. Collagen based TE vessels, which were treated with vitamin A and/or C, were tested by constant strain rate tests, step strain tests and sinusoidal strain tests. To characterize the compliance, the UTS, rate of relaxation and elastic efficiency were measured. The latter was defined as the ratio of the areas under the stress-strain curve during unloading and loading. The central finding of the study was that constructs treated with vitamin A and C exhibited mechanical properties that, in terms of strength and elasticity, more closely mimicked those of native vessels than their untreated counterparts.

### **Burst pressure / compliance**

Measures of tensile stresses can be used to estimate the pressure-strain relationship, and the corresponding burst strength, using thin wall assumptions and Laplace's relationship. The starting point is Hooke's law. In case of uniaxial stress tests, this law reads:

$$\sigma_{\text{uniaxial stress}} = E \varepsilon \quad (3.2)$$

where E is the Young's modulus and  $\varepsilon$  the strain  $(l-l_0)/l_0$ . For the purpose of burst pressure experiments, the construct is fixated in axial direction. Hooke's law under these plane strain conditions reads:

$$\sigma_{\text{plane strain}} = \frac{E}{1-\nu^2} \varepsilon \quad (3.3)$$

where  $\nu$  is the Poisson ratio, which equals 0.5 in case of incompressibility. Laplace's relationship, which couples the pressure to the wall stress, reads:

$$P r = \sigma_{\text{cauchy}} h \quad (3.4)$$

where P is the pressure, r the radius and h the wall thickness. Combination of (3.1)-(3.4) gives a relationship between the pressure P and the measured stress in a tensile test:

$$P = \frac{\sigma_{\text{tensile}} h_0}{(1-\nu^2) \lambda r_0} \quad (3.5)$$

where  $\sigma_{\text{tensile}}$  is defined as the engineering stress measured in a uniaxial tensile test,  $h_0$  the initial wall thickness,  $\lambda$  the stretch  $l/l_0$  and  $r_0$  the initial radius. This relationship is valid under thin wall and incompressibility assumptions.

Berglund and co-workers (2003) used a similar approach to estimate the burst pressures of collagen/elastin based constructs. In another study the same investigators (Berglund

2004) performed burst pressure measurements by inflating tubular constructs to failure. To this end the constructs were submerged in saline buffer and filled with saline at a constant flow rate, while simultaneously measuring the luminal pressure. Besides burst pressure measurements, Niklason (2001) also measured dynamic compliance and static compliance. Changes in external vessel diameter were measured over a range of static and pulsatile pressures from 0 to 200mmHg. The compliance was calculated from systolic and diastolic diameters and pressures. In addition to the compliance and burst pressure, also the suture retention strength of tissue-engineered constructs, which is a critical measure in surgical handling, was measured by several investigators (Hoerstrup, 2001; Prabhakar, 2003). These measurements were performed by fixing one end of the specimen to a tensile tester, while the other end was connected to a clamp by a suture material. A tensile force was applied until the constructs were torn off and the construct rupture stress was recorded.

In conclusion, to characterize and analyze TE blood vessels, many measurement methods can be applied. Histology and biochemical assays provide general information about the tissue content and structure. Mechanical testing of tubular constructs should include tensile tests, burst pressure experiments and measurements of compliance and suture retention strength.

Using a selection of the above described characterization methods, the present study describes the culture of 3 different tubular constructs, which resulted from the scaffold concepts described in chapter 2. The constructs were seeded with myofibroblasts isolated from human saphenous veins (HVSC). These cells were used as they show good in-vitro tissue generation and are easily obtainable and therefore suitable for human tissue engineering applications (Schnell, 2001). The tubular constructs were cultured for 4 weeks under static conditions. The tissue morphology was investigated by histology using toluidine blue and Masson's trichrome stains. Tissue properties were quantified by biochemical assays measuring DNA, GAG and hydroxyproline. To study the mechanical properties of the static cultured tubular constructs, the properties were, in a first approach, measured in two directions by uniaxial tensile tests, in circumferential direction as ring samples and in axial direction as strip samples. To investigate the influence of the tubular geometry on the tissue development, also a strip construct was cultured and analyzed. Mechanical properties were measured along the long and short axis of the strip.

## **3.2 Materials & Methods**

### **3.2.1 Materials**

Poly( $\epsilon$ -caprolactone) (PCL) with an average molecular weight of 80.000 was dissolved in 99.9% HPLC-grade chloroform at a concentration of 17.5% w/v respectively (Sigma, Aldrich, USA). Polyglycolic acid (PGA) sheets (thickness 1.0mm; specific gravity 69 mg/cm<sup>3</sup>; Cellon, Luxembourg) were coated with a thin layer of 1% w/v poly-4-hydroxybutyrate (P4HB) (Symetis Inc., Switzerland) dissolved in tetrahydrofuran (THF).

### 3.2.2 Constructs / 4 week static culture

One rectangular (45x10x1mm) and three different types of tubular constructs were manufactured based on the concepts described in chapter 2. The constructs were all based on PGA coated with P4HB. The rectangular and one type of tubular construct consisted of PGA/P4HB only. The P4HB coating on the PGA construct was mainly located at the outside of the tube as was shown in chapter 2 (Fig 2.5). Therefore, for comparison, also the rectangular construct was coated from one side only. The two other types of tubular constructs consisted of PGA/P4HB in combination with electrospun PCL. One type was expanded with an inner PCL layer, the other with an outer PCL layer (Fig. 2.5).

From each type, three constructs were cultured for 4 weeks under static conditions as described in chapter 2. In short, sterile constructs were seeded with HVSC ( $30\text{-}40 \times 10^6$  cells/ml) using fibrin gel as a cell carrier. The constructs were placed in culture flasks and the fibrin gel was allowed to polymerize for 20 minutes in the incubator. Afterwards the flasks were filled with 25 ml of TE medium consisting of DMEM Advanced (Gibco, USA), supplemented with 10% fetal bovine serum (FBS; Biochrom, Germany), 1% Glutamax (Gibco, USA), 0.3% gentamycin (Biochrom, Germany) and 0.25mg/ml L-ascorbic acid 2-phosphate (Sigma, USA). All constructs were kept in the incubator during the next 4 weeks. After this culture period the constructs were first photographed in order to evaluate their macroscopic appearance. Afterwards the constructs were analyzed histologically, by mechanical testing and via biochemical assays, as described below. To this end 2 rings were cut from the middle of the tubes for histology, while 3 other rings and 3 strips were cut for circumferential and axial tensile tests as depicted in Fig 3.1. Afterwards, the mechanically tested tissue was analyzed by means of biochemical assays in which the amounts of DNA, GAG and hydroxyproline were measured.

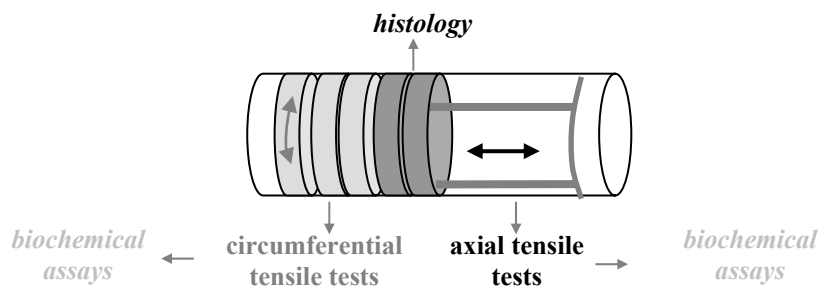


Fig. 3.1: Characterization of the tubular constructs by histology, mechanical testing in two directions and biochemical assays.

### 3.2.3 Histology

From each construct two rings were fixed in 4% phosphate-buffered formalin. One ring was embedded in Technovit 7100 (Kulzer, Klinipath, the Netherlands) and one in paraffin. The constructs containing electrospun PCL could not be embedded in paraffin

because the PCL melted during the embedding process. Sections of 5 and 10 $\mu\text{m}$  thickness, respectively, were cut from both samples. The Technovit sections were stained with toluidine blue for general tissue morphology. From these slices the average inner diameter and wall thickness of the tubular constructs was determined. The paraffin sections were stained with Masson's trichrome to visualize collagen. As a reference for the construct dimensions, non-seeded PGA/P4HB scaffolds ( $n=3$ ) were embedded in Technovit. From sections of these constructs initial values of the wall thickness and diameter could be determined.

### 3.2.4 Mechanical testing

Of each tubular construct, three rings were tested circumferentially while three strips were tested axially (Fig.3.1, 3.2). The rectangular constructs were tested in the direction of the short and long axis. Tensile tests were performed using an uniaxial tensile tester (custom-built, equipped with a load cell of 20N) at a constant strain rate of the initial length/min. The engineering stress was calculated as the measured force  $F$  divided by  $2*d*h$  for circumferential tests and  $b*h$  for axial tests (Fig. 3.2). In the first case the initial length was equalized to  $\pi r$ . In case of the axial tests the initial length was fixed at 6mm. The averaged values of  $b$  and  $d$  were 2-3mm. From the stress-strain curves, the ultimate tensile strength (UTS) was determined, as well as the elongation at break as a percentage of the initial length. The Young's modulus ( $E$ ) was defined as the slope of the linear portion of the curve.

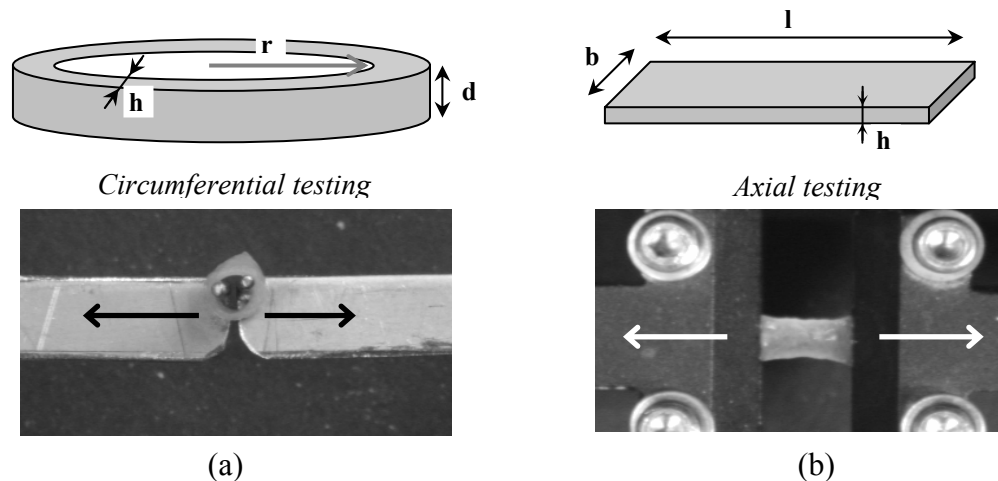


Figure 3.2: Mechanical testing in circumferential (a) and axial direction (b).  $r$  is the radius of the construct,  $h$  the wall thickness,  $d$  the thickness of the ring and  $l$  and  $b$  the length and width of the strip.

To validate the two measurement protocols and to confirm that both tests provided the same results when applied to identical samples, electrospun PCL tubes ( $r=1.5\text{mm}$ ,  $h=0.2\text{mm}$ ) and silicone tubing ( $r=1\text{mm}$ ,  $h=0.25\text{mm}$ ) were tested as rings and as strips that were cut in circumferential direction. These two materials were chosen because the Young's moduli were estimated to be in the same order of magnitude as the moduli of

the TE constructs. In case of the circumferential tests the constructs were lubricated with a soap solution to decrease the friction. In this way the surface of the test samples mimicked the low-friction surface properties of tissue. The stress-strain curves and resulting Young's moduli and UTS were compared.

### 3.2.5 Biochemical assays

Tissue formation was analyzed quantitatively by biochemical assays for DNA, GAG and hydroxyproline. The amounts of DNA, GAG and hydroxyproline were expressed as  $\mu\text{g}$  per mg dry weight. It was not possible to compare the constructs with and without a PCL layer as the final constructs included different amounts of remaining scaffold material. The amounts of GAG and hydroxyproline were also normalized for the amount of DNA. In this way information was gained about the extracellular matrix synthesis by the cells. In addition, it enabled comparison between the different scaffold constructs as this result was not affected by the amount of remaining scaffold material.

#### DNA/GAG assay

To determine the amount of DNA and GAG in the tissue samples (about 2-3 mg dry weight), the samples were digested in papain solution (100mM phosphate buffer, 5mM L-cystein, 5mM EDTA and 125-140  $\mu\text{g}$  papain per ml) at 60°C overnight. The samples were centrifuged after digestion. One part of the supernatant was used for the DNA assay and one part was used for the GAG assay. The amount of DNA was determined using the Hoechst dye method (Cesarone, 1979). The samples were diluted in TE buffer (10mM Tris, 1mM EDTA, pH 7.4) and 100 $\mu\text{l}$  was pipetted into a black 96-wells plate (Corning, USA) in duplo. A similar amount of working solution containing the Hoechst dye (10mM Tris, 1mM EDTA, 2M NaCl and 2.5 $\mu\text{g}$  Hoechst dye per ml) was added to each well. The plate was incubated at room temperature for 10 minutes, protected from light, to allow binding of the Hoechst dye to the DNA. Subsequently, the fluorescence was measured (excitation: 355nm, emission 460nm). The amount of DNA in the samples was determined from a standard curve prepared from calf thymus DNA (Sigma, USA). The GAG content was determined using a modification of the assay described by Farndale et al (1986). Briefly, 40 $\mu\text{l}$  of each sample was pipetted in duplo into a flat bottom 96 wells plate. 150 $\mu\text{l}$  of DMMB color reagents (46 $\mu\text{M}$  dimethylmethylene blue, 40.5mM glycin, 40.5mM NaCl, pH 3.0) was added to each well and the plate was gently shaken. The absorbencies at 540 and 595 nm were read within 5 to 10 minutes before precipitation occurred and subtracted from each other. The amount of GAG in the samples was determined from a standard curve prepared from chondroitin sulphate from shark cartilage (Sigma, USA).

#### Hydroxyproline assay

For the hydroxyproline assay, a modified version of the protocol provided by Huszar et al. (1980) was followed. The tissue samples (about 2-3 mg dry weight) were hydrolyzed in 4M NaOH (Fluka, USA) for 10 minutes at 120°C. The hydrolyzed samples were subsequently neutralized by addition of a similar amount of 1.4M citric acid (Fluka,

USA). Chloramin-T (62mM) was added to the supernatant and the samples were allowed to oxidize for 25 minutes at room temperature. For color development, aldehyde/ perchloric acid solution (1M) was added and the samples were incubated for 15 minutes at 65°C. The absorbency was read at 550nm. The amount of hydroxyproline in the samples was determined from a standard curve prepared from trans-4-hydroxyproline (Sigma, USA).

### 3.2.6 Statistics

All quantitative data were averaged per construct, 2-3 samples per tube, subsequently averaged per group, i.e. per different scaffold type, and represented as the average value of each group  $\pm$  the standard error of the mean. Comparisons between groups were performed by one-way ANOVA, assuming equal variances, using Bonferroni post-hoc tests (STATGRAPHICS Plus 15.0.04, Statistical Graphics Corp., USA) to determine significant differences ( $p < 0.05$ ). For the uniaxial tensile tests, two-tailed student t-tests were used to elucidate differences between the properties in axial and circumferential direction within each group.

## 3.3 Results

### 3.3.1 Histology

Figure 3.3 shows the macroscopic photographs and histological slides of the 4-week cultured constructs. The strip of PGA/P4HB (Fig. 3.3a), which could compact freely throughout the culture period, showed distinct compaction. Also in the tubular PGA/P4HB construct compaction was visible, although less pronounced. After a 4-week culture period the decrease in diameter of these constructs was 27% on average, as derived from histology. In the constructs with a layer of electrospun PCL (Fig. 3.3c,d) no compaction was visible. Toluidine blue staining of the constructs, which was already partly shown in Fig. 2.7, revealed homogeneous cell distribution in constructs of PGA/P4HB (Fig. 3.3a, b) and in the construct with an outer PCL layer (Fig. 3.3d). In case of the construct with an inner layer of PCL, cells were mainly present in the PGA/P4HB and only penetrated marginally into the electrospun PCL. In the PGA/P4HB strip, the tissue was most dense at the inner side of the compacted strip. This was confirmed by the Masson's trichrome staining, showing only collagen at this site. The collagen distribution in the tubular construct was more homogeneous, but most pronounced at the outside of the construct. The toluidine blue stained sections were used to quantify the wall thickness and, in case of the tubular constructs, the inner diameter, the results of which are shown in Fig. 3.6a. The initial value of the wall thickness and inner diameter of the PGA/P4HB construct is depicted as a dashed line. The decrease in wall thickness and, more pronounced, in the diameter confirms the compaction of the PGA/P4HB constructs.



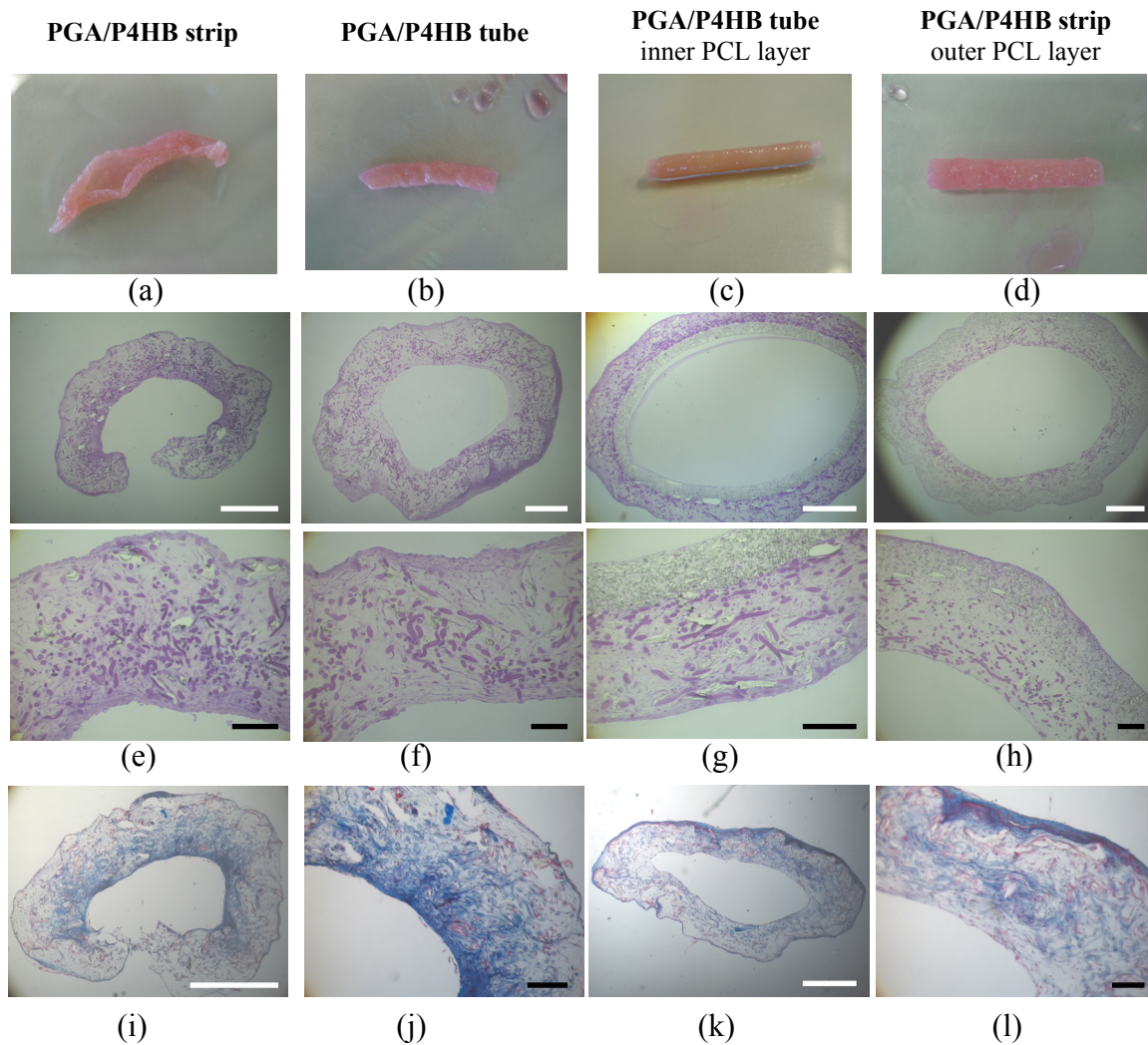


Figure 3.3: Macroscopic appearance and histology of 4-week cultured constructs: strip of PGA/P4HB, tube of PGA/P4HB, tube of PGA/P4HB with inner and outer PCL layer. Photographs visualize the compaction of the PGA/P4HB constructs (a,b). Toluidine blue staining of constructs, i.e., in overview and detail images, is shown in figures e-h. Masson's trichrome staining of the strip (i,j) and the tubular (k,l) PGA/P4HB construct visualizes collagen in blue. The white bars indicate 1mm, the black bars indicate 200µm.

### 3.3.2 Mechanical properties

#### Validation test

Figure 3.4 shows the results of the validation tensile tests on ring and strip samples of silicone tubing and electrospun PCL tubes. The stress-strain curves resulting from the ring and strip measurements were very similar. Some deviations occurred at very low strains. In circumferential tests, due to remaining friction forces, the stress slightly increased before the samples were actually strained. Based upon the measurements on electrospun PCL, the error in the elongation at break was in the order of a few percent. This deviation did not affect the Young's modulus or UTS. The resulting Young's moduli of the silicone tubing were  $E_{\text{ring}}=1.61\pm 0.06\text{MPa}$  and  $E_{\text{strip}}=1.63\pm 0.10\text{MPa}$ . The

Young's moduli and UTS for the electrospun PCL samples were  $E_{\text{ring}}=3.6\pm 0.4\text{MPa}$ ,  $E_{\text{strip}}=3.5\pm 0.8\text{MPa}$ ,  $UTS_{\text{ring}}=1.6\pm 0.3\text{MPa}$  and  $UTS_{\text{strip}}=1.7\pm 0.2\text{MPa}$ , respectively. No significant differences were found between E and UTS for the ring versus strip samples.

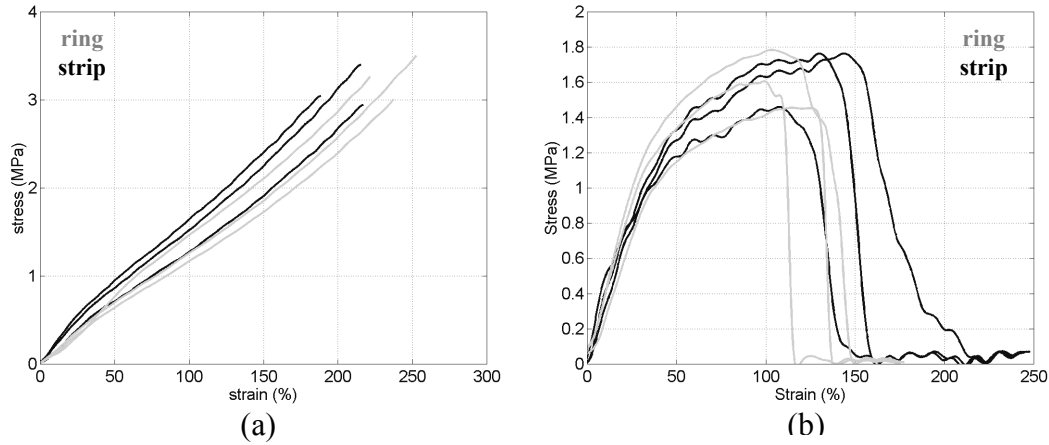


Figure 3.4: Stress strain curves of silicone tubing (a) and electrospun PCL (b) measured as ring (grey curves) and strip (black curves) samples.

### Tissue engineered constructs

Representative stress-strain curves of the four types of engineered constructs are shown in Fig. 3.5. These curves show the mechanical behavior of all constructs in circumferential and axial direction. In case of the rectangular constructs, this refers to the short and long axis. Averaged values of the various parameters, derived from these stress-strain curves, i.e. E, UTS and the elongation at break are depicted in Fig. 3.6. The stress-strain curves of the cultured rectangular samples showed a difference in mechanical behavior between both directions, quantified by a higher modulus and UTS in the axial direction ( $p<0.01$  and  $p<0.05$ , respectively). This was also the case for the PGA/P4HB tubular constructs ( $p<0.01$ ). The most striking difference between the stress-strain curves of the rectangles and the tubes (Fig. 3.5a,b), is the high value of the elongation at break in circumferential direction of the tubular construct. The stress-strain curves of the constructs with inner electrospun PCL layer (Fig. 3.5c) mainly display the behavior of the PCL layer as the stress immediately increases at low strain levels, comparable to the behavior of pure electrospun PCL as shown in Fig. 2.8b. At higher strains the constructs showed yielding. During the tensile tests the constructs did not fail. Therefore, instead of the elongation at break, the strain at the yield point, i.e. the starting point of plastic deformation, is depicted in Fig. 3.6d. The constructs with an outer electrospun PCL layer show a combination of the behavior of the cultured tissue and the PCL. At low strain values, the curves show resemblance to the curves of the PGA/P4HB construct without a PCL layer, although the Young's modulus is significantly higher. At higher strain values the PCL takes over, the constructs did not break during the tensile tests but could be stretched over 100%. This behavior, i.e., the PCL taking over at higher strains, was confirmed at visual inspection of the constructs during the tensile tests. At a certain strain-level the PGA/P4HB part of the construct broke and only the PCL part was further stretched.

It must be emphasized that the properties of the inner and outer PCL layer were not the same, as was already illustrated in chapter 2 (Fig. 2.5). The inner PCL layer consisted of a separate dense electrospun tube, whereas the outer layer was spun as a far more open structure, on top of the PGA/P4HB construct.

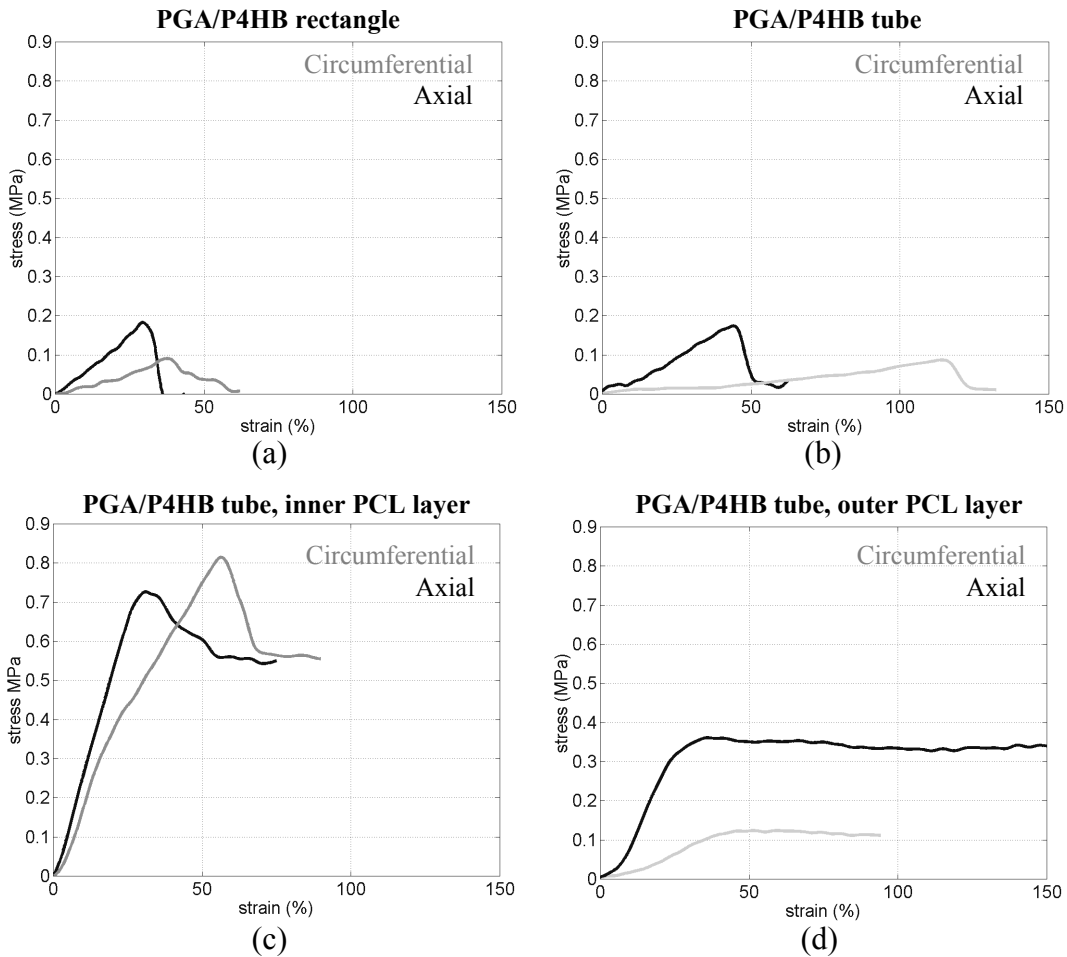


Figure 3.5: Representative *stress-strain* curves for 4-week static culture of the *PGA/P4HB* rectangle (a), the *PGA/P4HB* tube (b), the *PGA/P4Hb* tube with inner(c) and outer (d) PCL layer. Black curves result from tensile tests in axial direction, grey curves refer to circumferential testing. In case of the rectangular construct, this refers to the long and short axis.

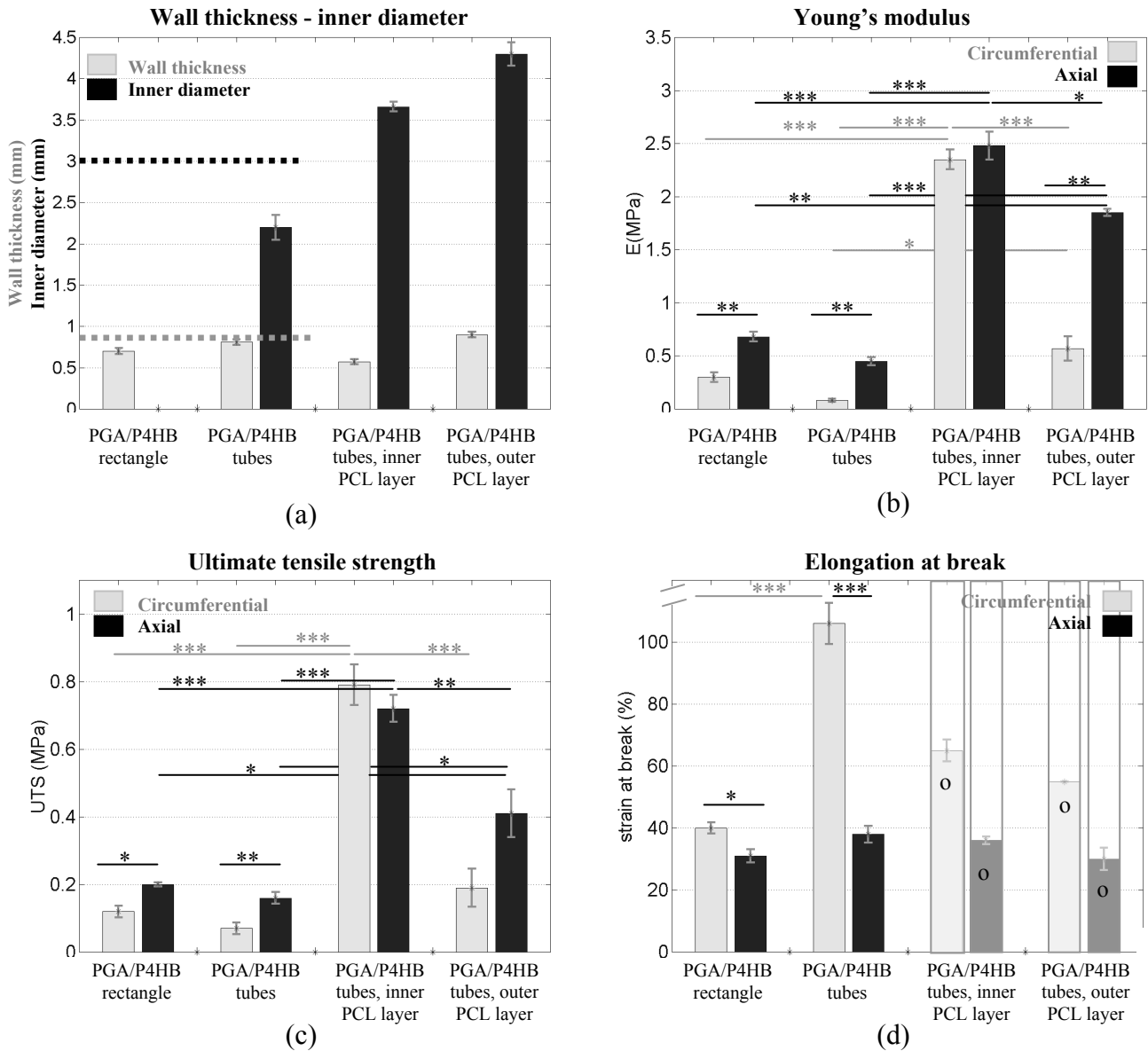


Figure 3.6: Geometry and mechanical properties constructs after a 4-week static culture period: wall thickness and diameter (a), Young's modulus (b), ultimate tensile strength (c) and elongation at break (d). In case of the rectangular constructs, circumferential and axial refer to the short axis and long axis, respectively. In case of the constructs with a PCL layer, instead of the elongation at break, the strains at the yield point, i.e. the strain at the starting point of plastic deformation, are depicted (o). The dashed lines in figure a, which only apply to the PGA/P4HB rectangles and tubes, indicate the initial wall thickness and diameter of the PGA/P4HB constructs, respectively. Data are presented as mean values  $\pm$  standard error of mean (\* represents  $p < 0.05$ , \*\* represents  $p < 0.01$ , \*\*\* represents  $p < 0.001$ ).

### 3.3.3 Biochemical assays

An overview of the amount of DNA, GAG, and hydroxyproline for all constructs is shown in Fig. 3.7. The amounts per dry weight (Fig. 3.7a) can only be compared between groups with the same scaffold composition, i.e. the rectangle and the tube of

PGA/P4HB. The relative amounts of scaffold material in both constructs with PCL layer are different. No comparison can be made between these two constructs. Tubes of PGA/P4HB contained more DNA than the rectangles ( $p < 0.05$ ). There were no significant differences between the amounts of GAG and hydroxyproline.

The values per  $\mu\text{g}$  DNA allowed comparison between all four groups (Fig. 3.7b). There were no significant differences in the amounts of GAG and hydroxyproline, meaning that the cells in all static cultured

constructs synthesized approximately the same amount of matrix, independent of the scaffold structure.

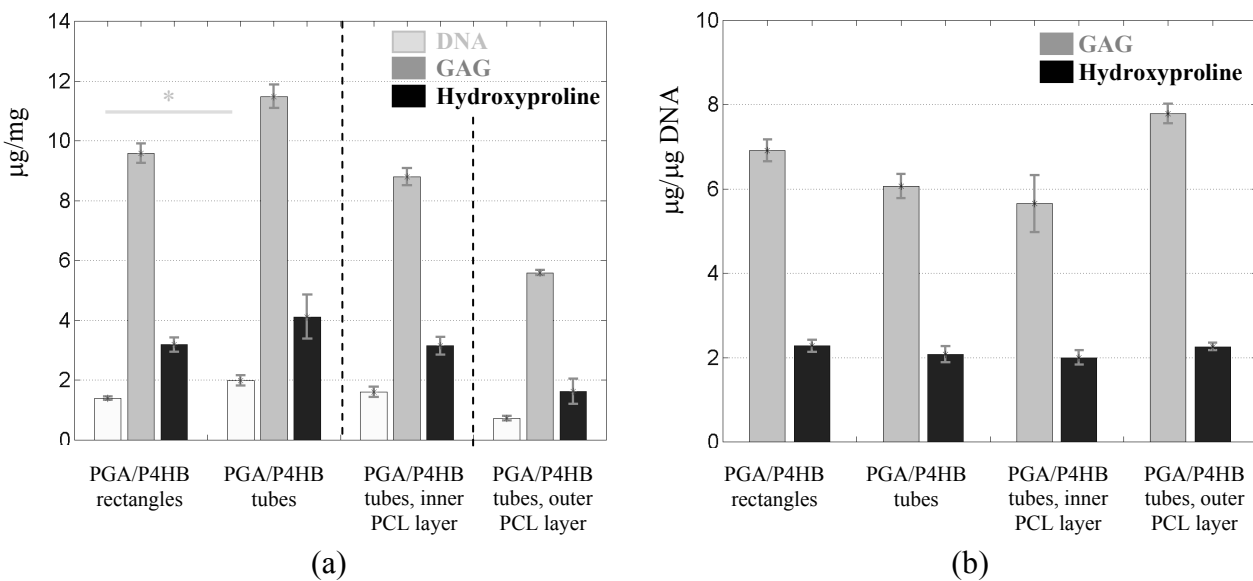


Fig. 3.7: The amount of DNA, GAG, and hydroxyproline per dry weight (a) and per  $\mu\text{g}$  DNA (b) in the static cultured constructs. Data are presented as mean values  $\pm$  sem (\* represents  $p < 0.05$ ). The dashed lines in figure a indicate that only the PGA/P4HB strips and tubes can be compared with each other, the other constructs contain different amounts of remaining scaffold material.

### 3.4 Discussion

In this study various methods for the characterization of TE blood vessels were reviewed. A distinction was made between the tissue content and the mechanical properties. In addition, static cultures of different tubular TE constructs were analyzed using these methods. On the basis of tissue development and mechanical properties, a scaffold type is selected for future studies, as described below.

Histology and biochemical assays, for e.g., DNA, hydroxyproline and GAG, are, in a first approach, reliable methods to characterize the tissue and its biochemical contents. For a more detailed study, biological functionality tests, immunostaining for e.g., SMC-specific proteins, determination of phenotype, genetic profiling, blood performance or measurements of matrix metalloproteinases can be useful. Mechanical properties of TE constructs are often characterized by a Young's modulus and ultimate tensile strength

(UTS) resulting from uniaxial tensile tests. These measures, extended with a representative stress-strain curve, are sufficient to compare different scaffold concepts, as described in this study. However, to evaluate the mechanical behavior and functionality of TE blood vessels in more detail, more data and more elaborate measurement protocols will be necessary. This should include the whole range of measured stress-strain curves, measurements of compliance, burst pressure and suture retention strength. In addition, measurements should be performed to assess the visco-elastic behavior of the artificial grafts.

In this study, tubular constructs of different scaffold composition were cultured for 4 weeks under static conditions. No significant differences in the amount of tissue, i.e. the number of cells and ECM protein, were found between the PGA/P4HB constructs with or without an electrospun PCL layer. However, the cell and tissue distribution in the constructs with an inner PCL was not homogeneous, i.e. the cells were mainly present in the PGA/P4HB part.

The stress-strain curves of the various constructs showed distinct differences depending on the remaining scaffold material. In case of PGA/P4HB constructs, the scaffold material did not contribute to the mechanical properties. This was illustrated in chapter 2 (Fig. 2.8), which showed that the properties of this scaffold material already declined drastically after 11 days. Therefore, it can be concluded that the mechanical properties of these constructs are solely determined by the cultured tissue itself. On the other hand, the stress-strain curves of the constructs with a PCL layer clearly demonstrated the contribution of this layer. The Young's moduli and UTS were significantly higher compared to the constructs of PGA/P4HB only. In constructs with an inner PCL layer the mechanical behavior was dominated by PCL, illustrated by stiff and non-compliant behavior. Constructs with an outer PCL layer showed a combination of the behavior of the cultured tissue and the PCL. The contribution of the two PCL layers was different as they had a distinctly different structure, as was shown in chapter 2 (Fig. 2.5).

The selection of the most promising scaffold concept has to be based on several aspects. Artificial grafts should have appropriate mechanical properties, at least in terms of stiffness and strength. In addition, cells should be distributed homogeneously and produce acceptable amounts of extracellular matrix proteins. Furthermore, in the ideal case, there is no remaining scaffold material in the final construct. This excludes possible problems concerning the degradation products and the inflammatory potential of the material.

Applying these requirements to the proposed scaffold concepts it can be concluded that the PCL degrades slowly and, consequently, will be part of the graft much longer than the PGA/P4HB. The cells in all constructs produced comparable amounts of extracellular matrix. Furthermore, the mechanical properties, in terms of stiffness and strength, were better in the constructs with a PCL layer. However, it has been shown that mechanical conditioning of PGA/P4HB constructs can result in a large improvement of the mechanical properties (Mol, 2006). Aside from that, the same investigators emphasized the positive effect of internal static strain on tissue development. This strain develops when compaction of the tissue is counteracted by e.g., constraining the construct in a bioreactor. To some extent this effect was also visible in the statically cultured PGA/P4HB constructs in the present study. In the rectangular as well as in the tubular constructs the stiffness and strength, i.e., E and

UTS, were significant lower in the direction in which most compaction was visible. It is therefore hypothesized that the geometry allowed less compaction in the axial direction and thereby induced internal static strain. As such, the mechanical properties were increased in this direction in terms of a higher value of E and UTS. On the contrary, the constructs with a PCL layer showed hardly any compaction. Therefore it can be assumed that internal static strain will not develop in these constructs when attached in a bioreactor. It might be hypothesized that the PCL layer would induce static strain, as it resists the compaction of the PGA/P4HB part of the scaffold. However, this could not be confirmed because no differences in the amount of extracellular matrix were found when compared to the constructs without a PCL layer.

Based on the fast degradation of PGA/P4HB and the promising results of this material in TE heart valves (Mol, 2006), mechanical conditioning protocols will be applied, in a first approach, to the PGA/P4HB constructs only (chapter 4-6). The construct reinforced with an outer electrospun PCL layer might be a candidate when the strength of the TE constructs of PGA/P4HB will prove not to be sufficient. This scaffold exhibited a homogeneous cell and tissue distribution and tissue-like mechanical behavior. It should, however, be investigated if the PCL layer does not counteract the additional tissue formation due to mechanical conditioning.

# 4

## Axially strained tissue-engineered blood vessels



## 4.1 Introduction

Tissue-engineered constructs grown under static culture conditions often lack sufficient tissue development and, consequently, exhibit weak mechanical properties compared to those of native equivalents. Many studies have demonstrated that cell and tissue growth is enhanced in response to mechanical conditioning (Kim, 2000; Seliktar, 2003; Hoerstrup, 2002; Isenberg, 2003; Mol, 2003). To improve the mechanical properties of small diameter TE blood vessels, axial straining can be applied to condition tubular constructs, as it is known that axial strain is an important element in the growth of arteries during the embryonic vascular development. In addition, also adult human coronary arteries are, in contrast to other arteries, continuously subjected to a substantial axial strain of approximately 10% (Zilla, 1999). To study the effect of axial strain on arteries, Jackson and co-workers (2002) developed an in-vivo model in which axial strain in rabbit carotid arteries could be artificially elevated via a surgical procedure. It was found that by wall tissue remodeling, the strain was reduced within 3 days and completely normalized in 7 days. A substantial increase in DNA, elastin and collagen was recorded. These data indicate that axial strain of arteries is an important mechanical stimulus for accelerated cell proliferation, the production rate of the extracellular matrix, and vascular remodeling. These findings were confirmed in a study of Han (2003). Porcine carotid arteries were longitudinally stretched which promoted cell proliferation in the arteries. Meng and co-workers (1999) applied longitudinal stretch to human saphenous vein grafts, i.e. the cell source of the presented TE blood vessels. A large increase in the amount and activity of matrix metalloproteinases, which affect vascular remodeling, was found when compared to controls.

To test strain-induced vascular remodeling, Mironov and co-workers (2003) developed a bioreactor in which axial and circumferential strain could be applied. The capacity of the bioreactor to perform both strains was tested on silicone tubes and natural arteries. However, to our knowledge, no experiments have been reported regarding cultures of TE blood vessel constructs in such bioreactor. Therefore, to investigate the effect of axial straining on TE blood vessels, we developed a bioreactor in which tubular constructs were investigated. P4HB coated PGA constructs were seeded with human myofibroblasts, harvested from the saphenous vein (HVSC). These cells show good in-vitro tissue generation and are easily obtainable, making them suitable for human tissue engineering applications (Schnell, 2001). The constructs were subsequently cultured under static and dynamic axial strain conditions. The produced extracellular matrix and the mechanical properties of the strained constructs were compared to those of control constructs cultured without applied strain. A distinction was made between the mechanical properties in axial and circumferential direction.

## 4.2 Materials and Methods

### 4.2.1 Tubular constructs

Tubular scaffolds were produced as described in chapter 2 and 3. In short, a non-woven polyglycolic acid (PGA) sheet of 8\*0.5\*0.1cm was wrapped around a rod with a diameter of 3mm. The ends were fixed with suture and the construct was dip-coated in a 1w/v% poly-4-hydroxybutyrate (P4HB, Symetis Inc., Switzerland) in tetrahydrofuran (THF). After evaporation of the solvent, the tubular construct was removed from the rod. The scaffolds were further dried under vacuum overnight to remove solvent remnants. The length of the resulting tubes was approximately 3.5cm.

### 4.2.2 Bioreactor design

The axial straining device consists of 4 separate vented culture chambers made of polycarbonate (Fig 4.1). In each chamber one tubular construct can be secured to stainless steel tubes with sutures. One stainless steel tube per chamber is coupled to a rigid arm that is connected to a pneumatic drive (Festo, Germany). The amplitude of the

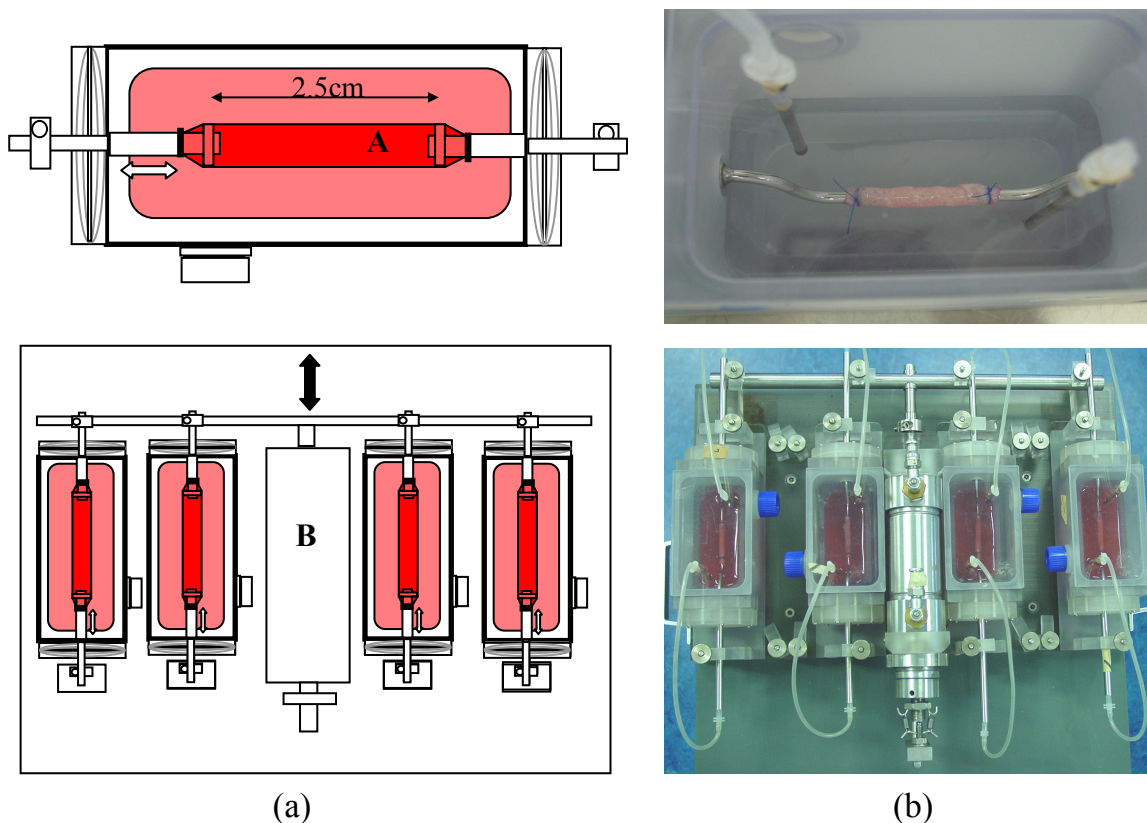


Figure 4.1: Schematic drawings (a) and photographs (b) of the axial straining device: constructs (A) are attached to stainless steel tubes, one of which is coupled to a rigid arm that is connected to a pneumatic drive (B) that can strain the constructs to various degrees, and at various frequencies. The construct chambers are filled with culture

pneumatic drive movement can be adjusted. All chambers can be sterilized in an autoclave. Sterility is maintained by silicone membranes. Through the stainless steel tubes a balloon catheter can be inserted inside the constructs. This catheter prevents leakage of the cell/fibrin solution into the lumen of the constructs during seeding. The stainless steel tubes can also be perfused, allowing the application of flow through the constructs during culture.

### **4.2.3 Cells / Seeding procedure**

Human venous myofibroblasts were harvested from the saphenous vein (HVSC) and expanded using regular culture methods (Schnell, 2001). The medium to culture these cells consisted of DMEM Advanced (Gibco, USA), supplemented with 10% fetal bovine serum (FBS; Biochrom, Germany), 1% Glutamax (Gibco, USA) and 0.1% gentamycin (Biochrom, Germany). The medium for seeding and subsequent tissue culture, referred to as TE-medium, contained 0.3% gentamycin and additional L-ascorbic acid 2-phosphate (0.25 mg/ml, Sigma, USA) to promote extracellular matrix production.

Tubular PGA constructs were mounted to the stainless steel tubes in the bioreactor and fixed by sutures. To prevent leakage of the cell/fibrin solution into the lumen of the tubes, a balloon catheter was inserted inside the tubes. The constructs were sterilized in the set-up by exposure to UV for 45 minutes and subsequent soaking in 70% ethanol for 3h. Afterwards the constructs were washed in phosphate-buffered saline (PBS) and placed in medium overnight. The seeding was performed per construct using fibrin as a cell carrier (Mol, 2005). The HVSC were suspended in a sterile thrombin solution (10 IU/ml medium; Sigma, USA). The cells-thrombin solution was mixed with an equal amount of sterile fibrinogen solution (10mg actual protein/ml medium; Sigma, USA). The total solution ( $20\text{-}30 \times 10^6$  cells/ml) was mixed with a pipette until the starting point of the polymerization process of the gel. Then the cell-fibrin solution was immediately dripped on the scaffold. Afterwards the balloon catheter was removed and the device was placed inside an incubator to allow the fibrin gel to further polymerize for 20 minutes. Afterwards the chambers were filled with 35ml of TE-medium, which was changed every 3 to 4 days.

### **4.2.4 Culture and mechanical conditioning**

After seeding, the constructs were statically cultured in the bioreactor (37° C, 5% CO<sub>2</sub>) during 1 week. Afterwards, one group (n=4) was cultured under the same conditions for another three weeks. It was manually checked that the constructs were minimally stretched. Another group of constructs (n=5) was exposed to 5% axial strain at 1Hz during the remaining 3 weeks. Control constructs (n=4) were put in culture flasks directly after seeding and cultured for 4 weeks without any applied strain.

#### 4.2.5 Evaluation of tissue formation

After 4 weeks of culture, TE constructs were evaluated by histology, mechanical testing and biochemical assays. To this end, 2 rings were cut from the middle of the tubes for histology, while 3 other rings and 3 strips were cut for circumferential and axial tensile tests as depicted in Fig. 4.2. The tissue that was used for mechanical testing was afterwards analyzed for their amounts of DNA, GAG and hydroxyproline.

##### Histology

Of each construct two rings were fixed in 4% phosphate-buffered formalin. One ring was embedded in Technovit (Kulzer, Klinipath, the Netherlands) and one in paraffin. Sections with a thickness of 5 and 10 $\mu$ m, respectively, were cut from both samples. The Technovit sections were stained with toluidine blue and analyzed for general tissue formation by light microscopy. Besides, these slices were also used to determine the inner diameter and the wall thickness of the constructs. When the cross-section of the tubes could not be measured due to flattening caused by the cutting of the ring segments, the inner circumference was approximated by an ellipse and the diameter was estimated as  $(\frac{1}{2}(a^2+b^2))^{1/2}$ , where a and b are the long and short axes of the ellipse. The paraffin sections were stained with Masson's trichrome stains to visualize collagen.

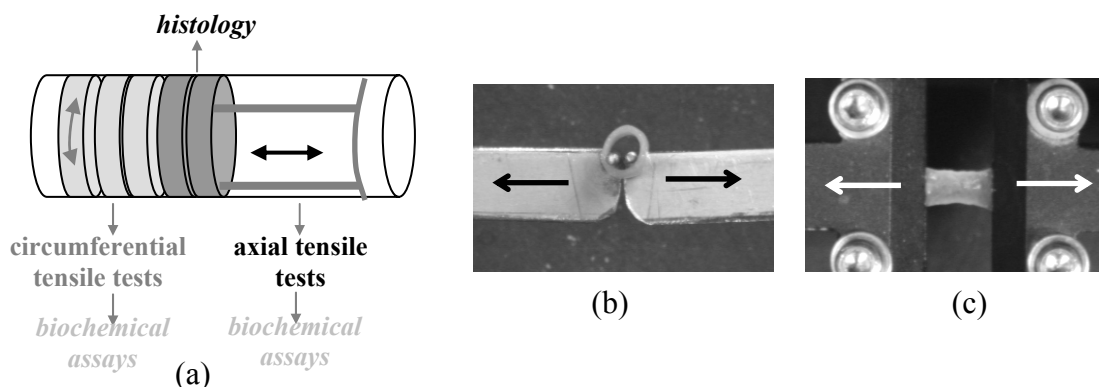


Figure 4.2: Characterization of TE constructs by histology, mechanical testing and biochemical assays(a). Mechanical tests were performed on ring samples in circumferential direction (b) and on strip samples in axial direction (c)

##### DNA/GAG assay

To determine the amount of DNA and GAG in the tissue, the samples (2-3 mg dry weight, n=3 per construct) were digested in papain solution (100mM phosphate buffer, 5mM L-cystein, 5mM EDTA and 125-140  $\mu$ g papain per ml) overnight at 60°C. The samples were centrifuged after digestion. The amount of DNA was determined using the Hoechst dye method (Cesarone, 1979) as described in chapter 3. The GAG content was measured using a dimethylmethylene blue (DMMB) spectrophotometric assay (Farndale, 1986), as described in chapter 3.

##### Hydroxyproline assay

Collagen content was assessed from the hydroxyproline content after acid hydrolysis in 4M NaOH for 10 minutes at 120°C and reaction with chloramine-T and

aldehyde/perchloric acid solution. A full description of the protocol is given in chapter 3.

### **Mechanical testing**

The mechanical properties of the engineered blood vessels were determined by uniaxial tensile tests in both circumferential and axial direction, as described in section 3.2.4. Of each construct 3 rings were tested for their circumferential characteristics while three strips were tested in the axial direction (Fig 4.2). Stress-strain curves were obtained using an uniaxial tensile tester (custom-built, equipped with a 20N load cell) and a constant strain rate of the initial length/min. From the engineering stress-strain curves, the ultimate tensile strength (UTS) was determined, as well as the elongation at break as a percentage of the initial length. The Young's modulus was calculated from the slope of the linear portion of the engineering stress-strain curve.

### **4.2.6 Statistics**

All quantitative data were averaged per construct (2-3 samples per tube), and subsequently averaged per group. Data are presented as the average value of each group  $\pm$  the standard error of the mean. Comparisons between groups were performed by one-way ANOVA, assuming equal variances, using Bonferroni post-hoc tests (STATGRAPHICS Plus 15.0.04, Statistical Graphics Corp., USA) to determine significant differences ( $p < 0.05$ ). For the uniaxial tensile tests, two-tailed student t-tests were used to elucidate differences between the properties in axial and circumferential direction within each group.

## 4.3 Results

### 4.3.1 Macroscopic appearance

Figure 4.3 shows photographs of the tubular constructs in the bioreactor immediately after seeding and after a 4-week culture period. After 4 weeks, the static control, i.e. the tubular construct cultured in a culture flask, as depicted in Fig. 3.3 (chapter 3) showed some compaction. Figure 4.3a shows the tubular construct immediately after the seeding protocol. The PGA/P4HB scaffold is filled with the cell/fibrin solution and therefore has a shiny appearance. The constructs cultured under static strain (Fig. 4.3b) show distinct compaction as illustrated by the significantly decreased vessel diameter. This effect is even more pronounced in the dynamically strained constructs (Fig. 4.3c). The compaction started to be visible 2½-3 weeks after seeding and gradually increased for the remaining culture period. The compaction was quantified by the values of the inner diameter and the wall thickness of the constructs, as determined from histological slides. The average decrease in inner diameter amounted to 28, 24 and 47% for the constructs cultured in a culture flask, and under static and dynamic strain conditions, respectively. For the wall thickness the corresponding decrease was 5, 32 and 35%, respectively (Fig 4.6a).

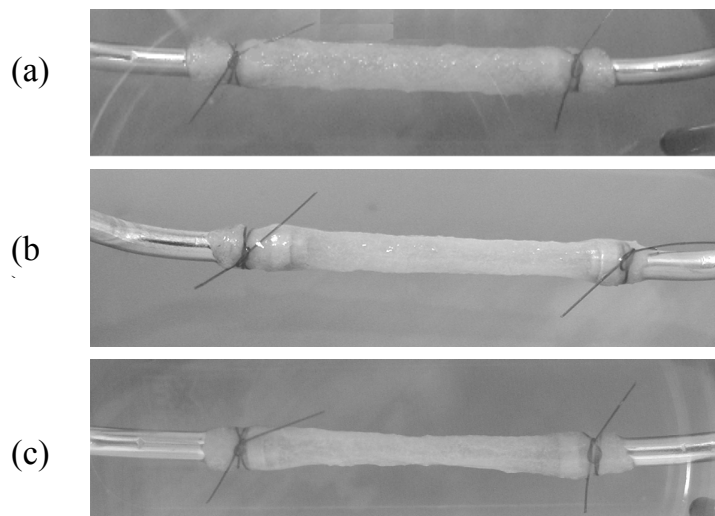


Figure 4.3: *Macroscopic appearance of tubular constructs in the bioreactor just after seeding (a) and after a 4-week culture period under static (b) or dynamic (c) strain conditions. Tissue compaction of the cultured constructs is visualized by the decrease in construct diameter.*

### 4.3.2 Histology

Histological slides stained with toluidine blue are depicted in Fig. 4.4. All constructs showed, to a certain extent, uniform cell and tissue distribution. At some locations, most clearly illustrated in Fig. 4.4a, a denser cell layer is present at the outer side. Both



strained constructs contained more tissue than the static control tubes. In addition, the statically strained construct showed denser tissue than the dynamically strained equivalents. Masson's trichrome staining revealed that the statically cultured control constructs contained collagen only at the outside layer of the tubular wall (Fig. 4.4g). The statically strained constructs showed a more dense and homogeneous distribution of collagen (Fig. 4.4h). The dynamically strained tubes showed more collagen than the static controls but the distribution was less homogeneous compared to the static strained constructs (Fig. 4.4i).

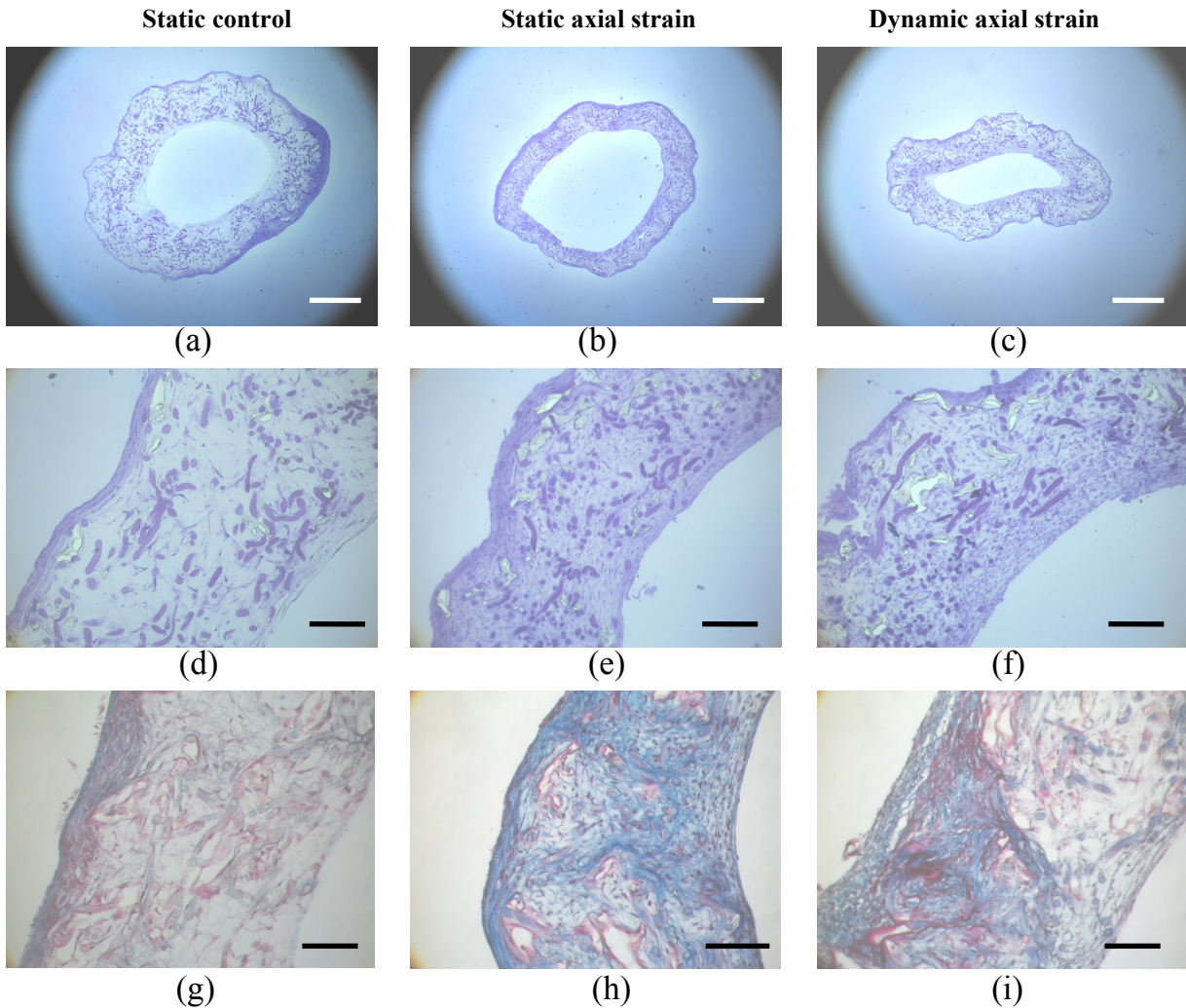


Figure 4.4: *Histological slides stained with toluidine blue (a-f) and Masson's trichrome (g-i) of 4 week statically cultured control constructs, statically strained and dynamically strained tubes. Both strained constructs show more dense tissue than the control constructs. The white bars indicate 1mm, the black bars indicate 200 $\mu$ m.*

### 4.3.3 Quantitative evaluation of tissue formation

An overview of the amount of DNA, GAG, and hydroxyproline in the different types of constructs is given in Fig. 4.5. The amount of DNA and GAG in the tubular constructs showed no differences between the static controls and both types of strained constructs.

The statically strained tubes contained significantly more hydroxyproline per dry weight and per DNA ( $p < 0.01$  and  $p < 0.05$  respectively) than the static controls. The dynamically strained did not contain more hydroxyproline than the static controls.

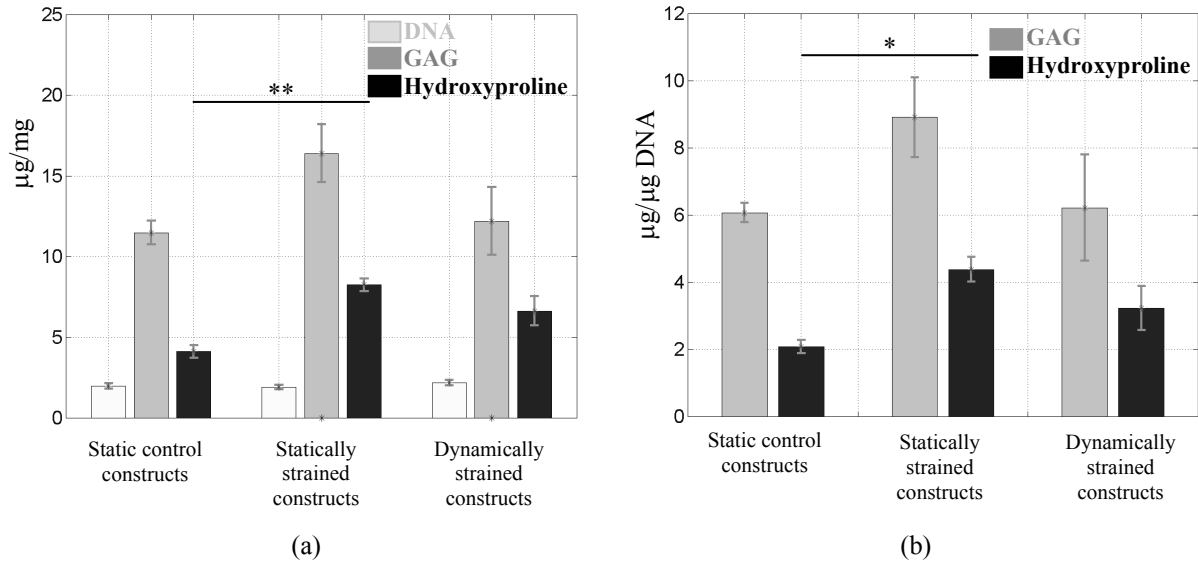


Figure 4.5: The amount of DNA, GAG and hydroxyproline per dry weight (a) and per DNA (b) in the tubular constructs after four weeks of culture, data are presented as mean  $\pm$  sem (\* represents  $p < 0.05$ , \*\* represents  $p < 0.01$ ).

#### 4.3.4 Mechanical testing

The mechanical properties of the cultured tubular constructs were assessed via uniaxial tensile tests in two directions. Figure 4.6 shows an overview of the measured stress-strain curves of the control and strained constructs. Both measurements in axial and circumferential direction are shown in each plot. The mean values of the derived parameters, i.e. E, UTS and the elongation at break, are given in Fig. 4.7. In all types of constructs the behavior in axial and circumferential direction was different. This was illustrated by a higher Young's modulus and UTS, and a lower elongation at break value in the axial direction, the significance levels are depicted in Fig. 4.7. The Young's moduli and the UTS in axial direction of both strained constructs were significantly higher ( $p < 0.005$  and  $p < 0.05$  respectively) than in the static controls. The Young's moduli and the UTS in circumferential direction of the static strained constructs were also significantly higher ( $p < 0.01$  and  $p < 0.05$ , respectively) than in the static controls. However, the properties of the dynamically strained constructs, in terms of Young's modulus and UTS, did not improve in this direction compared to the static controls. In addition, the properties in circumferential direction of these constructs varied to a large degree as illustrated by the grey stress-strain curves shown in Fig. 4.6c.



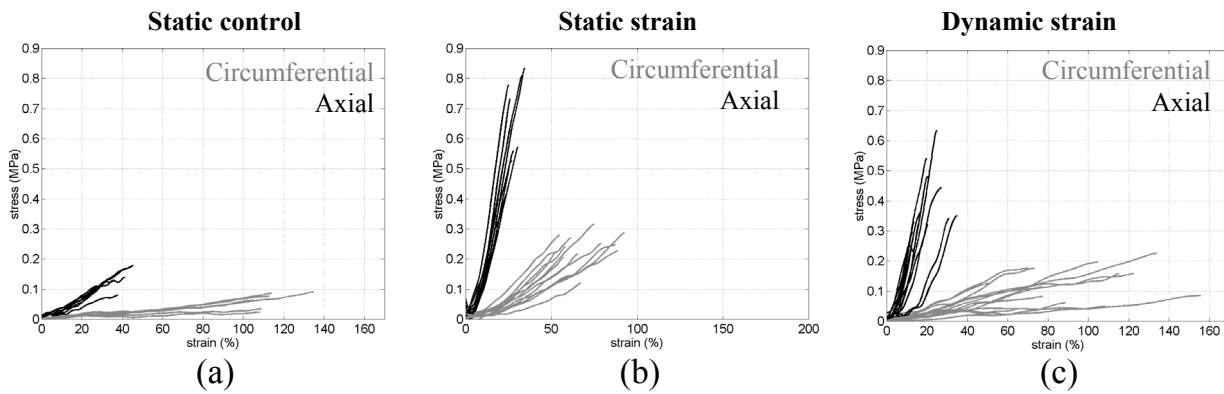


Figure 4.6: *Stress-strain curves of static control (a), statically strained (b) and dynamically strained constructs (c) in circumferential (grey) and axial (black) direction*

#### 4.4 Discussion

Coronary arteries are, in contrast to other arteries, continuously subjected to a substantial axial strain. Furthermore, several studies have demonstrated that axial strain, applied to arteries or veins, is an important mechanical stimulus for accelerated cell proliferation, production of extracellular matrix, and vascular remodeling (Jackson, 2002; Han, 2003; Meng, 1999). Therefore, in the present study, axial strain was used to stimulate the culture of tissue-engineered (TE) blood vessels. Tubular constructs of P4HB coated PGA were seeded with human saphenous vein cells in combination with fibrin gel. The constructs were cultured for 4 weeks under static or dynamic axial strain conditions. Static axial strain developed through fixation of the constructs in axial direction, thereby counteracting the compaction of the tissue in this direction. Both strained constructs contained more extracellular matrix than the control constructs, as illustrated by the higher amount of hydroxyproline. In addition, the mechanical properties in the direction of the applied strain, i.e. in axial direction, improved significantly in terms of a higher Young's modulus and UTS. In case of the static strained constructs, also the mechanical properties in circumferential direction improved. However, large differences existed between the properties in axial and circumferential direction. The Young's modulus and UTS of the static strained constructs were a factor 7.5 and 3, respectively, higher in axial direction compared to those in circumferential direction. Dynamic axial straining, compared to static axial straining did not further improve the properties, it even had a negative effect on the Young's modulus in circumferential direction.

It was found that the mechanical properties and the amounts of produced extracellular matrix varied largely within the separate groups. This was especially true in case of the strained constructs. It is believed that the amount of strain, i.e. static as well as dynamic, largely affects the outcome of the mechanical properties of TE constructs (Mol, 2003; Isenberg, 2003). Because the attachment of the constructs in the bioreactor and the determination of the zero-stress point were performed manually, it can be assumed that

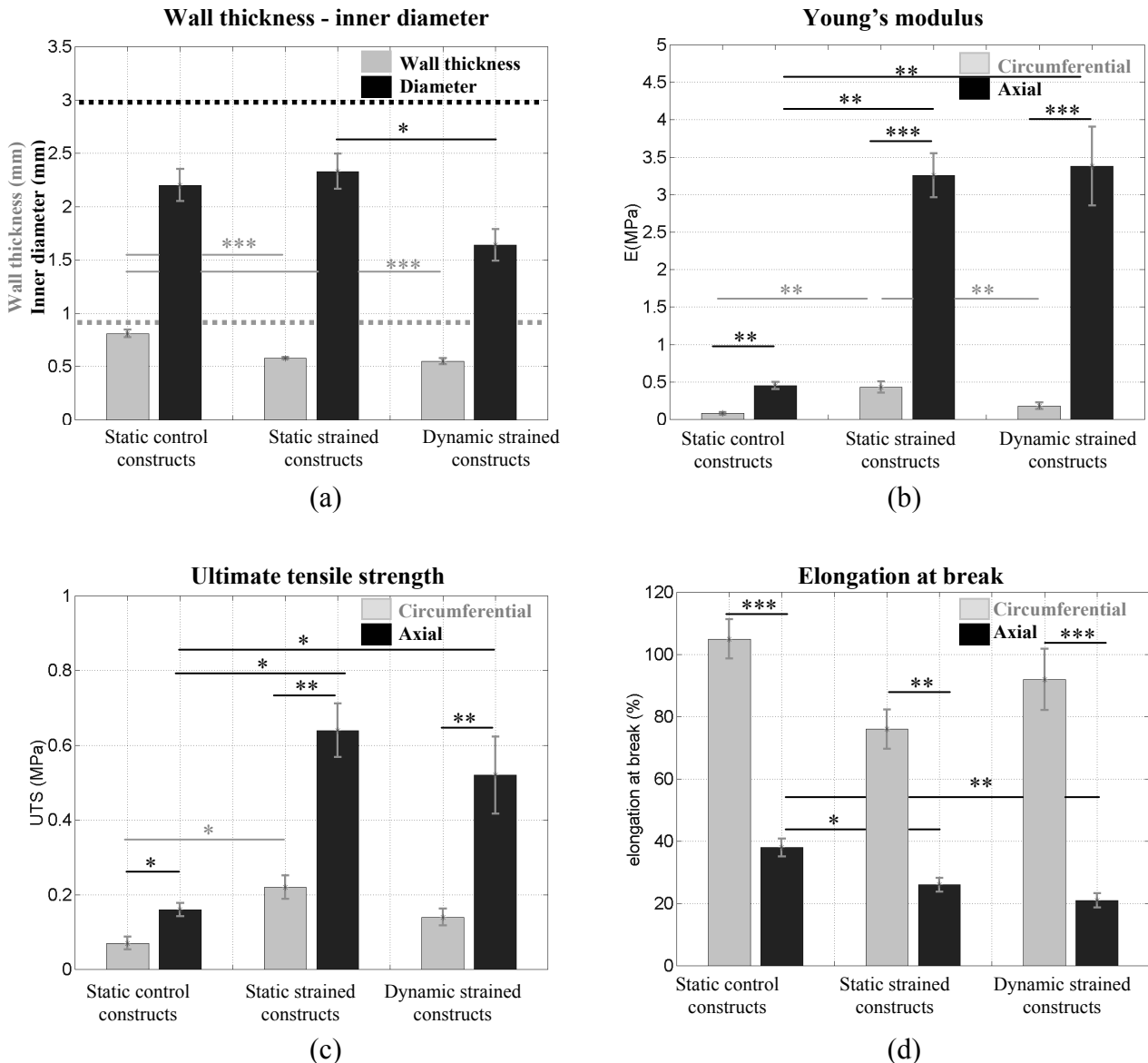


Figure 4.7: Geometrical and mechanical properties of static and axially strained constructs after a 4-week culture period: wall thickness and inner diameter (a), Young's modulus (b), UTS (c) and elongation at break (d), the latter three are given in axial as well as circumferential direction. The dashed lines in figure a indicate the initial wall thickness (grey) and inner diameter (black) of the PGA/P4HB constructs. Data are presented as mean  $\pm$  sem (\* represents  $p < 0.05$ , \*\* represents  $p < 0.01$ , \*\*\* represents  $p < 0.001$ ).

the large variations found are due to these less well controlled circumstances. In addition, strained constructs within one group were not cultured in one session. In these sessions different batches of fetal bovine serum (FBS) were used for the various cultures. These FBS batches resulted, as it subsequently appeared, in a distinct difference in the growth rate of the cells, and, likely, also in the matrix production of these cells. This might, besides the arguments mentioned above, contribute to relative large variations in the measured properties of the strained constructs.

It can be concluded that the effect of static axial strain, induced by counteracting the compaction of the tissue in this direction, has a positive effect on the tissue development and mechanical properties in axial direction of TE blood vessels. The additional effect of dynamic straining in this direction is limited or even negative. The mechanical properties in circumferential direction did also improve in the static strained constructs, in terms of stiffness and strength, although the constructs were much stronger in the axial direction. To further improve the properties in circumferential direction a bioreactor has to be developed that applies static axial strain in combination with circumferential strain. This bioreactor and the TE blood vessel constructs cultured in this device are described in chapter 5.

# 5

## Circumferentially strained tissue-engineered blood vessels

## 5.1. Introduction

The culture of tissue-engineered (TE) blood vessels that could ultimately be used for coronary artery bypass surgery is the subject of ongoing research. Investigators try to mimic the properties of native tissue by varying the scaffold material, the culture time, the cell source and the culture conditions. Circumferential straining of these constructs during culture is a widely applied conditioning protocol to optimize the properties of TE blood vessels. Differences exist in the applied methods, the levels of strain and the culture time. Circumferential strain levels of 1 and 5% were applied for 7/8 weeks by threading tubular PGA constructs over compliant silicone tubing (Niklason, 2001; Poh, 2005). A pulsatile flow through this tubing provided the circumferential straining. The same principle was used by Seliktar and co-workers (2003). These investigators applied a strain of 10% to their collagen-based tubular constructs for 4-8 days. Hoerstrup and co-workers (2001) directed the pulsed flow immediately through the vascular lumen, thereby generating direct shear stress to the luminal surface as well as periodical radial distension of the vessel wall. Using this method also strain levels of 5 and 10% were applied to tubular constructs (Jeong, 2004; Xu, 2005).

All these studies indicate that the mechanical conditioning of TE blood vessels by circumferential straining clearly improves the mechanical properties. However, as compared to constructs with human cells, better results, at least in terms of burst pressure, have been obtained in constructs cultured with cells from (young) animals. Therefore, it is plausible that the cell species and the age of the donor have a large influence on the outcome of the construct. Niklason harvested cells from bovine aorta, porcine carotid and human saphenous vein. Although the constructs seeded with bovine cells resulted in TE blood vessels with a burst pressure of  $2150 \pm 709$  mmHg (Niklason, 1999), equivalent constructs seeded with cells harvested from human saphenous veins had significantly lower burst pressures, i.e. in the order of 500 mmHg (Klinger, 2006). In addition, the results on these human TE blood vessels could only be obtained by using genetically modified human cells, i.e. telomerase-expressing SMC (Poh, 2005). This transfection increases the replicative capacity of the fibroblasts. However, under different circumstances, Mol and co-workers (2006) cultured strong TE heart valves with human saphenous vein myofibroblasts. As described and applied in chapter 4, the basis of such constructs was a P4HB coated PGA scaffold in combination with a fibrin gel. It can be postulated that the combination of the above scaffold material, conditioning protocol and human cells does indeed lead to strong tissue-engineered constructs. In order to test this hypothesis on tubular constructs, we used this approach in combination with circumferential strain to culture TE blood vessels. A bioreactor set-up was developed that allowed static axial straining as well as dynamic circumferential straining of tubular constructs. PGA/P4HB constructs were seeded with human saphenous vein cells, cultured for 4 weeks and afterwards analyzed by histology, immunohistochemistry, biochemical assays, and mechanical testing, including tensile tests and burst pressure measurements.

## **5.2. Materials and Methods**

### **5.2.1 Tubular constructs**

Blood vessel constructs were produced as described in chapter 2 and 3. In short, a non-woven PGA sheet (specific gravity 69mg/cm<sup>3</sup>; Cellon, Luxemburg) of 80\*5\*1mm was wrapped around a rod with a diameter of 3mm and dip-coated in a 1w/v% poly-4-hydroxybutyrate (P4HB, Symetis Inc., Switzerland) in tetrahydrofuran (THF). The scaffolds were dried under vacuum overnight to remove solvent remnants.

### **5.2.2 Cells / Seeding procedure**

Cells were cultured and seeded as described in section 4.2.3. Human myofibroblasts were harvested from the saphenous vein of two patients (age 65 and 47 years) and expanded using regular culture methods (Schnell, 2001) up to passage 7. Seeding of the cells was performed per construct using fibrin as a cell carrier. The cell containing fibrin gel (20-30\*10<sup>6</sup> cells/ml) was mixed with a pipette until the starting point of the polymerization process of the gel. The cell-fibrin solution was subsequently dripped on the scaffold and the bioreactors were placed inside an incubator to allow the fibrin gel to further polymerize for 20 minutes. The petridishes containing the constructs were filled with 20ml of TE medium. Every 3 to 4 days the medium was changed.

### **5.2.3 Bioreactor design**

The total bioreactor set-up (Fig. 5.1) consisted of a bioreactor (A) in which the tubular construct (B) was mounted, a pressure device (C) that generated pulsatile flow, and a syringe (D) that acted as a compliance. Silicone tubing (Rubber, the Netherlands) and polypropylene connectors (Neolab, Germany) connected the different parts, while check valves (Qosina, NY, USA) were fitted on either side of the pressure device. The bioreactor, which can be placed on top of a glass petridish, and the pressure device were made of polycarbonate (KUBRA kunststoffen, the Netherlands).

The pressure device consisted of a PBS containing silicone tube that was compressed and decompressed by air from a proportional pressure valve (Festo, Germany). The silicone rubber tube was coated with polyurethane to prevent leakage of air through the silicone rubber. As the pressure device was connected to two check valves, a unidirectional, pulsatile flow (1Hz) could be created. A teflon pipe with large punched holes was placed inside the coated silicone tube to prevent it from collapsing and not returning to its original state. A certain level of pressure was applied to the coated tube. The pressure inside the silicone tubing, and thereby the level of straining of the construct, was adjusted per construct by a clamp (F) on the silicone tubing behind the construct which served as a resistance.

To enable measurements of the pressure inside the silicone tubing, at the location of the tubular constructs, a pressure sensor was connected to a pressure measurement dome

(Beckton Dickinson, Belgium) which was located just before the construct. During culture the bioreactors could be placed on top of an inverted microscope to visualize straining of the construct. The separate parts of the set-up were autoclaved before use. Afterwards, tubular TE constructs were placed over silicone tubing and mounted in the bioreactor (Fig. 5c-e). The construct was sterilized in the set-up by exposing it to UV for 45 minutes and subsequent soaking in 70% alcohol for 3h. Subsequently the constructs were washed in phosphate-buffered saline (PBS) and placed in medium overnight.

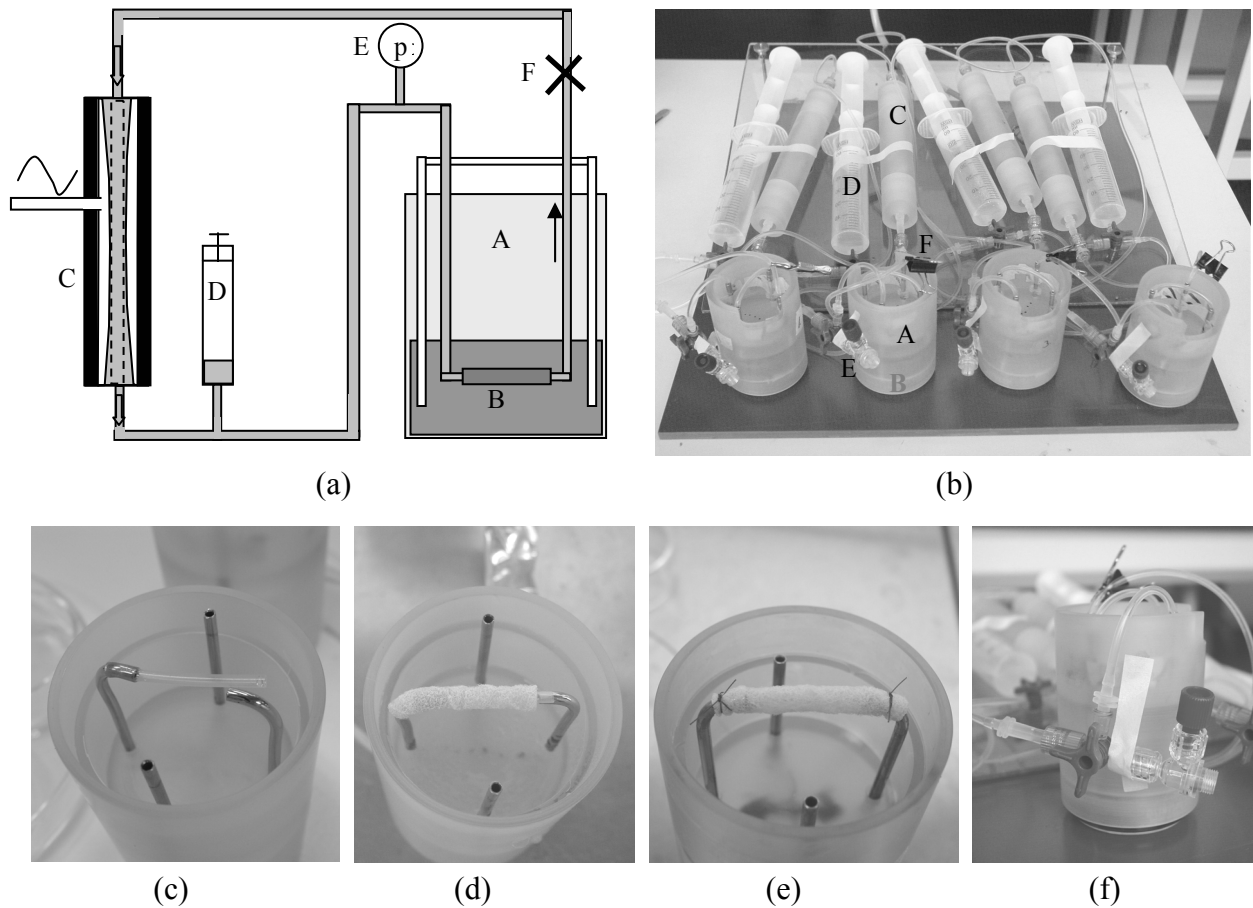


Fig. 5.1 *Bioreactor set-up: schematic drawing (a) and photograph (b) of the total set-up, consisting of 4 separate bioreactors. The tubular construct is mounted over a silicone tubing(c) in the bioreactor (d,e), picture f shows a detailed image of the bioreactor with pressure measurement dome. The capital letters are referred to in the text.*

#### **5.2.4 Measurement of strain and pressure**

Bioreactors could be placed on top of an inverted microscope to visualize the straining of the constructs during culture. A camera (Sony) captured the straining and resulting movies were analyzed using Matlab (version 5.3, the MathWork, Inc.) to quantify the level of applied circumferential strain. The pressure was measured simultaneously using a pressure sensor (BD, Belgium). Pressure-diameter measurements were performed on the silicone tubing to assess its strain-pressure relationship. These measurements were performed at different pressure levels, which were adjusted by either changing the pressure applied to the coated tube in the pressure device or by changing the position of the clamp behind the bioreactor. A strain level of 1% was achieved at an internal pressure of approximately 350mmHg.

#### **5.2.5 Culture and mechanical conditioning**

After seeding, the constructs were statically cultured in the bioreactor (37° C, 5% CO<sub>2</sub>) during 1 week. Subsequently, constructs were exposed to a circumferential strain of approximately 1% at 1Hz for the remaining 3 weeks (n=8). To maintain a strain of 1% the pressure inside the silicone tube was measured on a daily basis and adjusted, if necessary, to approximately 350mmHg by changing the position of the clamp behind the construct. The straining of the construct was captured twice a week by using a camera, as described in section 5.2.4.

Two types of control constructs were cultured under static conditions for 4 weeks in culture flask, i.e. single PGA/P4/HB constructs (static control I, n=3) and constructs that were placed over silicone tubing (static control II, n=2).

#### **5.2.6 Evaluation of tissue formation**

After a 4-week culture period, TE constructs were evaluated by histology, mechanical testing and biochemical assays, as explained in former chapters. The static controls and one part of the strained constructs (n=4) were analyzed as described in section 4.2.5. The other strained constructs (n=4) were subjected to burst pressure experiments (see below). Afterwards, representative parts of these constructs were tested by tensile tests and biochemical assays as well.

As described in chapter 4, the tensile tests were performed both in circumferential and axial direction. The tissue used for mechanical testing was afterwards analyzed by means of biochemical assays, measuring the amounts of DNA, GAG and hydroxyproline (see below).

#### **Histology and immunohistochemical assay**

Two rings of each construct were fixed in 4% phosphate-buffered formalin. One ring was embedded in Technovit and one in paraffin. Sections of 5 and 10µm thickness,



respectively, were cut from both samples. The Technovit sections were stained with toluidine blue and analyzed for general tissue formation. The paraffin sections were stained with Masson's trichrome stains to visualize the collagen.

To demonstrate the presence of the contractile protein,  $\alpha$ -smooth muscle actin was visualized in a static and strained construct through immunohistochemical analysis by antibody binding. To this end, paraffin sections were deparaffinized, washed in PBS containing 0.1% Tween 20 and subsequently treated with an antigen retrieval solution (0.04% pepsin, 0.5% milk powder in PBS, pH 2.0). After permeabilization, slides were incubated overnight at 4°C with the primary mouse antibody against human  $\alpha$ -SMA (diluted: 1:100 a2547, Sigma, The Netherlands). Afterwards, a secondary antibody (GaM-IgG2a Alexa 350, Invitrogen Molecular probes, The Netherlands) was diluted 1:200 in PBS and incubated for 90 minutes at room temperature. A short wash with a 0.1% Tween 20 solution in PBS was performed to diminish background staining from non-specific antibody binding. Cell nuclei were counterstained using an incubation with propidium iodide (Invitrogen Molecular probes, The Netherlands). Finally, slides were embedded in Mowiol (Sigma, The Netherlands). Digital pictures were captured using a Zeiss Axiovert 200 fluorescent microscope (Zeiss, Germany) mounted with a monochrome Axiocam, using appropriate filters and post-hoc color definition.

### **DNA/GAG assay**

To determine the amount of DNA and GAG in the tissue samples (n=3 per construct, 2-3 mg dry weight) the samples were digested in papain solution (100mM phosphate buffer, 5mM L-cystein, 5mM EDTA and 125-140  $\mu$ g papain per ml) overnight at 60°C. The samples were centrifuged after digestion. The amount of DNA was determined using the Hoechst dye method (Cesarone, 1979) as described in chapter 3. The GAG content was measured using a dimethylmethylene blue (DMMB) spectrophotometric assay (Farndale, 1986, chapter 3).

### **Hydroxyproline assay**

Collagen content was assessed by hydroxyproline measurements after acid hydrolysis in 4M NaOH for 10 minutes at 120°C and reaction with chloramine-T and aldehyde/perchloric acid solution. A detailed description of the protocol is given in chapter 3.

### **Tensile testing**

The mechanical properties of the engineered blood vessels were determined by uniaxial tensile tests in both circumferential and axial direction. Of each construct 3 rings were tested circumferentially ( $d \approx 2$ mm, Fig. 3.2) while three strips ( $b \approx 3$ mm) were tested axially. Engineering stress strain curves were obtained using an uniaxial tensile tester (custom-built, equipped with a 20N load cell) and a constant strain rate of the initial length/min.

From the engineering stress-strain curves, the ultimate tensile strength (UTS) was determined, as well as the elongation at break as a percentage of the initial length. The Young's modulus was calculated, defined as the slope of the linear portion of the curve.

### Burst pressure

Burst pressure experiments were performed by inflating tubular constructs to failure. To this end, the cultured constructs were taken out of the bioreactor and both construct ends were secured with a suture to a vessel-cannula (Medtronic, the Netherlands). The experimental set-up is shown in Fig. 5.2. The constructs were filled with PBS at a constant 7.5 ml/min flow rate. One cannula was connected to a pressure measurement dome (Ohmeda, Finland) and the luminal pressures were measured using a pressure sensor (BD, Belgium). The change of the diameter of the constructs was simultaneously captured by a high speed camera (Phantom, V9.0, Photo-Sonics International Ltd, UK). Burst pressures were defined as the highest pressure values attained prior to rupture.

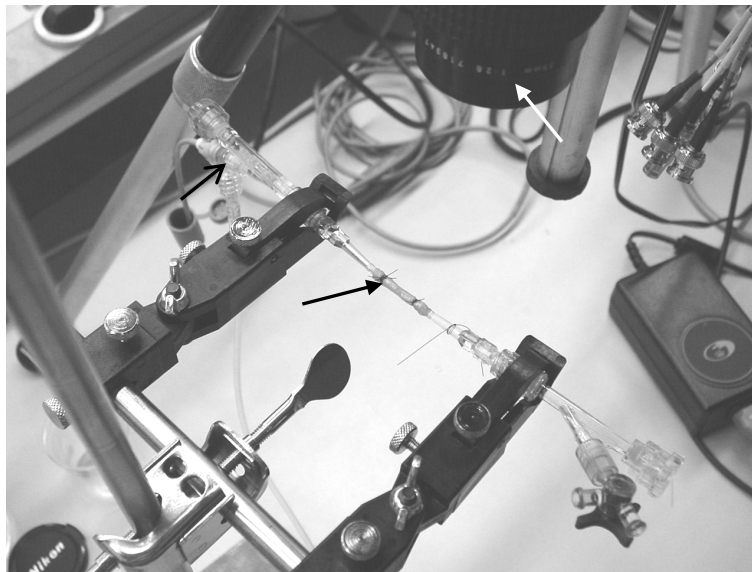


Fig. 5.2: *Burst pressure set-up: tubular constructs were filled with PBS at a constant flow rate, the flow passes a pressure measurement dome (open black arrow) and enters the construct (closed black arrow), the whole experiment is captured by a high-speed camera (white arrow).*

### 5.2.7 Statistics

All quantitative data were averaged per construct, 2-3 samples per tube, and subsequently averaged per group and represented as the average value of each group  $\pm$  the standard error of the mean (sem). Comparisons between groups were performed by one-way ANOVA, assuming equal variances, using Bonferroni post-hoc tests (STATGRAPHICS Plus 15.0.04, Statistical Graphics Corp., USA) to determine significant differences ( $p < 0.05$ ). For the uniaxial tensile tests, student t-tests were used to elucidate differences between the properties in axial and circumferential direction within each group.

## 5.3. Results

### 5.3.1 Quantification of circumferential strain

The straining of the silicone tubing, which equals the strain of the inside of the construct, was assessed during culture by measuring the pressure inside the tubing. An example of the pressure signal is given in Fig. 5.3c. Simultaneously, a camera captured the straining at the outside of the construct, which was approximately 0.5% (Fig 5.3b). The relation between the strain at the inner side and the outer side of the construct can be calculated, assuming wall incompressibility, and depends on the wall thickness. The outer diameter changed over time as a result of a decreasing wall thickness due to tissue compaction (Fig. 5.4). After 1 day of straining, i.e. 8 days after seeding, the outer diameter of the construct was on average 4.7mm (Fig. 5.4a). It decreased to 4.5, 3.8 and 3.7 mm after 14, 19 and 23 days after seeding, respectively (Fig. 5.4b-d). In addition to illustrating the decrease in outer diameter, Fig. 5.4 also shows a change in appearance of the surface of the construct. After 8 days of culturing (Fig. 5.4a), the surface looked rough with protruding scaffold fibers, whereas the surface became smoother over time (Fig. 5.4b-d).

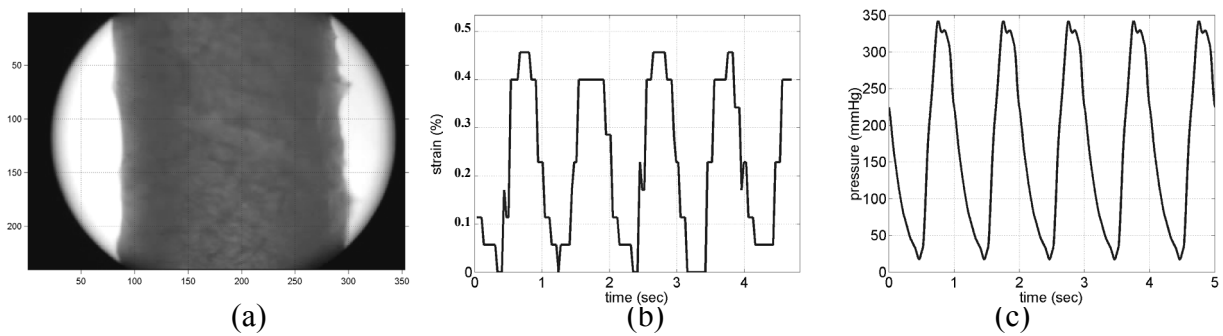


Fig. 5.3 Measurement of pressure and strain during culture. A camera captured the change in outer diameter of the construct (a), which was converted to circumferential strain (b), simultaneously the inner pressure was measured (c).

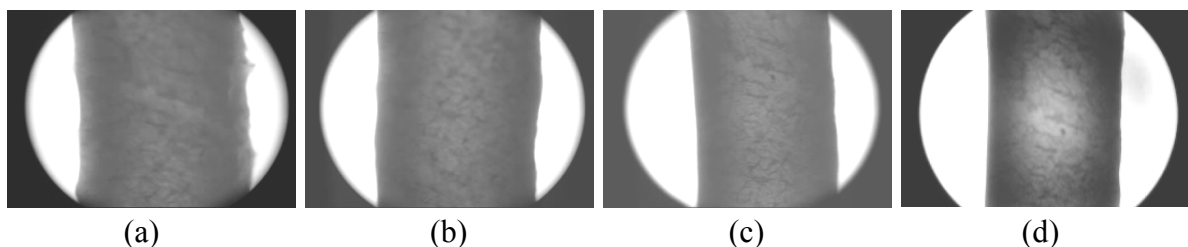


Fig. 5.4 Pictures of tubular construct, as part of the captured movies, at different time points, i.e. 8(a), 14(b), 19(c) and 23(d) days after seeding.

### 5.3.2 Histology

Macroscopic photographs and histological slides of the constructs are shown in Fig. 5.5. Histological investigation revealed no apparent differences in tissue density and/or distribution between the static cultured control constructs, i.e. the single PGA/P4HB constructs and the constructs cultured around a silicone tube. However, the dynamically cultured constructs showed much denser and more homogeneous tissue. This is

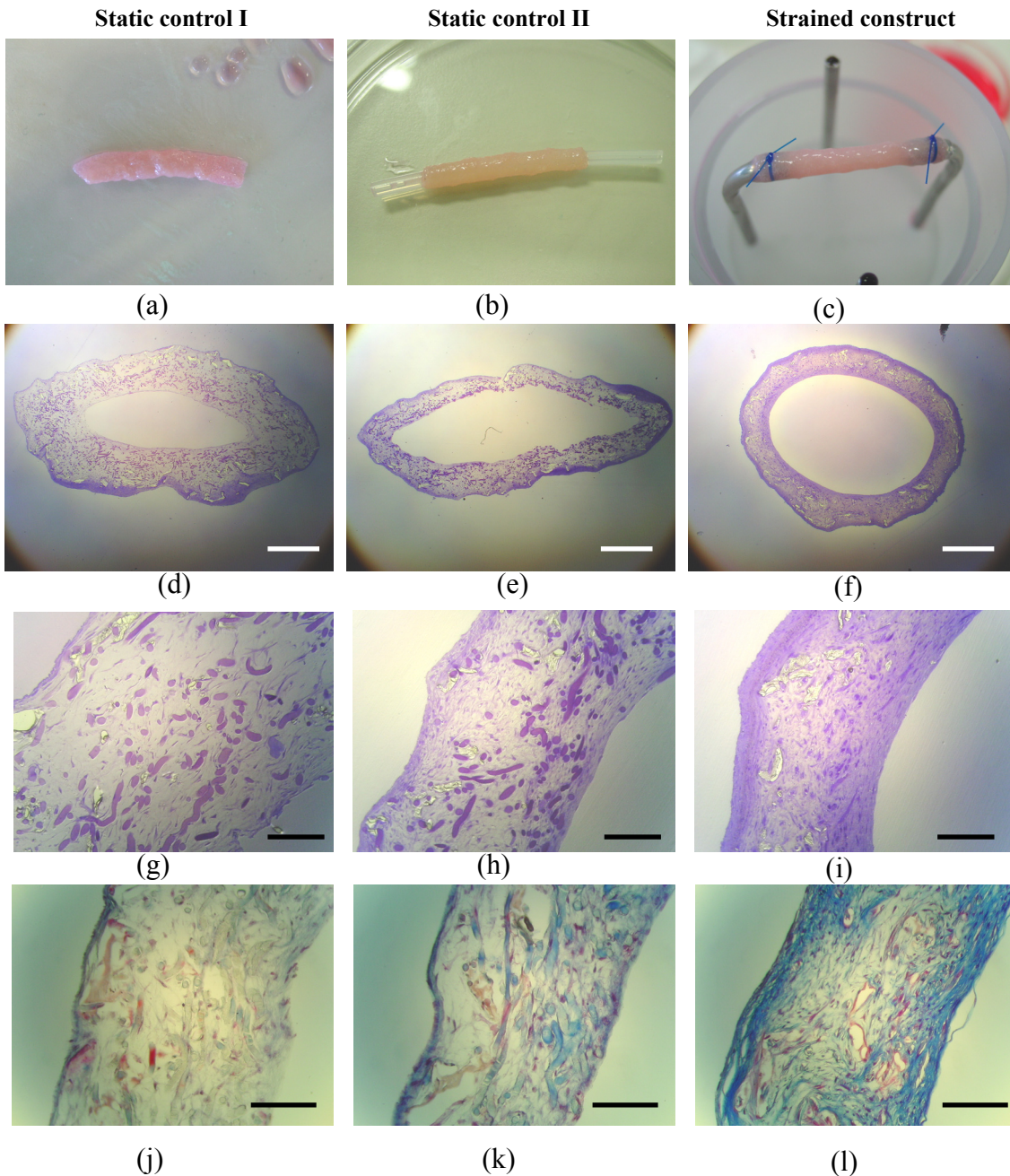


Figure 5.5: Macroscopic photographs and histological slides of static controls (a,b) and strained (c) constructs showing toluidine blue (d-i) and Masson's trichrome (j-k) staining of statically and circumferentially strained constructs. Static control II is cultured around a silicone tubing. The white bars indicate 1mm, the black bars indicate 200 $\mu$ m).

confirmed by the Masson's trichrome staining indicating much more collagen to be present in the strained constructs. The distribution of the collagen was not homogeneous throughout the whole construct, i.e., most collagen was found at the inner and outer side of the vessel wall.

Figure 5.6 shows the staining of the contractile protein  $\alpha$ -SMA in a static control (Fig. 5.6a) and strained construct (Fig. 5.6b,c). In addition, it shows a strong autofluorescence of the scaffold material. In the strained constructs more  $\alpha$ -SMA was present compared to the static controls. At some locations in the strained construct (data not shown)  $\alpha$ -SMA was more pronounced at the inner and outer surfaces than in the middle of the vessel wall. This correlated to the locations of high tissue density, as shown in Fig. 5.5i. Figure 5.6c shows a detailed image of the  $\alpha$ -SMA staining of the strained constructs, combined with cell nuclei staining.

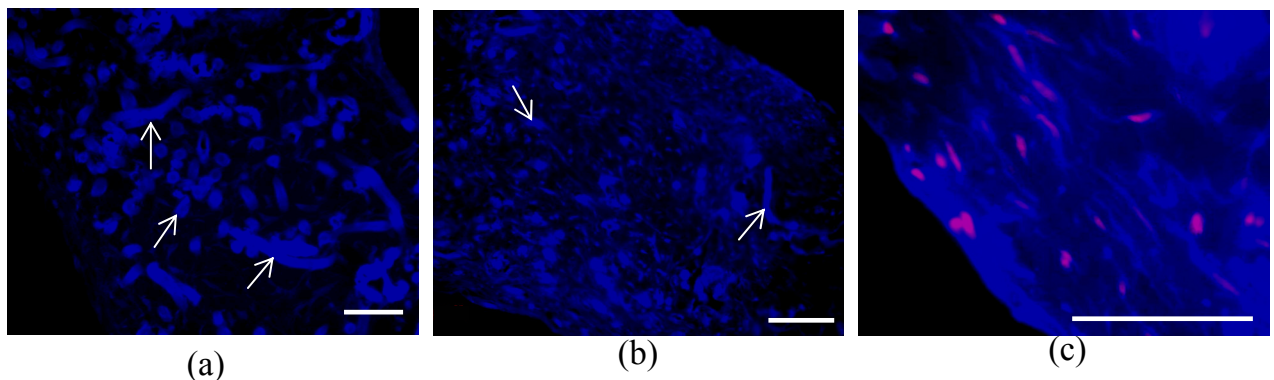


Figure 5.6:  $\alpha$ -SMA staining (blue) of a statically (a) and circumferentially strained (b,c) construct. A strong autofluorescence of the scaffold material (white arrows) is visible, most pronounced in the slide of the statically cultured construct (a). Figure c shows a detailed image of the strained construct including counterstained cell nuclei (pink). The bars indicate  $100\mu\text{m}$ .

### 5.3.3 Quantitative evaluation of tissue formation

The tissue content in the 3 different groups, i.e. the statically cultured control constructs whether or not around silicone tubing, and the circumferentially strained constructs, was quantified by the amounts of DNA, GAG and hydroxyproline (Fig. 5.7). No significant differences were found between the amounts of DNA found in the 3 types of constructs. However, the amounts of GAG and hydroxyproline in the strained constructs were significantly higher than in both types of static cultured constructs ( $p < 0.001$ ). No differences were found between the two static controls. The amount of GAG produced per  $\mu\text{g}$  DNA in the strained constructs was higher compared to that produced in the constructs statically cultured around silicone tubing ( $p < 0.05$ ). Also the amount of hydroxyproline per  $\mu\text{g}$  DNA was higher in the strained constructs than in both static control groups, ( $p < 0.01$  compared to the single constructs,  $p < 0.05$  compared to the constructs cultured around silicone tubing).

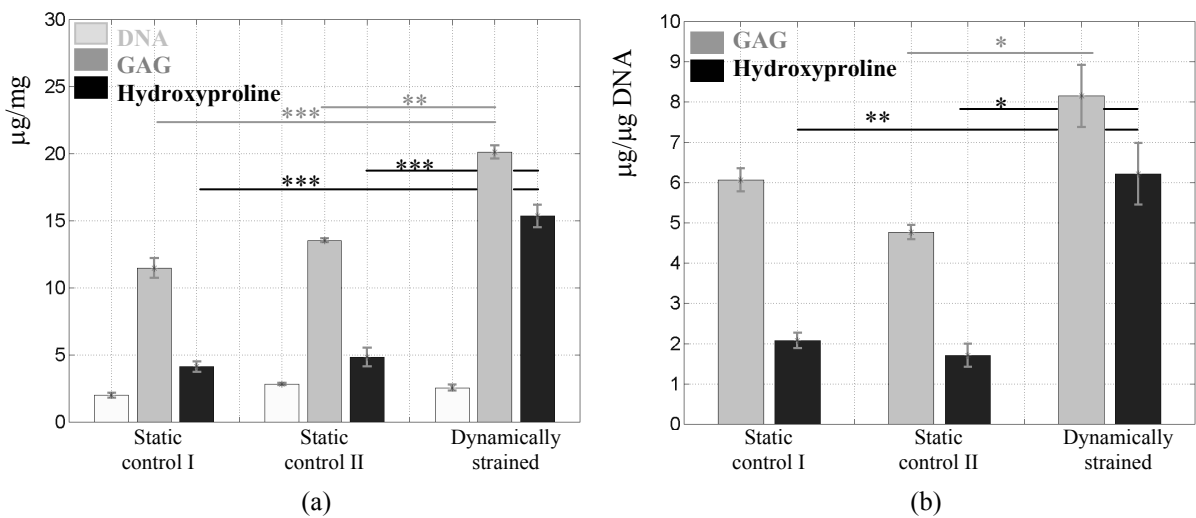


Figure 5.7: The amounts of DNA, GAG and hydroxyproline per dryweight (a) and per DNA (b) in the statically and dynamically cultured constructs after a 4-week culture period. Data are presented as mean  $\pm$  sem (\* represents  $p < 0.05$ , \*\* represents  $p < 0.01$ , \*\*\* represents  $p < 0.001$ ).

### 5.3.4 Mechanical testing

The stress-strain curves resulting from tensile tests in circumferential and axial direction are shown in figure 5.8. Measurements on the static cultured control (I) constructs revealed relative poor mechanical properties and a distinct difference between the mechanical behavior in both directions. This was quantified by the Young's modulus, UTS and the elongation at break (Fig. 5.9). As compared to these control constructs, the properties of the constructs statically cultured around silicone tubing improved in circumferential direction in terms of an increase of the averaged Young's modulus and UTS by a factor 4 and 2, respectively. On the other hand, the elongation at break in this



direction was lower compared to the single PGA/P4HB constructs ( $p < 0.05$ ). A large increase in mechanical properties was found for the constructs that were dynamically strained in circumferential direction (Fig. 5.8c, 5.9). The Young's modulus increased by a factor 4 and 5 in circumferential and axial direction, respectively, compared to the constructs cultured statically around silicone tubing (both  $p < 0.05$ ). For the UTS these factors equaled 3 and 5, respectively ( $p < 0.05$  and  $p < 0.001$ , respectively).

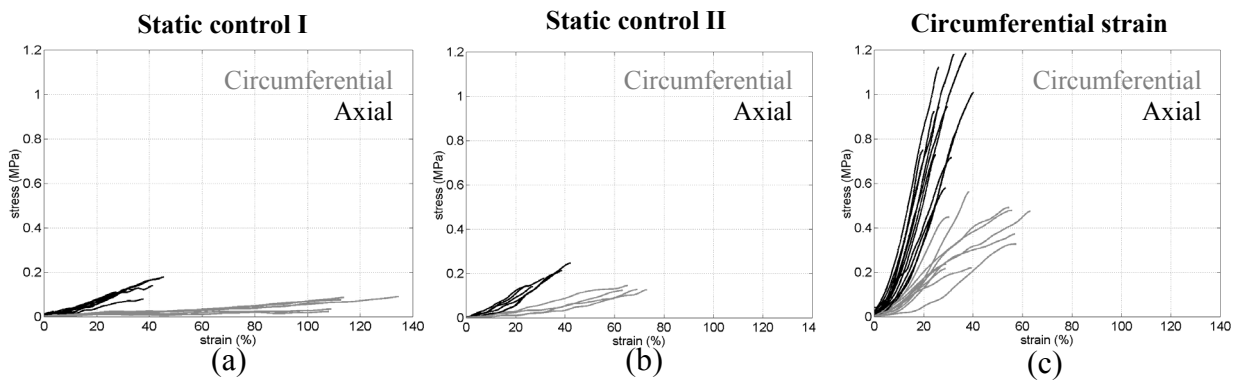


Figure 5.8: *Stress-strain curves of statically cultured, single (a) or around silicone tubing (b), and dynamically strained (c) constructs in circumferential (grey) and axial (black) direction.*

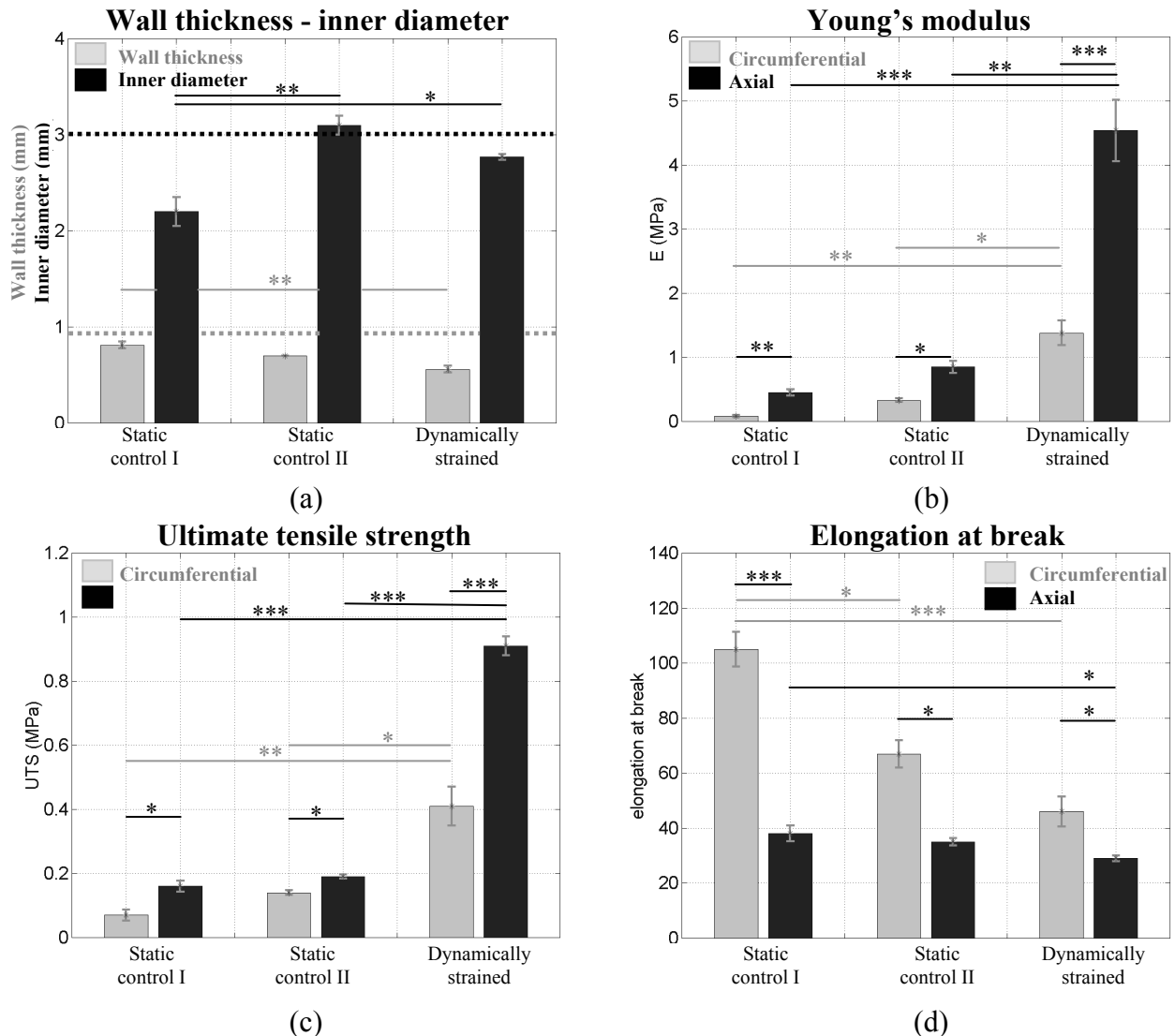


Figure 5.9 Geometrical and mechanical properties of static and dynamically cultured constructs after a 4-week culture period: wall thickness and inner diameter (a), Young's modulus (b), UTS (c) and the elongation at break (d). The latter three are given in axial and circumferential direction. The dashed lines in figure (a) indicate the initial wall thickness (grey) and inner diameter (black) of the PGA/P4HB constructs. Data are presented as mean  $\pm$  sem (\* represents  $p < 0.05$ , \*\* represents  $p < 0.01$ , \*\*\* represents  $p < 0.001$ ).

### 5.3.5 Burst pressure

The results of the burst pressure experiments are shown in Fig. 5.10. Changes in the vessel diameter during the experiment, captured by the high-speed camera, were analyzed at different positions (horizontal lines in Fig. 5.10a). Combination with the measured pressure signal (Fig. 5.10b) resulted in pressure versus circumferential strain (Fig. 5.10c), showing, among other things, that the circumferential strain of this construct at 100mmHg, i.e. in the physiological working range, was approximately 10%.



After the burst pressure experiment, uniaxial tensile tests were performed in two directions, the results of which are presented in Fig. 5.10d. As described in chapter 3 (section 3.1.2), the circumferential stress-strain curve can be used to estimate the pressure-diameter relation. Figure 5.10e includes both the measured (black line) and the estimated (grey line) pressure-strain curve. The elongation at break is significantly lower in the measured curve. The measured pressure-strain relationship resulting from the burst pressure experiment allows an estimation of the compliance of 0.03%/mmHg at 100mmHg (dashed line Fig. 5.10e).

The mechanical properties of the strained constructs, quantified by the Young's modulus and UTS, and the measured burst pressures are summarized in Table 5.1. The  $UTS_{circ}$  was used to estimate the burst pressure, as described by equation 3.5 (chapter 3). An  $UTS_{circ}$  of 0.48MPa can be converted to a burst pressure of 886mmHg, using the

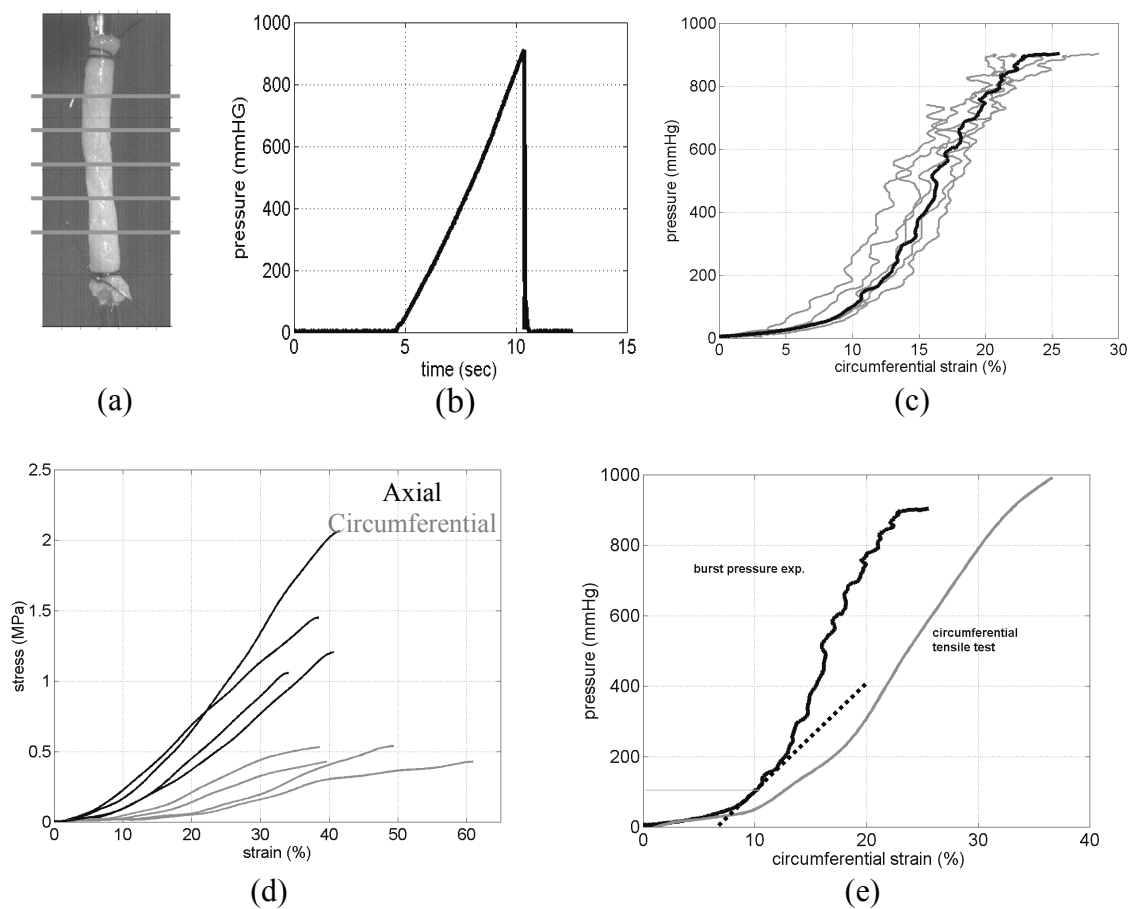


Figure 5.10: *Burst pressure experiment; the diameter change of the construct is analyzed at several positions (a) and related to the pressure signal (b), resulting in pressure versus circumferential strain (c), the thick black curve shows the average behavior of one construct. Figure d shows stress strain curves of all constructs ( $n=4$ ) in axial and circumferential direction which were obtained after the burst pressure experiment. Figure e shows the measured (black) and estimated (grey) pressure-strain relation, the latter is based on the circumferential tensile test. The dashed line indicates an estimation of the compliance at 100mmHg*

averaged initial radius (1.5mm) and wall thickness (0.41mm) of the constructs. This is in good agreement with the measured burst pressure of  $906 \pm 123$  mmHg.

As discussed earlier (chapter 3), some investigators use Cauchy stress instead of engineering stress. The relation between both stress measures in a uniaxial tensile test is given by  $\sigma_{\text{Cauchy}} = \lambda \sigma_{\text{eng}}$ , where  $\lambda$  is defined as the stretch  $l/l_0$ . This results in different values for the Young's modulus and UTS. To enable comparison between those studies and the constructs presented in the present study, table 5.1 also contains the values of E and UTS when Cauchy stress was applied.

Table 5.1: *Mechanical properties of circumferentially strained TE constructs. Young's modulus and UTS are calculated using engineering or Cauchy stress. Data are presented as mean  $\pm$  sem.*

	$E_{\text{axial}}$ (MPa)	$E_{\text{circ}}$ (MPa)	$UTS_{\text{axial}}$ (MPa)	$UTS_{\text{circ}}$ (MPa)	Burst pressure (mmHg)
$\sigma_{\text{eng}}$	$5.0 \pm 0.6$	$2.0 \pm 0.2$	$1.4 \pm 0.1$	$0.48 \pm 0.02$	$906 \pm 62$
$\sigma_{\text{cauchy}}$	$7.3 \pm 0.5$	$3.0 \pm 0.1$	$1.9 \pm 0.1$	$0.72 \pm 0.02$	

## 5.4. Discussion

The properties of tissue-engineered blood vessels, in terms of tissue formation and mechanical properties, can be improved by mechanical conditioning during culture. Particularly circumferential straining protocols have proven to be effective (Niklason, 2001; Niklason, 2005; Seliktar, 2003; Hoerstrup, 2001). The most promising results have been obtained with the use of animal cells. The present study describes the culture of human vascular grafts based on a scaffold of PGA/P4HB and fibrin. Constructs seeded with human saphenous vein myofibroblasts, which were subjected to static axial strain and 1% dynamic circumferential strain for a 4-week culture period, displayed strongly increased tissue formation and improved mechanical properties compared to static controls. Comparison between the presented strained constructs and the constructs presented in chapter 4, which were only subjected to an axial strain, reveals the additional effect of circumferential straining. The combination of strain in axial and circumferential direction resulted in constructs that contained significantly more collagen. In addition, it improved the mechanical properties, in terms of a higher Young's modulus and UTS, in both axial and circumferential direction. Burst pressure experiments revealed that the presented constructs could withstand pressures up to at least 800mmHg.

To demonstrate the effect of static circumferential strain, control constructs were statically cultured around silicone tubing. This tubing induces static internal strain by counteracting the compaction in circumferential direction. However, the mechanical

properties of these constructs improved only to a minor extent compared to the static controls that were not cultured around tubing. The effect of the silicone tubing, and thereby the effect of static internal circumferential strain, might be enhanced by increasing the diameter of the internal tubing.

When comparing different TE constructs, it should be mentioned that in most studies on TE blood vessels animal cells have been used. Comparing human and animal TE constructs is not straightforward. Indeed, experiments in our lab showed that a similar conditioning protocol applied to valvular constructs seeded with human and ovine saphenous vein cells resulted in different outcomes. For one thing, compared to human cells, the ovine cells proliferated much faster resulting in thicker valve leaflets (unpublished results). This finding suggests that care should be taken when comparing TE constructs cultured with human and animal cells.

Niklason and co-workers (Poh, 2005; Klinger, 2006) cultured TE blood vessels by using the same cell source as in our study, i.e. human saphenous veins, and a comparable tubular PGA scaffold. In comparison to our study, no P4HB coating or fibrin gel was added to the PGA scaffold. After a 7-8 week culture period under 1% circumferential strain conditions, applied via silicone tubing, constructs displayed a significantly lower burst pressure than in our experiments, in the order of 500mmHg. In addition, these results could only be obtained when the cells were genetically modified, i.e., via human telomerase reverse transcriptase (hTERT) gene transfection. This transfection increases the replicative capacity of the fibroblasts. Constructs cultured with non-modified cells resulted in weak blood vessels, possessing burst pressures in the order of 100mmHg (Poh, 2005). As the main difference between this study and our findings is the use of fibrin gel, it might be concluded that fibrin strongly promotes the tissue formation and the mechanical properties. The strongest human TE blood vessels, in terms of burst pressure, were cultured by L'Heureux and co-workers (1998). Constructs were based on rolled cell sheets and consisted of sheets of human umbilical vein SMCs and human dermal fibroblasts. The resulting constructs had a burst pressure greater than 2200mmHg, which exceeds the reported value of 2000mmHg reported for native arteries (L'Heureux, 2006). It should be mentioned that the production of these grafts involved a culture period of up to 3 months, including a 7-week period for the adventitial maturation. Therefore it can be concluded that, considering the relative short culture period of 4 weeks, our TE blood vessels are strong compared to other engineered vascular grafts. In this comparison we excluded grafts that still contain scaffold material that contributes to the mechanical properties.

In the present bioreactor, and in bioreactors of the research group of Niklason (Niklason, 1999; Poh, 2005), a silicone tube inside the tubular constructs is used to apply a circumferential strain. In contrast, in a study by Hoerstrup (2001), tubular constructs were directly subjected to flow with only limited circumferential straining. Constructs based on a PGA/P4HB scaffold and seeded with ovine SMCs resulted in TE vessels with a burst pressure of 325mmHg. With the bioreactor described in this chapter, we performed experiments using a similar approach. A pulsatile flow was directly applied to the constructs inducing a circumferential strain varying from 3-10%. However, the tissue in the resulting constructs was not homogeneous and did not improve significantly compared to static controls (data not shown). This could have been partly due to inappropriate bioreactor dimensions in terms of inflow-length, which caused a non-

uniform flow to the construct, as was estimated by numerical simulations (van Lith, 2005). However, we believe that a silicone tubing inside the constructs, which directly counteracts the compaction and thereby induces internal static strain, plays an important role in the development of the presented strong TE constructs.

In the present study cells were isolated from human saphenous veins from two different patients. Constructs seeded with these cells were subjected to identical culture protocols. Afterwards, one group (male donor, age 65) was mechanically analyzed by tensile tests, the other group (female donor, age 47) by burst pressure experiments, followed by tensile tests. Despite the different cell sources, no significant differences were found in the amount of DNA and extracellular matrix. The mechanical properties of the second group, in terms of Young's modulus and UTS, were higher than in the first group, although only significantly in the  $UTS_{axial}$ . In contrast, the group of Niklason (Klinger, 2005) found a strong dependence of the strength of the construct and the donor age. A blood vessel cultured from cells of a 47-year-old donor resulting in a burst pressure of 450mmHg, whereas donor ages of 55, 67 and 74 resulted in values of approximately 225, 130 and 120mmHg, respectively. This age-dependency was not confirmed in our study although we used cells from only two different donors. In a comparable study in our laboratories strong TE heart valve leaflets were cultured, based on the same scaffold and conditioning protocol, from a 77-year old donor (Mol, 2006). Therefore, we do not expect that our method is strongly donor-age dependent, although more experiments with different donors have to be performed.

The burst pressure experiment revealed information about the compliance of the TE constructs. It showed that the strain at 100mmHg of the presented TE construct was approximately 10%, which correlates well with the reported values of 4-10% for coronary arteries (Zilla, 1999). The estimated compliance of the TE constructs was 0.03%/mmHg. For human coronary arteries this value is in the order of 0.06%/mmHg (Zilla, 1999). Direct comparison should, however, be performed with care. First, the burst pressure experiment was not designed for compliance measurements and therefore did not include pre-conditioning or dynamic measurements. Second, we did not apply an axial pre-strain to the constructs during the performed experiments. This affects the measurement of the pressure-diameter relation and compliance, and should therefore be adjusted to in-vivo values, as was demonstrated in studies by e.g. van Andel (2003) and Billiar (2001). In addition, it must be recognized that differences exist between ex-vivo and in-vivo measurements. This was demonstrated, among others, by Tajaddini and co-workers (2003) who examined vascular properties of intact porcine coronary artery ex-vivo and in vivo. The in-vivo vessels appeared less compliant than ex-vivo, likely influenced by in-vivo factors such as myocardial support and vascular tone. Therefore, although the compliance of the TE construct seems to be in the right range, more experiments are needed.

In the present study, the mechanical properties of TE constructs were assessed via uniaxial tensile tests and burst pressure experiments. It was investigated whether tensile tests can predict the outcome of the burst pressure experiment and, as such, suffice for the mechanical characterization of TE constructs. The group of constructs that was subjected to a burst pressure experiment was therefore subsequently tested by tensile tests, performed on the remaining parts of the constructs. In this case the burst pressure experiment can be regarded as a pre-conditioning of the tissue of 15-20% of the initial

length in circumferential direction, i.e. the strain at which the weakest point of the construct failed (fig. 5.10c). It was shown that the value of the  $UTS_{circ}$  can be used for obtaining a good estimation of the burst pressure, using thin wall assumptions and the LaPlace's relationship. However, the averaged elongation at break of the constructs, resulting from the burst pressure experiment, was significantly lower than the values measured in the subsequently performed circumferential tensile test. This was probably due to the fact that these tensile tests were performed on the stronger parts of the constructs as the weakest point had failed in the burst pressure experiment. However, the lowest values of the elongation at break of the constructs that were only subjected to tensile tests, were in good agreement with the outcome of the burst pressure experiment. As such, the circumferential tensile tests predict the pressure-strain relationship of the engineered blood vessel relatively well. In addition, compared to the burst pressure analysis, uniaxial tensile measurements have the advantage that significant less sample material is required and that more information is provided about yielding, modulus, and homogeneity and anisotropy of the constructs.

In conclusion, the presented TE constructs cultured from human saphenous vein cells possessed better mechanical properties, in terms of burst pressure, than constructs cultured in comparable studies with similar culture times. The main difference with other studies is the use of fibrin gel. The use of internal silicone tubing, through which circumferential strain was applied, appeared to be necessary for culturing strong constructs. To expand the evaluation of the cultured constructs presented in this study, we compared the properties of the TE blood vessels with those of native equivalents. The results of these experiments are shown in the next chapter.

## 5.5. Acknowledgements

We gratefully acknowledge Reinout Hesselink for his work on the immunostainings.

# 6

Comparison between tissue-engineered blood vessels and native equivalents

## 6.1. Introduction

The feasibility of the application of tissue-engineered (TE) blood vessels in coronary artery bypass grafting should, as a first approach, be tested by comparing the properties of TE constructs with those of human native coronary arteries. However, coronary arteries (CA) are difficult to study since they are small and relatively inaccessible, with numerous branchings. The number of studies on the mechanical properties of CA is therefore limited, although recently some data have become available. Because of the limited availability of human CA and the good morphological resemblance between human and porcine CA (Weaver, 1986), several studies have concentrated on porcine vessels, whether or not in combination with human arteries. Van Andel and co-workers (2003) investigated the *ex-vivo* mechanical properties of porcine and human coronary arteries by measuring the pressure-diameter and circumferential and axial stress-strain relations by inflating cannulated artery segments. Lally and co-workers (2004) applied uniaxial and equibiaxial tensile tests on porcine coronary arteries. Tensile testing on human CA was performed by Holzapfel (2005). This study focused on layer-specific mechanical properties, quantifying the ultimate stresses and strain in circumferential and axial direction for the separate intima, media and adventitia layers.

Although data on the mechanical properties of (human) coronary arteries have been published, large differences exist between the measurement circumstances, protocols and calculation methods. Therefore, to enable the comparison between the TE constructs, as presented in chapter 5, and native equivalents, identical analysis methods and protocols need to be applied. In the present study, measurements of the mechanical properties and biochemical contents were performed on human saphenous veins (HSV) and left internal mammary arteries (LIMA), i.e. the two human grafts routinely used for coronary bypass grafting. In the course of this study it was not feasible to perform measurements on human coronary arteries due to the limited availability. To enable comparison with other studies, as described above, measurements were also performed on porcine coronary arteries. Resulting properties are compared to those of the TE constructs, which were already partly presented in chapter 5.

## 6.2. Materials & Methods

### 6.2.1 Tissue-engineered blood vessels

Tissue-engineered blood vessels were cultured as described in chapter 5. In short, tubular constructs of P4HB coated PGA were seeded with human vena saphena cells (donor age 47 and 65 years). Fibrin gel was used as a cell carrier. The constructs (n=8) were statically cultured in a bioreactor during 1 week, followed by a 3-week culture period with 1% circumferential straining at 1Hz.

## **6.2.2 Human and porcine native blood vessels**

From 4 pigs (1-1.5 years old, approximately 150kg), segments of approximately 2-3cm of the left anterior descending (LAD) and left circumflex coronary artery (LCX) were excised. The hearts were obtained from the local abattoir and transported to the laboratory in an insulating box containing phosphate buffered saline (PBS) at approximately 4°C. Measurements were performed within 6 hours post mortem.

Segments of discarded human saphenous veins (HSV, n=5, patient age 65±7 years) and left internal mammary artery (LIMA, n=3, patient age 49±7 years) were obtained after completion of coronary-artery bypass grafting (CABG) from a local hospital. The specimens were transported in DMEM to the laboratory. Measurements were performed within 2 hours. Loose adventitial tissue was removed from the segments as much as possible.

During surgery, in order to prevent spasms, segments of the LIMA are treated with papavarine, a well-known vasodilator. Since the lumen of the LIMA is very narrow without papavarine, we included this drug to enable proper measurements of the mechanical properties. For comparison reasons, also the HSV and the porcine coronary arteries were treated with this vasodilator. Furthermore, the use of papavarine excluded any interference on the tensile tests by contractile smooth muscle cells. Thus, the mechanical properties of the extracellular matrix of the TE and native vessels could be compared.

## **6.2.3 Histology**

Depending on the length of the blood vessel segments, which was limited in case of the human HSV and LIMA, one or two rings of the TE and native vessels were fixed in 4% phosphate-buffered formalin. The rings were embedded in Technovit and/or in paraffin. Sections of 5 and 10µm thickness, respectively, were cut from the samples. The Technovit sections were stained with toluidine blue and analyzed for general tissue formation. The paraffin sections were stained with Masson's trichrome to visualize the tissue content and, more specific, smooth muscle and collagen. Measures for the inner diameter and the wall thickness were obtained from the Technovit sections.

## **6.2.4 Biochemical assays**

The tissue of the TE constructs and the native vessels was quantified by biochemical assays, measuring the amount of DNA, GAG and hydroxyproline, as described in chapter 3. In short, the amount of DNA and GAG was determined in the tissue samples (n=2-3 per construct, 2-3 mg dry weight) by digestion of the samples in papain solution (100mM phosphate buffer, 5mM L-cystein, 5mM EDTA and 125-140 µg papain per ml) overnight at 60°C. The samples were centrifuged after digestion. The amount of DNA was determined using the Hoechst dye method (Cesarone, 1979). The GAG content was measured using a dimethylmethylene blue (DMMB) spectrophotometric assay (Farndale, 1986). Collagen content was assessed from hydroxyproline measurements



after acid hydrolysis in 4M NaOH and reaction with chloramine-T and aldehyde/perchloric acid solution.

### **6.2.5 Mechanical testing**

The mechanical properties of the engineered and native blood vessels were determined by uniaxial tensile tests in both circumferential and axial direction. Depending on the available length of the vessel segment, of each construct 1-3 rings were tested circumferentially while 1-3 strips were tested axially, as described in chapter 3. The native human and porcine blood vessels were pre-conditioned to a strain of approximately 10% of the estimated elongation at break, which was determined from a test sample prior to the actual measurements. From the engineering stress-strain curves, the ultimate tensile strength (UTS) was determined, as well as the elongation at break as a percentage of the initial length. The Young's modulus (E) was calculated, defined as the slope of the linear portion of the curve.

### **6.2.6 Statistics**

All quantitative data was averaged per construct, 1-3 samples per blood vessel, and subsequently averaged per group and represented as the average value of each group  $\pm$  the standard error of the mean (sem). Comparisons between groups were performed by one-way ANOVA, assuming equal variances, using Bonferroni post-hoc tests (STATGRAPHICS Plus 15.0.04, Statistical Graphics Corp., USA) to determine significant differences ( $p < 0.05$ ).

## **6.3. Results**

### **6.3.1 Histology**

Histological slides of a TE construct, LIMA, HSV and porcine CA are presented in Fig. 6.1. Masson's trichrome staining clearly distinguished between muscle tissue (red) and collagen (blue). The walls of the arteries, i.e. the human LIMA (Fig. 6.1b) and porcine CA (Fig. 6.1d), demonstrated an abundant presence of smooth muscle. The loose adventitial tissue mainly contained collagen. The HSV had a distinct different appearance demonstrating much more collagen in the vessel wall (Fig. 6.1c). In addition, the lumen was much more irregular, which is a general characteristic when compared to the lumen of arteries. The 'folded' structure can explain the highly compliant behavior of veins at low pressures as under these circumstances the wall unfolds rather than resists to the pressure. The collagen shown in the TE construct appears to be much less and not as organized as in the native vessels.

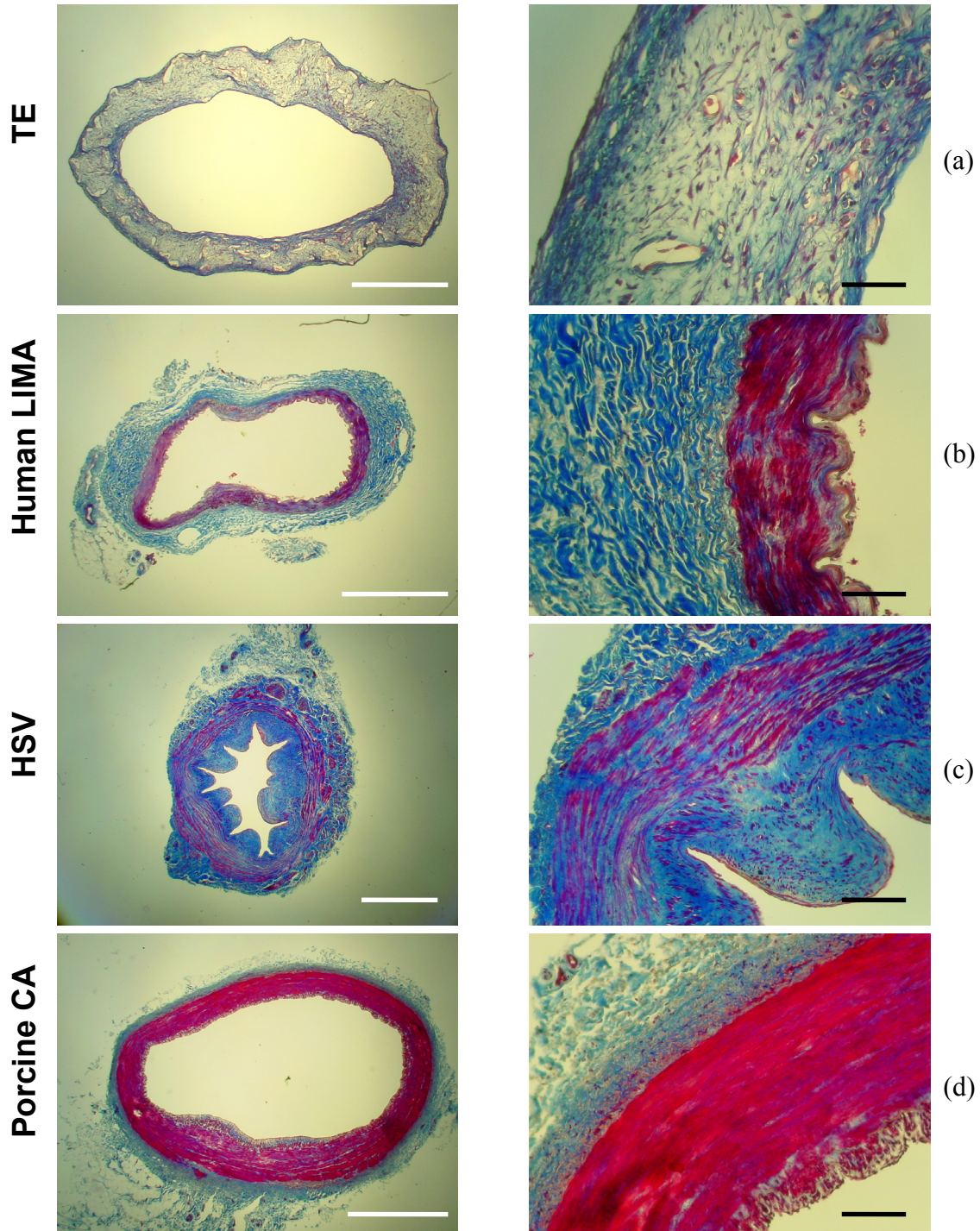


Figure 6.1: Masson's trichrome staining of cross-sections of TE (a) and native (b-d) small diameter blood vessels, where red indicates smooth muscle and blue collagen. The white bars represents 1mm, the black bars indicate 100µm.

### 6.2.2 Quantitative evaluation of tissue formation

The tissue content of the engineered and native blood vessels was quantified by the amounts of DNA, GAG and hydroxyproline (Fig. 6.2). No significant differences were

found between the amount of DNA in the TE, LIMA, HSV and porcine CA. This might seem inconsistent with the histology shown in Fig. 6.1. However, DAPI staining (data not shown) confirmed that the amount of cell nuclei did not differ much for the TE and native constructs. The amount of GAG in the TE vessels (Fig. 6.2a) was significantly higher than that in the native vessels ( $p < 0.001$  compared to the LIMA and HSV, and  $p < 0.05$  compared to the porcine CA). Conversely, the amount of hydroxyproline in the TE constructs was significantly lower than that in the native equivalents ( $p < 0.01$ ). On average, the hydroxyproline content of the TE constructs was about 50% compared to the analyzed native vessels. When normalized for the DNA content, the amount of GAG in the TE constructs was significantly higher than in the LIMA ( $p < 0.01$ ) and the porcine CA ( $p < 0.05$ ) (Fig. 6.2b). The amounts of hydroxyproline per DNA were higher for the native vessels compared to the TE constructs, although only significantly for the HSV ( $p < 0.05$ ).

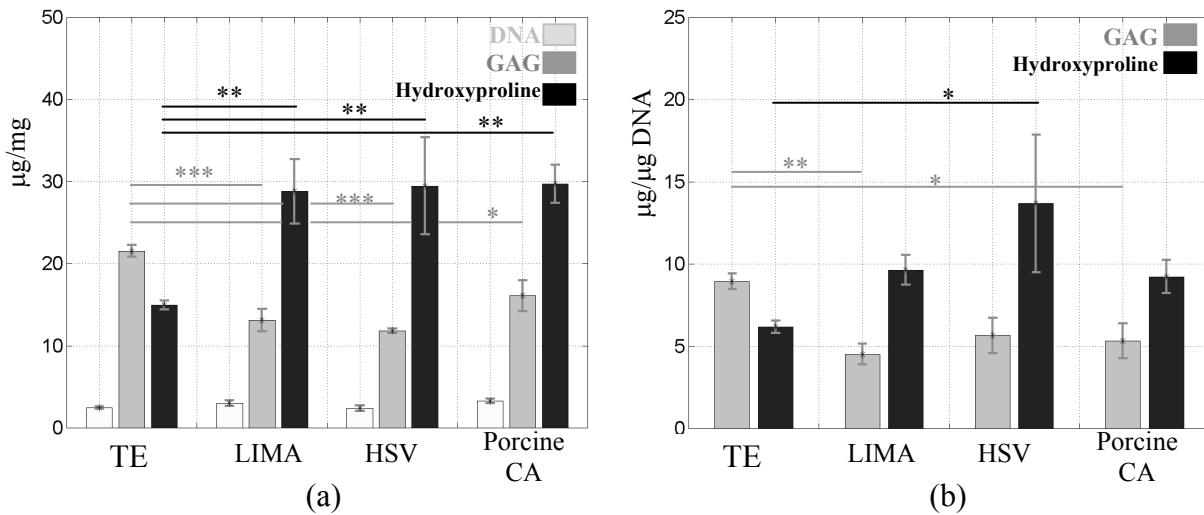


Figure 6.2: The amounts of DNA, GAG and hydroxyproline per dryweight (a) and per DNA (b), for the engineered vessels (TE), the human LIMA and HSV, and the porcine CA. Data are presented as mean  $\pm$  sem (\* represents  $p < 0.05$ , \*\* represents  $p < 0.01$ , \*\*\* represents  $p < 0.001$ ).

### 6.2.3 Mechanical testing

All four types of blood vessels were subjected to uniaxial tensile tests in circumferential and axial direction. For the sake of clarity, Fig. 6.3a shows one representative curve, in both directions, for each blood vessel type. The resulting Young's moduli, UTS and elongation at break are presented in Fig. 6.4. In terms of Young's moduli and UTS, all blood vessels demonstrated stronger behavior in axial than in circumferential direction. This difference was most pronounced in the HSV. The TE constructs and the LIMA show most resemblance in this respect. The tensile tests in circumferential direction, reflecting the most important functional characteristic of vessels, are shown in more detail in Fig. 6.3b. To illustrate the variation in the behavior, the stress-strain relations in this direction are presented as envelopes, within which all individual stress-strain

relations are situated for each type of blood vessel. Comparison between the LIMA and HSV demonstrates that the vein is far more compliant compared to the artery. Furthermore, the envelopes of the two arteries, i.e. the human LIMA and porcine CA, overlap, indicating relatively small differences between these vessels. However, at low stress values, the porcine vessel appeared to be more compliant.

In general, the mechanical properties of the TE constructs were not up to those of the native vessels. Compared to the LIMA, which is the most used graft for CABG, TE vessels demonstrated significantly lower Young's moduli and UTS ( $E_{\text{circ}}$  ( $p < 0.05$ ),  $E_{\text{axial}}$  ( $p < 0.01$ ),  $UTS_{\text{circ}}$  ( $p < 0.001$ )). Also the elongation at break in circumferential direction is significantly smaller for the TE constructs, when compared to the LIMA ( $p < 0.05$ ).

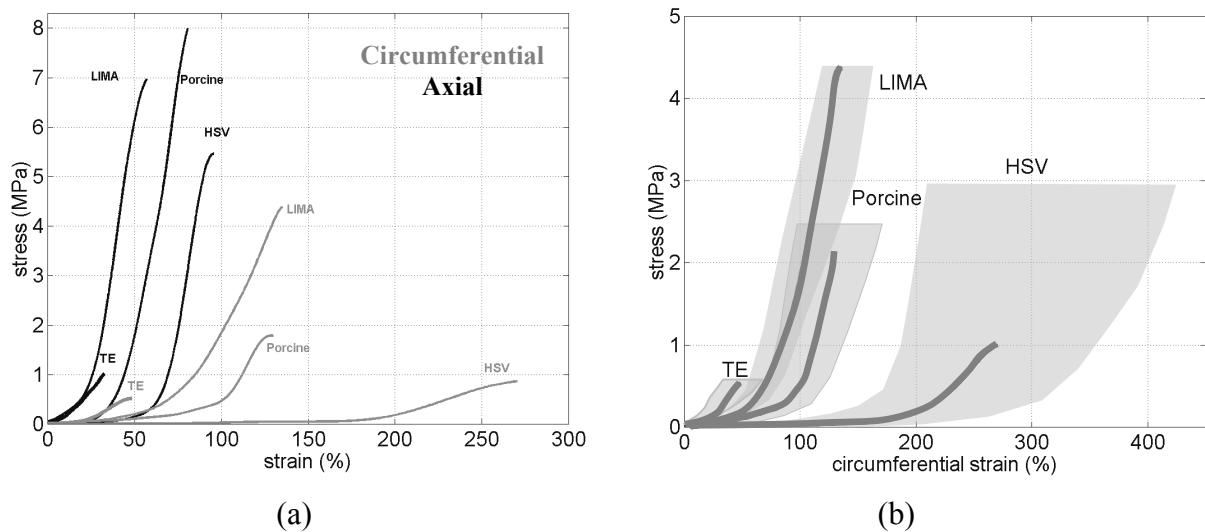


Figure 6.3: Representative stress-strain curves in circumferential and axial direction for the TE constructs and native equivalents, i.e., the human LIMA, HSV and porcine CA (a). Figure b shows in more detail the curves in circumferential direction and includes envelopes, within which all individual stress-strain relations are situated for each type of blood vessel.

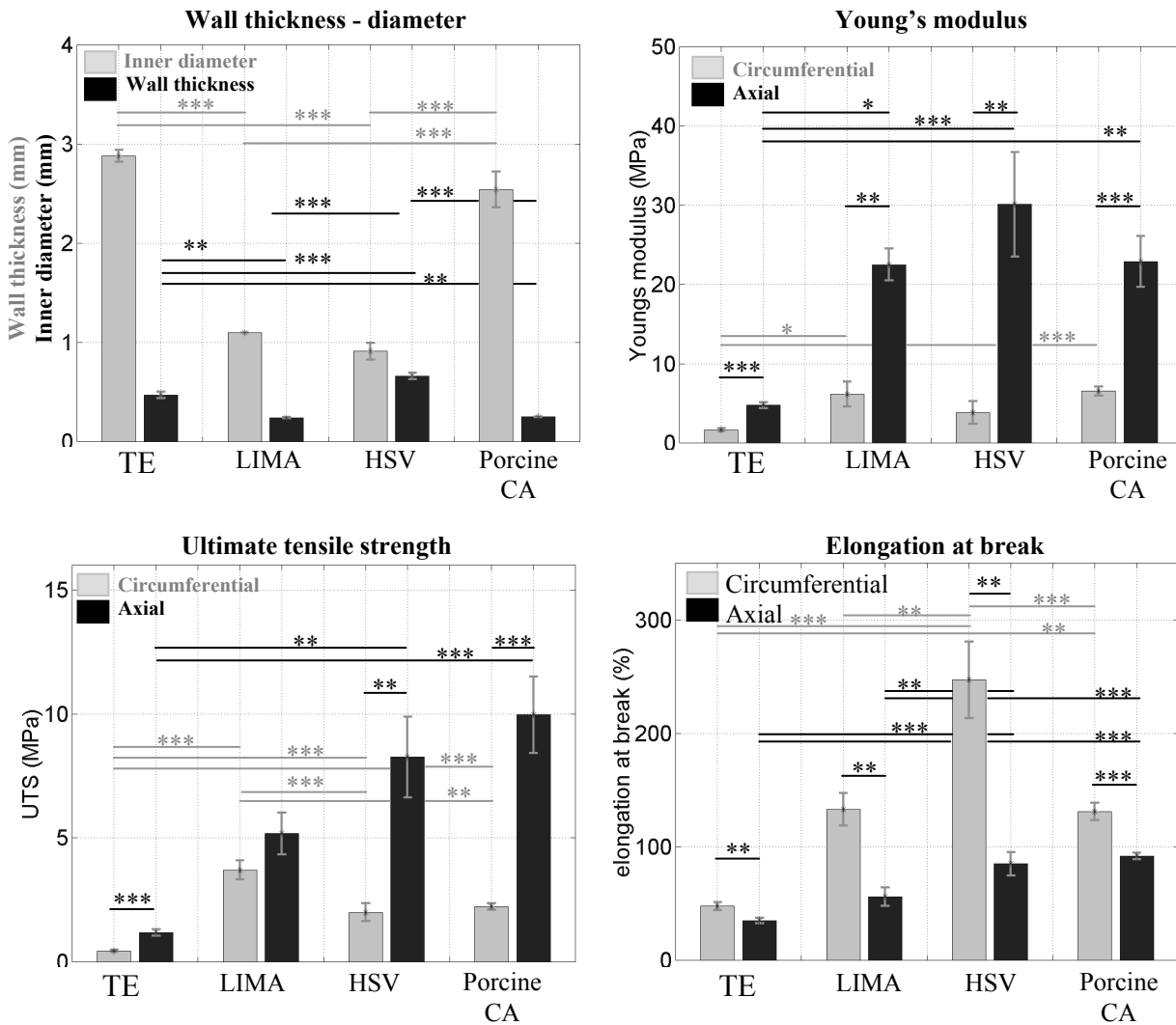


Figure 6.4: Geometrical and mechanical properties of TE constructs and native equivalents, i.e., the human LIMA, HSV and porcine CA. The Young's modulus, UTS and the elongation at break are given in axial (black) and circumferential (grey) direction. Data are presented as mean  $\pm$  sem (\* represents  $p < 0.05$ , \*\* represents  $p < 0.01$ , \*\*\* represents  $p < 0.001$ ).

The stress-strain curves in Fig. 6.3 are displayed over the whole measurement range up to stress values of 8MPa. However, it should be kept in mind that the physiological relevant stress range is much lower. In terms of pressure, the range from 0-500mmHg well displays all the relevant information about the mechanical behavior of the blood vessels. The measured wall stress in the tensile tests was converted to pressure values as described in chapter 3 (equation 3.5). The relevant wall stresses range approximately from 0 to 0.5 MPa. Figure 6.5 shows representative stress-strain curves in this range in circumferential direction for the TE construct, LIMA and the porcine CA (Fig. 6.5a). In addition, it shows the estimated pressure-strain curves (Fig. 6.5b). The curve for the HSV is included (dashed line) although the thin wall assumption is grossly violated ( $h > r$ ), as shown in Fig. 6.4). Fig. 6.5 shows that the behavior of the TE constructs at

relative low values of the wall stress and pressure does not deviate much from that of the LIMA.

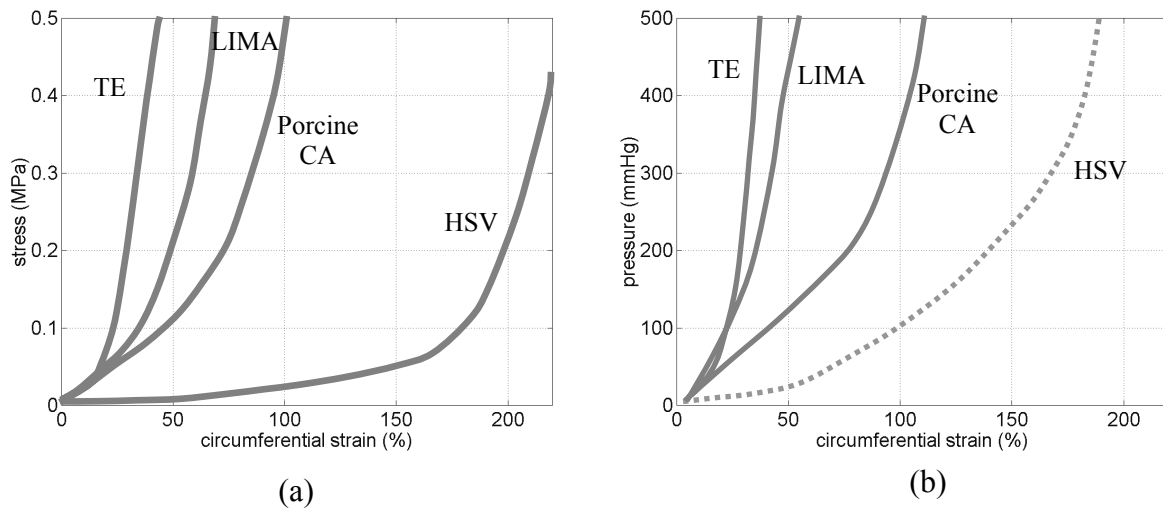


Figure 6.5: Circumferential stress-strain (a) and pressure-strain (b) curves at physiological relevant values for TE constructs and native equivalents, i.e., the human LIMA, HSV (dashed because the thin wall assumption is grossly violated), porcine CA.

#### 6.4. Discussion

Matching the mechanical properties of TE grafts to those of the host artery may enhance the post implantation performance of these grafts. On the other hand, at implantation, the mechanical properties may not need to be identical to those of a native artery as a TE vessel is composed of viable tissue with the potential to remodel, repair, and grow. The TE vessel is expected to adapt to local hemodynamic conditions and gradually acquire the structural and mechanical characteristics of the vessels it replaces. Nevertheless, some critical minimum demands remain. The construct should be strong enough to withstand surgical handling at implantation, it should withstand physiological pressure and it should consist of viable tissue that is able to remodel. To characterize the TE constructs of the present study, the properties were compared to native equivalents, while keeping the above considerations in mind. Measurements were performed on human left internal mammary artery (LIMA) and human saphenous vein (HSV), as these vessels are the most applied grafts in coronary artery bypass grafting. In addition, measurements were performed on porcine coronary arteries (CA) as these arteries show good morphological resemblance to human CA and are far easier to obtain.

The present study demonstrated that, although the tissue of the TE constructs was less developed than that of native vessels, the mechanical properties in the physiologically relevant range, assessed by tensile tests, did not differ much from that of the native human artery. The amount of collagen in the TE constructs was approximately 50% of that of the measured native blood vessels, whereas the amount of GAG was approximately 60% higher than that in native equivalents. The mechanical properties, in terms of the modulus and UTS, were much lower compared to those of native vessels.



This illustrates that not only the amount of collagen was less in the 4-week old constructs, but more importantly, the extent of its cross-linking and organization level. This aspect is likely to improve after implantation when the construct will remodel in the in-vivo environment.

At physiological relevant wall stresses and pressures, the mechanical properties of the TE construct, as assessed by tensile tests, were very similar to that of the native LIMA, i.e. the most successful vascular graft in coronary artery bypass grafting (CABG). It must be mentioned that the geometry of the TE vessel and the LIMA differed substantially, i.e. the diameter of the engineered vessel was on average 2.9mm, whereas this was 1.1mm for the LIMA. This difference influences the mechanical behavior in terms of pressure versus strain as described by Laplace's law (equation 3.5).

The burst pressure of the presented TE blood vessels was 900mmHg. Using thin wall assumptions and the Laplace relationship, it is possible to estimate the burst pressures of the native vessels from the circumferential tensile tests, as described in chapter 3 and applied in chapter 5. The measurements on the human LIMA and porcine CA result in an estimated burst pressure of 7000mmHg and 2000mmHg, respectively. No estimation can be obtained for the HSV, as the thin wall assumptions are grossly violated in this case. The estimation for the human artery seems to be fairly high, as reported values for the LIMA are in the order of 2000mmHg (L'Heureux, 2006). Reported values for the burst pressure of HSV are between 1680 and 3900 mmHg (L'Heureux, 1998; Yu, 1990). An aspect that could have influenced the accuracy of the measurements is the determination of the geometry of the vessels. The wall thickness and the vessel diameter were difficult to determine from the histological slides, especially in case of the irregular lumen structure of the HSV. The embedding process, necessary for the histological examination, might also have changed the original dimensions of the samples.

Ideally, the properties of the TE constructs should have been compared to those of human CA. However, in the course of the present study it was not feasible to perform measurements on these arteries, therefore human LIMA were investigated instead. Measurements of the mechanical properties of both these arteries were performed by van AnDEL (2003). Pressure-diameter and circumferential and axial stress-strain relations were obtained for both human CA and LIMA, and for porcine CA. Besides the principal finding that the porcine vessel wall was far more elastic than that of a human vessel, a small difference in elasticity was found between the human CA and LIMA (He, 2003). Thus, properties of the LIMA can be used as target properties for TE blood vessels. The more so because this artery is the most successful graft for CABG.

The properties of TE constructs and native equivalents were measured in-vitro. It should be acknowledged that differences exist between the in-vivo and ex-vivo behavior. To get more insight into these differences, Tajaddini and co-workers (2003) used intravascular ultrasound in conjunction with mechanical testing to examine vascular properties of intact porcine coronary artery ex-vivo and in-vivo. The in-vivo vessels appeared less compliant than ex-vivo, likely influenced by in-vivo factors such as myocardial support and vascular tone. Therefore care should be taken when extrapolating in-vitro measurements to in-vivo behavior.

In the present study, native blood vessels were treated with papavarine, a vasodilator, to enable proper measurements. In addition, it enabled a comparison between the mechanical properties of the extracellular matrix of the TE constructs and the native

vessels, excluding any interference by contractile smooth muscle cells. Pilot studies on treated and non-treated HSV demonstrated that the effect in the stress-strain curve was limited to the initial toe region of the curve. As such, the non-treated vessels showed an increased slope. No effects were found in the modulus and UTS of the non-treated and treated vessels.

Whereas a substantial amount of collagen was produced in the TE constructs, the constructs are likely to lack the right amount of elastin, compared to the native vessels. Although no measurements of elastin were performed in the present study, it is a general finding that TE constructs do not contain a significant amount of elastin after in-vitro culture (Mitchell, 2003). Because of the lack of elastin, the TE constructs are likely to creep, i.e. form an aneurysm, when subjected to physiological arterial pressure levels for longer periods of time. Further mechanical testing has to reveal to what extent this happens. Depending on the outcome of these measurements, it might be necessary to incorporate some sort of elastic layer in the construct. A possible solution might be adding an electrospun elastic layer to the construct, as described in chapter 3. Further experiments have to confirm whether such a construct shows as good a tissue development as the presented constructs and whether the functional behavior at physiological pressures will be improved.

In conclusion, the mechanical properties, at least those assessed by tensile testing, of the TE constructs and native arteries were remarkably similar in the physiological relevant range. The ultimate strength of the native vessels was, however, much higher. Further measurements of compliance, elasticity and long term behavior under physiological load should reveal whether these TE constructs are suitable for in-vivo investigation in animal models.





7

Endothelial cells

## 7.1. Introduction

In the field of vascular tissue engineering, many investigators concentrate on the development of tissue-like structures with high tensile strengths that provide mechanical support. Another critical issue for a tissue-engineered (TE) blood vessel substitute is to provide nonthrombogenicity. To achieve this, a functional endothelial layer is required. Research in humans and animal models has shown that endothelial cell (EC) function is more complex than was originally believed. Besides ‘simply’ providing a nonthrombogenic inner layer for a blood vessel, the endothelium is nowadays recognized as being a dynamic participant in vascular biology. It serves as a signal-transduction interface, linking the chemical and mechanical signals associated with flowing blood to the underlying vessel wall (Nerem, 1998). In addition, ECs residing in different mechanical environments exhibit different characteristics. This implies that the endothelium in, e.g., aorta, coronary artery and microcirculation behave substantially different. The apparent need for an EC-layer in TE vascular constructs initiated a new research domain. Several investigations showed rapid re-endothelialization of synthetic vascular grafts after implantation in animals, fast enough to prevent occlusions (Hertzler, 1981; Marquez, 1985; Zhang, 2004). This was explained by the inherent ability of the animals to self-endothelialize vascular lumens (Tebken, 2003). However, the endothelialization characteristics in animals and humans are incomparable, a problem that was only realized when initial clinical trials in humans provided poor results (Berger, 1972; Sauvage, 1974). Therefore, it is generally accepted that human vascular TE grafts should possess a confluent, functional EC layer prior to implantation. To achieve this target, two separate goals are defined. The first consists of a successful EC seeding method, the second addresses the functionality of the EC layer.

Several techniques exist for EC seeding. These techniques are commonly differentiated based upon the physical force applied in each seeding process, i.e. gravitational, hydrostatic and electrostatic. The most basic and extensively studied of these three techniques is the one that uses gravitational forces of seeding. To this end, the graft is filled with the EC solution and rotated periodically or continuously over a prolonged seeding time. For hydrostatic seeding techniques a pressure differential is used, either by increasing the internal pressure or by applying an external vacuum across the microporous graft wall. ECs are forced onto the luminal surface of the vascular graft. In the electrostatic cell seeding technique, the highly negatively charged surface, e.g., of synthetic grafts like e-PTFE, is changed in order to avoid the repulsion of negatively charged ECs (Pawlowski, 2004).

When ECs are seeded successfully, the identity and functionality should be tested. ECs can be characterized by immunohistochemistry for Von Willebrand factor (vWF), CD31, and eNOS staining. In addition,  $\alpha_1$ -fucosyl moieties identified by the plant lectin *Ulex Europaeus* Agglutinin I (UEA-1) can be used as a marker for ECs (Hamid, 2003). The nonthrombogenicity of the EC layer can be tested by exposing the grafts to flowing blood. The present study will only focus on the first goal, i.e. the EC seeding on vascular

grafts. Two different studies were performed, which should facilitate and allow further research on the functionality of the seeded EC layer. The first study concerns the seeding of the TE tubular constructs in the bioreactor presented in chapter 5. By applying the gravitational seeding technique, ECs harvested from human saphenous veins were seeded on fibrin-filled PGA/P4HB tubular constructs. The seeding protocol was evaluated by histology and fluorescent microscopy using the EC-specific staining Ulex Europaeus Agglutinin I (Holthofer, 1982). The second study focused on the co-culture of ECs and human saphenous vein myofibroblasts in TE constructs. Immunolabeling with Von Willebrand factor was used to identify the ECs on the construct.

## **7.2. Materials&Methods**

### **7.2.1 Cell culture**

Human myofibroblasts (HVSC) and endothelial cells (HVSEC) were harvested from human saphenous veins and expanded using regular culture methods up to passage 7. The medium to culture the HVSC consisted of DMEM Advanced (Gibco, USA), supplemented with 10% FBS (Biochrom, Germany), 1% Glutamax (Gibco, USA) and 0.1% gentamycin (Biochrom, Germany). The endothelial cells were cultured in EC medium containing EGM-2 (Cambrex, the Netherlands) supplemented with 20% FBS and growth supplements (EGM-2MV SingleQuots, Cambrex).

### **7.2.2 Bioreactor/seeding device**

The rotating device that enabled EC seeding in the bioreactor as presented in chapter 5, is shown in Fig. 7.1. The bioreactor was clamped in the rotation device and could be rotated continuously. The total system could be placed inside an incubator. The rotation frequency is 0.1Hz, which resulted in a velocity of the substrate relative to the cells of 0.1cm/s. This velocity was in the same order of the substrate velocity in a commercially available cell roller bottle system (Micronic, the Netherlands). As such, the frequency was expected to be sufficiently slow to facilitate cell attachment.

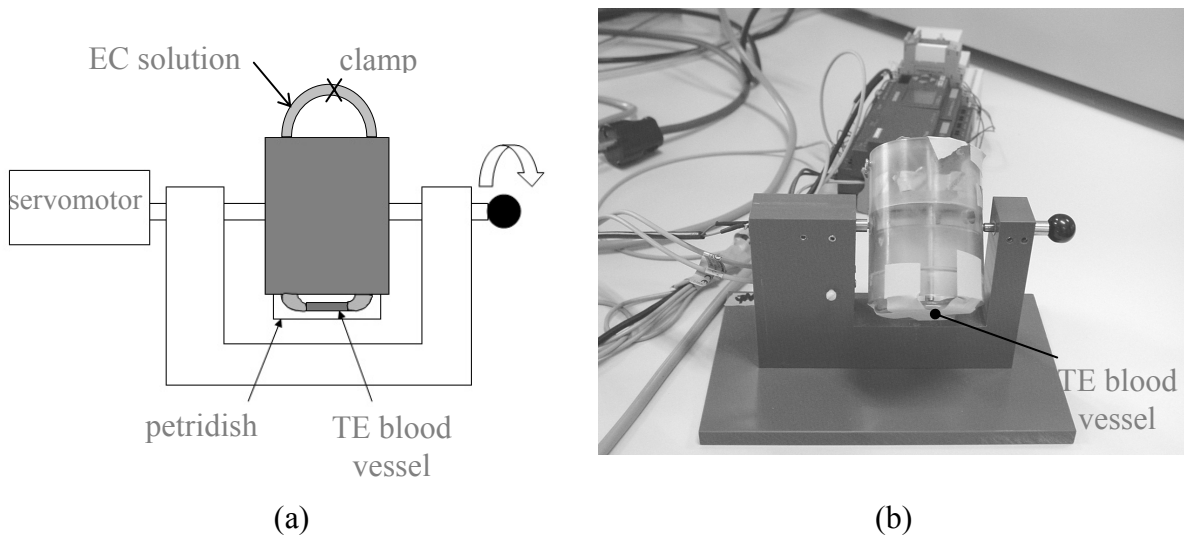


Figure 7.1: Schematic representation (a) and photograph (b) of the custom-made rotation set-up in which the bioreactor, as described in chapter 5, is placed for EC seeding.

### 7.2.3 Constructs and cell seeding

#### Seeding tubular scaffolds

In a first approach, tubular constructs of PGA/P4HB ( $n=3$ ), manufactured as described in chapter 2 (section 2.2.2), were attached in the bioreactor. A 3.0mm balloon catheter was inflated within the lumen of the scaffold. The construct was sterilized by soaking in 70% ethanol during 3 hours. Afterwards, the construct was washed in PBS and filled with a fibrin gel. The gel consisted of thrombin (10 IU/ml) and fibrinogen (10mg actual protein/ml, Sigma, USA) both dissolved in HVSC culture medium. The fibrin gel was left to polymerize for several minutes, after which the balloon catheter was deflated and removed from the lumen. The bioreactor was then placed inside an incubator to allow the fibrin gel to further polymerize during 20 minutes. Subsequently, the construct was flushed with EC medium to ensure that there was no leakage. HVSEC's were then trypsinized, centrifuged at 220g during 5 minutes and resuspended in EC medium, resulting in a final concentration of approximately  $4 \cdot 10^5$  cells/ml. A volume of 1 ml was injected via a silicone tube into the lumen of the construct. Subsequently, the bioreactor was placed in the rotation device and placed in the incubator. After 3 hours of rotation, the bioreactor was detached from the rotation device, the petridish was filled with EC medium, and the bioreactor was placed back in the incubator. After 1 day, the lumen of the construct was flushed with fresh EC medium. After 5 days of culture EC seeding was evaluated as described below.

#### Co-culture of EC and HVSC in a TE construct

In a second study, a rectangular PGA/P4HB construct was seeded with HVSC in combination with a fibrin gel, as described in chapter 3 (section 3.2.2). The constructs

were attached in a 6-wells plate by gluing the ends to the bottom of the plate. Due to this fixation, static strain was developed in the constructs which was assumed to stimulate tissue development, as discussed in chapter 4. The constructs were cultured in HVSC medium supplemented with ascorbic acid 2-phosphate (0.25 mg/ml, Sigma, USA) during 4 weeks. After this culture period, HVSEC were seeded on the constructs by carefully dripping an EC solution on top of the sample ( $10^5$  cells/cm<sup>2</sup>). Finally, after 4 hours, the well was filled with 7ml EC medium. After another 5 days of culture, the co-culture was evaluated as described below.

#### 7.2.4 Evaluation of EC seeding

##### Seeding tubular scaffolds

The EC-seeded tubular constructs were cultured for 5 days in the bioreactor. The results of the EC-seeding via the rotating device was evaluated by histology and fluorescence microscopy. For histology, a ring sample of each construct was fixed in 4% phosphate-buffered formalin and embedded in Technovit 7100 (Kulzer, Klinipath, the Netherlands). Sections of 5µm thick were stained with toluidine blue in order to visualize the seeded cells. The success of the seeding protocol and the appearance of the ECs was further analyzed by fluorescence staining. To this end, part of the seeded construct was stained with the EC-specific agent Ulex Europaeus Agglutinin I (UEA-I, Sigma, USA) labeled with fluoresceine isothiocyanate (FITC). In addition, the non-specific agent cell-tracker orange (CTO, Molecular Probes) was used to stain the cytoplasm of the cells. Confocal microscopy (Zeiss, CLSM 510) was used to visualize the constructs. Figure 7.2 shows an example of the UEA-I staining on a confluent monolayer of ECs. The staining was most pronounced at the edges of the ECs.

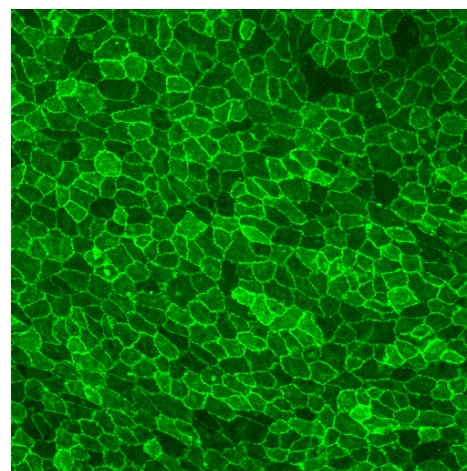


Figure 7.2: UEA-I staining of HVSECs

##### Co-culture of EC and HVSC in a TE construct

To analyze the HVSEC seeding on the cultured rectangular constructs, the ECs and myofibroblasts were labeled with CTO and UEA-I, as described above. In addition, immunolabeling with Von Willebrand factor (vWF) and DAPI was performed to characterize ECs and cell nuclei, respectively. To this end, 10µm thick paraffin sections were deparaffinized, washed in PBS containing 0.1% Tween 20 and subsequently treated with an antigen retrieval solution (0.04% pepsin, 0.5% milk powder in PBS, pH 2.0). After permeabilisation, slides were incubated at 4°C with the primary polyclonal rabbit antibody directed against human Von Willebrand Factor (a0082, Dako, The

Netherlands, dilution 1:500). Afterwards, a secondary antibody (GaR-IgG Alexa 555, Invitrogen Molecular probes, The Netherlands), diluted 1:200, was incubated for 90 minutes at room temperature. The secondary antibody was diluted in a DAPI solution to achieve counterstaining of the nuclei. After washing with a 0.1% Tween 20 solution in PBS to diminish background staining from non-specific binding antibody, slides were embedded in Mowiol (Sigma, The Netherlands). Digital pictures were captured using a Zeiss Axiovert 200 fluorescent microscope (Zeiss, Germany) mounted with a monochrome Axiocam, using appropriate filters and post-hoc color definition. Exposure times were kept similar in all slides to ensure that images of different sections were well comparable.

### 7.3. Results

#### Seeding tubular scaffolds

The cell seeding of the tubular constructs using the rotation device was evaluated histologically using toluidine blue staining. Figure 7.3 shows a cross-section of the PGA/P4HB constructs filled with a fibrin gel and seeded with ECs. From these slides it was estimated that approximately 50-75% of the lumen was covered with ECs. The appearance of the EC varied throughout the constructs. Some segments contained individual ECs that appeared rounded (Fig. 7.3b) while other areas showed well-spread and connected ECs (Fig. 7.3c).

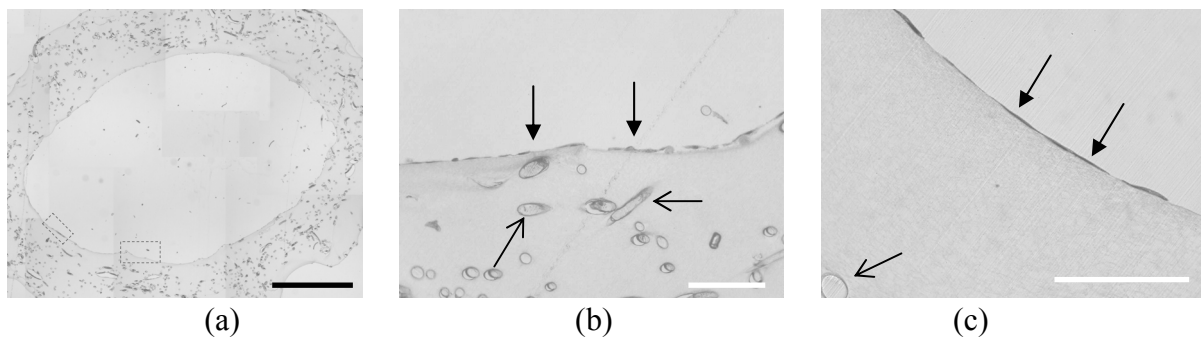


Figure 7.3: *Toluidine staining of EC seeded PGA tubular constructs, complete cross section (a) and higher magnification images (b,c) showing ECs (closed arrows) and PGA fibers (open arrows). The black bar indicates 1mm, the white bars indicate 100 $\mu$ m.*

The UEA-I/CTO staining confirmed the presence of ECs on the luminal side of the tubular constructs as shown in Fig. 7.4. A projection of the luminal area clearly showed the appearance of the cells (Fig. 7.4b). Some regions contained well-spread ECs (at the bottom half of the image), whereas at other locations, ECs appeared less confluent and more elongated (upper part of the image). Fig. 7.4 c and d show a higher magnification of a confluent lining of EC.

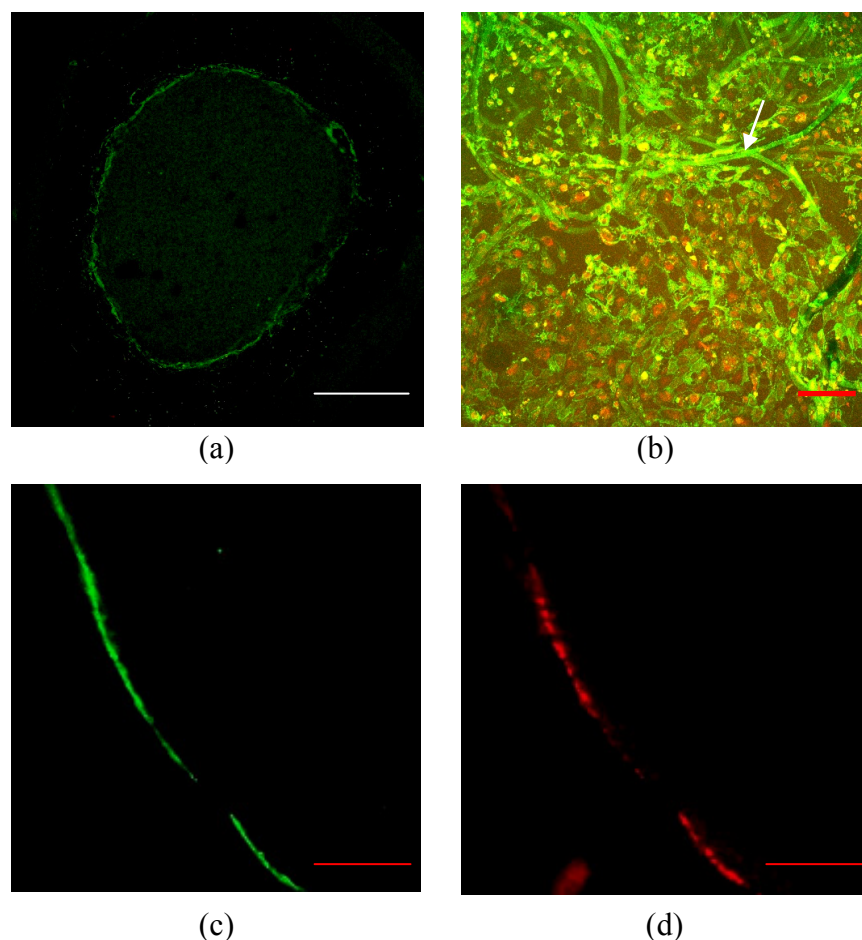


Figure 7.4: FITC-UEA-I / CTO staining of a tubular PGA/P4HB construct. Figure a shows a cross-section of the tubular construct (2.5x objective), figure c (UEA-I) and d (CTO) show the inner wall of the construct at a higher magnification (10x objective) visualizing a connected line of ECs. A projection of the lumen surface is shown in figure b. The white arrow indicates an autofluorescent PGA fiber. The white bar indicates 1mm, the red bars indicate 200 $\mu$ m.

#### Co-culture of HVSEC and HVSC in a TE construct

HVSECs were seeded on the surface of a 4-week cultured rectangular PGA/P4HB construct containing HVSCs. vWF staining revealed an endothelial lining on the surface of the constructs (Fig. 7.5a) which was confirmed by the DAPI staining of cell nuclei (Fig. 7.5b,c). In addition, a strong non-specific staining of polymer fragments was found deeper in the construct (Fig. 7.5a-c). The UEA-I/CTO staining demonstrated a sub-confluent layer of HVSECs on top of the seeded construct (Fig. 7.5d). The CTO-stained HVSC-seeded construct was visualized under the layer of HVSECs.



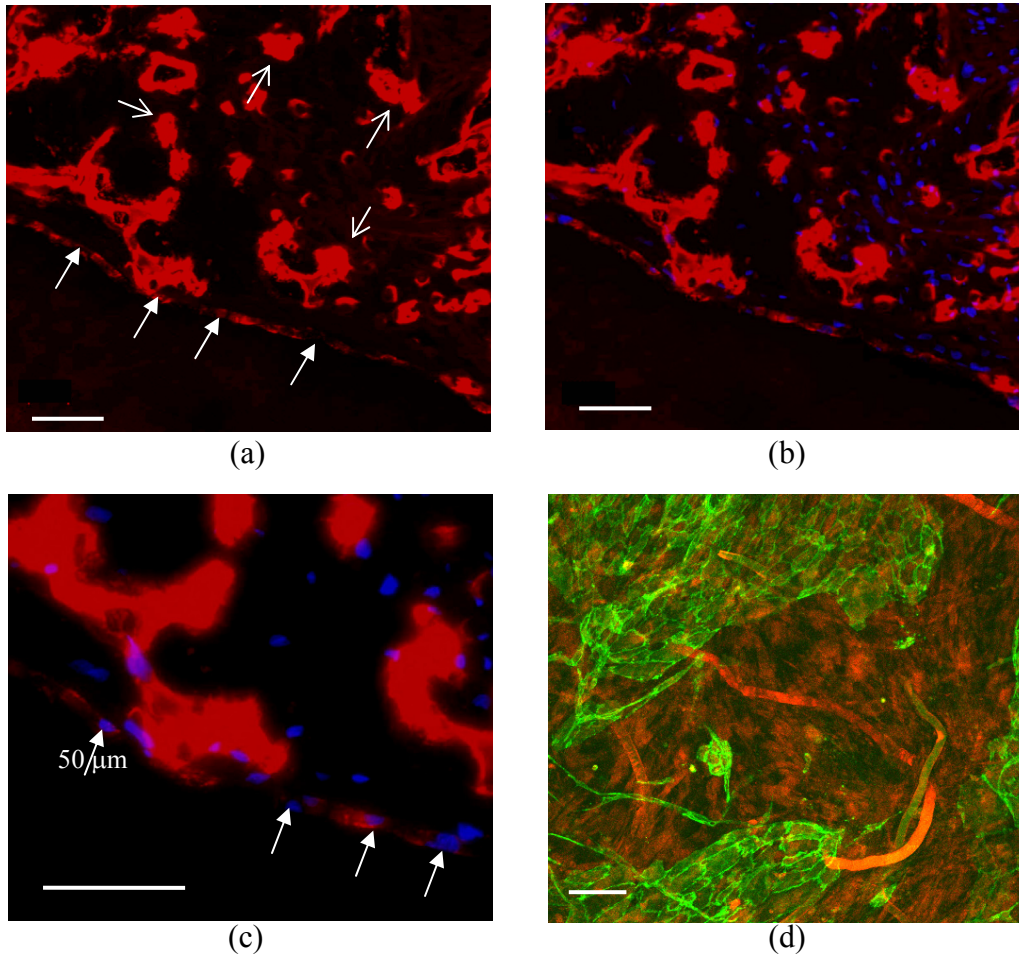


Figure 7.5: *Immuno-labeling with vWF (a-c, sideview) and UEA-I staining (d, top view) of HVSECs on top of the TE construct containing HVSC. Figure a shows the vWF staining (red) of a layer of HVSECs (closed arrows). In addition strong non-specific staining is visible of the autofluorescent PGA scaffold (open arrows). DAPI-stained cell nuclei (blue) of HVSEC and HVSC are shown in figure b and c. Figure c shows a higher magnification of figure c, illustrating the EC lining at the surface of the construct. FITC-UEA-I / CTO staining (d, topview) of the construct shows sub-confluent areas of HVSECs (green) and the underlying HVSC layer (red), autofluorescent PGA fibers appeared in red. The white bar indicates 100  $\mu\text{m}$ .*

## 7.4. Discussion

Aside from mechanical strength and elasticity, tissue-engineered (TE) vascular grafts should possess a confluent endothelium. This endothelial layer is not only required to prevent thrombosis, but also serves as a signaling interface and a

control for vasoactivity. TE blood vessels based on PGA, which resembled the TE constructs presented in chapter 5, have already been seeded with ECs followed by successful implantation into saphenous arteries of swines (Niklason, 1999). These investigators reported patency of the TE grafts up to 24 days, as recorded by digital angiography. The ECs in these constructs formed a sub-confluent layer before implantation. In another study, fibrin-based TE vascular grafts seeded with ECs were successfully implanted in jugular veins of lambs (Swartz, 05). Patency of these grafts was reported up to 15 weeks postgrafting. However, we should keep in mind that the endothelialization characteristics in animals and humans are incomparable. In contrast to animals, spontaneous endothelialization does not seem to occur in humans (Herring, 1985). Therefore, it can be concluded that, compared to animal grafts, the formation of a functional and confluent EC layer on human vascular grafts prior to implantation is more critical.

In the present study, two pilot studies were performed that facilitate further research towards obtaining a functional endothelium on the human TE blood vessels as presented in chapter 5. These studies concerned the first step in this process, i.e. the seeding of the EC on vascular constructs. Using the developed rotation device, it was possible to seed a layer of EC on scaffold constructs while attached in the bioreactor. In addition, we succeeded in seeding EC from human source, i.e. isolated from human saphenous vein, on rectangular TE constructs that were cultured with myofibroblasts. The cells attached to the surface but did not yet form a completely confluent layer. The identity of the EC was confirmed by UAE-I staining and immuno-labeling with vWF. To reach EC confluency on the TE vascular constructs, several aspects should be further investigated, which include the culture medium, the seeding density and the culture time. E.g., other pilot studies in our laboratories demonstrated that the applied EC medium counteracted the tissue formation in the constructs and, conversely, the EC did not survive in the applied TE culture medium. In current studies we aim to find a culture medium which promotes both tissue development and EC growth. In addition, an optimum has to be found between the seeding density and the culture time. Not shown data indicate that, in some cases, the EC layer developed well until a certain time point and then appeared to reduce. At present, it is not yet clear why this happened. A possibility is that the degradation products of the PGA accumulated in the construct, thereby lowering the pH of the local environment. The formation of a confluent EC layer might be stimulated by subjecting the cells on the construct to certain flow conditions. Several other studies applied this method and demonstrated that it allowed the EC to reach confluency and to make them more resistant against in-vivo shear stresses (Schnittler, 1987; Niklason, 1999).

In conclusion, EC were successfully seeded on tubular scaffolds and rectangular TE constructs. More research is necessary to reach a fully confluent EC layer on the TE blood vessels, which might include the application of flow during culture. In addition the functionality of this layer should be tested, e.g. by subjecting it to flowing blood. These experiments will be performed in the near future.

## **7.5. Acknowledgements**

We gratefully acknowledge Robert van Lith and Rolf Pullens for their contributions to this study. We further would like to thank Reinout Hesselink for his work on the immunostainings.

# 8

## General discussion

## 8.1. Introduction

The need for small diameter vascular grafts that are used for coronary arterial bypasses is large. The golden standards are the autologous saphenous vein (HSV) and left internal mammary artery (LIMA). Although the LIMA shows good results in terms of patency, its usable length is limited. The HSV performs poorer, approximately 15% to 30% of these grafts occlude in the first year, while 50% of the saphenous vein grafts are expected to be occluded within 10 years after implantation (Peykar, 2004). In addition to these limitations, 30% of patients do not have suitable veins or arteries (Bordenave, 2005). Current alternatives are prosthetic conduits based upon expanded polytetrafluoroethylene (ePTFE) and polyethylene terephthalate (Dacron). However, the patency of these prosthetic small diameter grafts at 5 years is only 20-50% (Baguneid, 2006). Tissue engineering of vascular grafts might be an alternative source. Such a graft should meet many requirements concerning, e.g., biocompatibility, mechanical behavior, biological function and processing properties. In general a vascular graft should at least meet the following functional criteria: it should possess tensile strength to provide mechanical support, an elastic component to provide recoil and prevent aneurysm formation. In addition, it should have a confluent endothelium to prevent thrombosis and to provide full functionality to the blood vessel. To reproducibly meet all these criteria in a single blood vessel remains a challenge.

A major advantage of a TE vessel is that, at implantation, it does not need to have properties identical to those of a native artery. Being composed of viable tissue with the potential to remodel, repair, and grow, a TE vessel might be able to adapt to local hemodynamic conditions and acquire the structural and mechanical characteristics of the vessel it replaces.

Starting from the critical functional criteria, the present thesis focuses on the first requirement for small diameter TE blood vessels, i.e. mechanical strength. The demands regarding strength, e.g. in terms of burst pressure, are not well defined. TE blood vessels should at least withstand physiological pressures. In addition, they should withstand surgical handling at implantation. It can be postulated that TE blood vessels should at least withstand pressures up to 500mmHg. In addition to the strength of TE blood vessels, the present study addresses issues regarding elasticity and endothelium.

The results of the present thesis are summarized and discussed in the next section. Future research is discussed in section 8.3

## 8.2. Tissue-engineered constructs

The TE blood vessels presented in this thesis consisted of a P4HB coated PGA scaffold. Myofibroblasts were harvested from human saphenous veins and seeded in combination with a fibrin gel into the scaffold. Mol and co-workers (2005; 2006) already showed that the combination of this scaffold, these cells and a strain-based mechanical conditioning protocol resulted in relative strong TE heart valve leaflets. In the present study, tubular

constructs were subjected to static and dynamic straining protocols in both axial and circumferential direction. For this, two separate bioreactors for tubular constructs were developed, one that allowed static and/or dynamic axial straining and another one that combined static axial strain with dynamic circumferential strain. Compared to static controls, static axial strain, which was induced by counteracting the compaction of the tissue in this direction, resulted in improved tissue formation and mechanical properties in the TE blood vessel. The mechanical properties were best developed in axial direction. The additional effect of dynamic strain in this direction was limited or even negative. The mechanical properties in circumferential direction, most critical for the mechanical behavior of a vessel, improved significantly when the tubular constructs were subjected to an additional dynamic strain in circumferential direction. After 4 weeks of in-vitro culture, the combination of static axial strain and dynamic circumferential strain resulted in the strongest TE blood vessels.

### 8.2.1 Tissue development

In the present study, the amount of developed tissue in the TE constructs was compared to that in native equivalents, i.e. human saphenous veins (HSV), human left internal mammary arteries (LIMA) and porcine coronary arteries (CA). The amount of DNA in the TE constructs equaled  $2.5 \pm 0.3 \mu\text{g}/\text{mg}$  and did not significantly differ from the measured amounts in the human and porcine native vessels. After conversion of the hydroxyproline tissue content to collagen, using a conversion factor of 8.8 based on the molecular weight of hydroxyproline and collagen, we found collagen contents of about  $0.13\text{g}/\text{g}$  tissue. Mol and co-workers (2006), who used a similar culture protocol although applied to valvular constructs, reported comparable amounts of collagen. In TE vessels cultured up to 8 weeks, the group of Niklason (Klinger, 2006) reported a collagen content up to  $0.22\text{g}/\text{g}$ . The measured amount of collagen in the native LIMA was on average  $0.26\text{g}/\text{g}$ , values that correspond well to the amount of collagen reported for human coronary arteries, i.e.  $0.30\text{g}/\text{g}$  (Ozolanta, 1998). The content of collagen in our TE constructs amounted to, on the average, 50% of that of native vessels. The amount of elastin in human CA is approximately  $0.06\text{g}/\text{g}$  (Ozolanta, 1998). Although we did not measure the amount of elastin, the TE construct likely did not contain any measurable amount of elastin (as discussed below). The amount of GAG in the engineered constructs was found to be  $22 \mu\text{g}/\text{mg}$ . A significantly higher value of  $33 \mu\text{g}/\text{mg}$  was reported by Mol (2006). Values as measured in the native human and porcine equivalents, amount to about  $14 \mu\text{g}/\text{mg}$ , which is significantly less than in our engineered constructs.

It can be concluded that the amounts of DNA and extracellular matrix proteins of the TE constructs are, to a certain extent, comparable to those of native vessels. However, in terms of structural organization, native vessels are much more developed and organized in a layered structure, as was very clearly indicated by histology (Fig. 6.1). Nevertheless, it is questionable whether or not the ideal design of a native artery has to be equaled in a TE vessel. As has been shown, at least in animal models, in-vivo remodeling of the construct occurs in response to the local hemodynamic conditions (Hoerstup, 2000).

## 8.2.2 Mechanical properties

In our approach, mechanical properties of the TE constructs were assessed by uniaxial tensile tests, both in axial and circumferential direction, and by burst pressure measurements. It is commonly agreed upon that the burst pressure is the key measure for comparison of the strength of (TE) blood vessels. The best TE constructs presented in this thesis achieved a burst pressure in the order of 900mmHg after a culture period of 4 weeks. These values suggest that our constructs reached high strength values when compared to the values reported by other researchers. For instance, Klinger and co-workers (2006) reported burst pressures up to 500mmHg in TE blood vessels after a 8-week culture period. As in our studies, these constructs were based on PGA and seeded with myofibroblasts isolated from human saphenous veins. In contrast to our study, the PGA scaffold was not extended with a P4HB coating and fibrin gel. Mol and co-workers (2003) already showed that the use of fibrin enables effective and homogeneous cell seeding and improves the production of extracellular matrix. In addition, in the study by Klinger (2006), the reported results could only be obtained when the cells were genetically modified, i.e., via human telomerase reverse transcriptase (hTERT) gene transfection. This transfection increases the replicative capacity of the fibroblasts. Constructs cultured with non-modified cells resulted in weak blood vessels, possessing burst pressures in the order of 100mmHg (Poh, 2005). The highest burst pressure of TE human blood vessels has been recently reported by L'Heureux (2006). Using a sheet-based method, this research group cultured TE blood vessels that possessed burst pressures up to 3500mmHg, which even exceeds the value of 2030mmHg that was found for human internal mammary arteries (patient age  $70 \pm 10$  years, L'Heureux, 2006). However, the time needed to produce these TE vessels was approximately 28 weeks. Reported values for burst pressures of human saphenous veins vary from 1680mmHg (L'Heureux, 1998), 2273mmHg (Lamm, 2001) to 3900mmHg (Yu, 1990). For the groin saphenous vein an even higher value of 4890mmHg was reported (Yu, 1990).

When the burst pressures of different blood vessel constructs are compared, one should realize that the burst pressure depends on the geometry of the vessel. In addition, what the vessel wall really has to withstand is not pressure but wall tension. The tissue has a stress limit that it can sustain without failure. The stress on the wall material of a thin-walled tube is given by  $(\Delta P * r / h)$ , i.e. the transmural pressure times the vessel radius divided by the wall thickness. Because the stress is finite for the tissue, the burst pressure will decrease with increasing diameter of the vessel and thinning of the vessel wall. As in our study the geometry of the TE vessels and the human equivalents significantly differed, e.g. the diameter of the TE constructs was 3 times larger, the outcomes of the tensile tests allowed a more reliable interpretation of vessel strength. In addition, tensile tests allowed comparison of the mechanical properties in circumferential and axial direction. These measurements revealed that both TE constructs and native blood vessels were stronger in axial direction, as indicated by a higher Young's modulus and ultimate tensile strength in this direction compared to that in circumferential direction. The tensile tests further demonstrated that the mechanical properties of the TE constructs, in terms of Young's modulus and ultimate strength,

could not compete with those of native equivalents. Within the physiological range, however, the differences in mechanical properties were minimal. More precisely, the behavior of the 4-week old TE constructs, as assessed by tensile tests, remarkably resembled that of the human adult internal mammary artery. As was demonstrated by Niklason (2001) and L'Heureux (1998), we can assume that longer culture periods will even further improve the mechanical strength of our TE constructs. In the study by Niklason, an increase of the burst pressure of bovine TE vessels was reported from 'unmeasurable' at three weeks, to 570mmHg after 5 weeks, and up to 2150mmHg after 8 weeks (Niklason, 2001). In case of human TE vessels, using the sheet-based approach, L'Heureux also reported a gradual increase of the burst pressure over time (L'Heureux, 1998). It is, however, questionable whether a further increase of the strength of the presented constructs, for instance by increasing the culture time, is worthwhile. Based on, e.g., the successful implantation of relatively weak vascular constructs in the veins of lambs (Swarz, 2005), it is likely that the strength of the presented constructs is sufficient.

Another critical criterion concerns the elasticity of the TE constructs. Without this property, vascular grafts will risk to creep permanently, eventually resulting in the formation of aneurysms. Although our TE constructs lack elastin, elaborate mechanical testing has to reveal to what extent and in what time scale the constructs will develop pathological creep.

### **8.3. Future research**

Although it can be agreed upon that acceptable strength has been achieved in the presented TE constructs, several other critical aspects have to be addressed. Further mechanical testing should elucidate the need for improvement of elasticity and compliance of the TE vessels. Second, human TE grafts require a functional endothelium. Although EC seeding experiments on the TE constructs were already performed, further investigation is necessary to achieve a confluent and functional EC layer. Only when the mechanical issues and the critical role of the endothelium are sufficiently solved, research on implantation into animal models might elucidate the potential of the presented constructs.

#### **8.3.1 Mechanical testing**

Uniaxial tensile and burst pressure tests, as described in this thesis, provide important information regarding the strength of TE constructs. However, as vascular TE grafts are intended for application in clinical studies, it will become increasingly important to understand how constructs will respond to mechanical loads, both acutely and as a function of time. Viscoelastic characterization describes time-dependent properties and can be used to predict material behavior (Berglund, 2005). Tests that should be performed to assess this behavior include stress relaxation and creep tests. Such measurements can be included in the tensile testing protocol. In addition, long-term validation, i.e. in the order of days to weeks, is necessary to predict the long-term mechanical behavior. TE vascular constructs should be subjected to physiological



pressures for a prolonged period of time, while monitoring the mechanical behavior. This will elucidate, e.g., the time frame in which creep possibly develops. It should be mentioned that although these measurements will predict the in-vivo mechanical behavior, they will not include the possible positive effects of in-vivo remodeling.

### **8.3.2 Elasticity / Compliance**

If the above mentioned mechanical tests will predict failure because of a lack of elasticity, it will be necessary to improve this mechanical characteristic prior to implantation. For this two different approaches can be distinguished, adjusting the scaffold characteristics or stimulating the in-vitro formation of elastin, as discussed below.

#### **Scaffold modification**

A temporary elastic scaffold layer at the inside of a TE construct might mimic the inner elastic layer of a native blood vessel. As such, it will improve its functional mechanical behavior in the physiological range. For this, adding an inner electrospun PCL layer, as described in chapter 3, might be a solution. However, such a layer of PCL is possibly not elastic enough. Rubber-like materials are more elastic and might therefore be better candidates. To improve the compliance of the TE graft, the elastic layer should determine the mechanical properties at low strain values while the collagen in the construct takes over at higher, supra-physiological, strain values. This can only be achieved when the elastic layer is under tension at physiological pressure values while the collagen-containing layer is not. These conditions, which are characteristic for a native blood vessel, should be considered when designing a more elastic, compliant scaffold.

#### **Elastin**

Elastin fibers, essential for vascular recoil, are mostly absent in vascular grafts before implantation (Mitchell 2003). Several animal post-implant studies, however, revealed in-vivo elastin development (Hoerstrup, 2000; Niklason, 1999). The question is whether this in-vivo process is fast enough to compensate for the lack of elastic properties of the TE graft at the time of implantation. In-vitro stimulation of insoluble elastin production remains difficult. This may be aggravated by the fact that TE constructs are often cultured in the presence of ascorbic acid (vitamin C) that promotes the formation of collagen (Niklason, 2005; L'Heureux, 1998; Mol, 2005). Ogle and co-workers (2002) showed that ascorbic acid negatively affects the elasticity of collagen-based constructs. To counterbalance this effect, these investigators also applied retinoic acid (vitamin A) in order to increase elasticity. TE constructs treated with such a combination of vitamin A and C showed a better elasticity than untreated constructs or constructs treated with vitamin C alone. Although not as strong as constructs treated with vitamin C alone, constructs treated with both vitamins exhibited mechanical properties that, at least at low stress values, more closely mimicked those of a native vessel. A refinement of dose, duration and administrative timing might further optimize the mechanical behavior of TE constructs.

### 8.3.3 Endothelial cells

To provide non-thrombogenicity, vascular grafts need a confluent functional endothelium. Whereas it has been demonstrated that animals are able to self-endothelialize the lumen of vascular grafts (Teebken, 2003), in humans endothelialization is extremely slow and almost never complete (Rahlf, 1986). Therefore, it seems to be unavoidable to seed human vascular grafts with endothelial cells (EC) prior to implantation. It has been shown that EC seeding improved patency of synthetic grafts (Seifalian, 2002). These studies demonstrated that cell density, seeding time and conditioning protocols were all important issues. One of the conclusions was that low density seeding fails, while seeding at a high density, referred to as sodding, improved clinical outcome (Tiwari, 2001). Swartz (2004) demonstrated that fibrin-based vascular constructs that were implanted in jugular veins of lambs 3 days after EC seeding displayed thrombogenicity with minimal space for blood flow 15 weeks after implantation. In contrast, the same type of implants cultured with EC for 10 days, under no-flow conditions, showed only minimal fibrosis without thrombus formation. Although performed in an animal model, this study demonstrated the influence of EC culture time prior to implantation. In addition, Dardik and co-workers (1999) tested the hypothesis that pretreatment with sustained in-vitro shear stress enhances subsequent EC retention on vascular grafts after implantation. To this end, polyurethane vascular grafts were seeded with rat aortic EC, cultured for 6 days and subsequently implanted as aortic interposition grafts in rats. In contrast to pretreatment with zero or low shear stress, relative high shear stress, i.e. 2.5Pa, resulted in the retention of fully confluent EC monolayers on the grafts 24 hours after implantation. In addition, the treated grafts demonstrated reduced neointimal thickening after 3 months.

In conclusion, it can be agreed upon that human TE vascular constructs have to be seeded with EC prior to implantation. Prolonged culture after EC seeding, all or not in combination with shear stress conditioning might stimulate the formation of a confluent EC layer and thereby improve the success of implantation.

### 8.3.4 Animal studies

In-vivo implantation in animal models is needed to further elucidate the potential of the TE vascular grafts. Information about, e.g., the functional mechanical behavior, patency rate, in-vivo scaffold degradation and remodeling properties can be obtained. Heart valves constructs based on the same scaffold material as used in the TE vessels presented in this thesis, i.e. a combination of PGA and P4HB, were already tested in lambs (Hoerstrup, 2000). To this end, scaffolds were seeded with autologous ovine myofibroblasts and endothelial cells and, after a culture period of 14 days in a pulse duplicator, implanted into lambs. Echocardiography demonstrated mobile functioning leaflets without stenosis, thrombus, or aneurysm up to 20 weeks after implantation. Complete degradation of the polymers, as determined by gas chromatography, occurred

by 8 weeks after implantation. It should, however, be mentioned that small amounts of P4HB, not detectable by the applied detection method, were likely to be present for a longer duration. DNA and extracellular matrix content, i.e. collagen, glycosaminoglycans, and elastin, increased to levels of native tissue and even higher at 20 weeks. This study showed that TE constructs based on a PGA/P4HB scaffolds are able to demonstrate functional behavior and yields promising tissue remodeling characteristics. In another related study, fibrin-based constructs, which were cultured for 2 weeks and subsequently seeded with EC, were implanted in jugular veins of lambs (Swartz, 2005). Angiography at 5 week postgrafting showed that the grafts were patent with no signs of aneurysm formation. At 15 week postgrafting, it was demonstrated that the vessels were still patent. Upon further investigation, significant amounts of produced collagen and elastin were found, although the fibrillar organization of elastin was not as extensive as that of control vessels.

To test the potential of the presented TE blood vessels in animal models, our constructs should be cultured with autologous animal cells. This likely implies some changes in the culture protocol as cells from different species react differently to mechanical conditioning (Seliktar, 2001). In addition, as the mechanical properties of TE vessels are highly species dependent (Niklason, 1999; McKee, 2003), the outcome of an autologous animal model might not be representative of the performance of a human TE vessel. Therefore, in another approach, human TE blood vessels could be implanted in immunodeficient animals, as was demonstrated by L'Heureux (2006). Prior to these experiments, EC functionality on the human TE grafts should be tested by subjecting them to human blood flow. These tests will elucidate on the risk of flow-induced thrombosis.

### 8.3.5 Cell sources

An important consideration in the field of tissue engineering is the cell source. To create tissues for transplantation into a patient the ideal donor cells are autologous. These cells should be easily obtainable, readily expandable in-vitro without the loss of differentiated phenotype or function, and implantable with little or no immune reaction (Shieh, 2005). In most cardiovascular tissue engineering approaches, cells are harvested from donor tissues, e.g. from peripheral arteries (mammary artery, radial artery) or veins (saphenous vein) which are routinely used in heart surgery. Recently, the role of cellular replicative lifespan, this is the number of times a cell population can divide, is gaining attention in the world of tissue engineering (Rhim, 2006). This seems to be logical because sometimes relatively long culture times are required for constructing adequate blood vessels. Autologous donor cells are not always feasible, particularly those derived from elderly patients. Some attempts have been made to overcome these problems. E.g., proliferative arrest was overruled by the ectopic expression of telomerase via human telomerase reverse transcriptase (hTERT) gene transfection (Klinger, 2006). This resulted in blood vessels that were stronger than control constructs. However, hTERT expression did not reverse or inhibit biochemical aging of cells. Therefore, the strength of the vessel constructs decreased with the age of the donors. A further drawback of harvesting vascular cells from donors is the necessity to sacrifice an intact vascular

structure of the patient. In addition, vessels from patients suffering from systemic atherosclerotic vascular diseases may not be a suitable cell source at all (Neuenschwander, 2004).

As a result of all these arguments, recent progress in stem cell biology has had a marked impact on the progress of tissue engineering. Stem cells, capable of self-renewal and differentiation into various cell lineages, hold great promise for treating affected tissue in which the source of cells for repair is limited or not readily accessible (Shieh, 2005). In a study by Matsumura (2003), bone marrow cells (BMC) were seeded on a polymer scaffold to create a TE blood vessel. The constructs were implanted in the inferior vena cava of dogs. These investigators demonstrated that the BMC contributed to vessel formation and ultimately differentiated into SMCs as well as ECs. The in-vivo study showed no evidence of stenosis after two years. In another approach, Schmidt and co-workers (2005) cultured living patches from human umbilical cord-derived fibroblasts and endothelial progenitor cells (EPC), which were obtained from the umbilical cord blood. However, it was not yet possible to culture strong vessels from these cells.

In conclusion, several promising cell sources are currently under investigation. Further research and long-term follow-up has to confirm the potential of these approaches.

### **8.3.6 Clinical implantation**

The transition from animal studies to clinical application in humans is not straightforward. Indeed, in-vivo implantation of (seeded) synthetic grafts already demonstrated the crucial differences between animal and human studies. Especially the differences in endothelialization properties appeared to be of high importance. In a first approach, constructs have to be implanted in 'low risk' positions, such as low pressure-sides in the vascular system. A few approaches of TE blood vessels have reached the phase of clinical trials. In a study by Shin'oka (2005), clinical results in young patients (1-24 years) showed promising results. Biodegradable grafts, based on a polymer tube of a copolymer of l -lactide and -caprolactone, were seeded with autologous bone marrow cells and used as an extracardiac total cavopulmonary connection graft. Normal function and good patency was reported up to a maximum follow-up of 32 months. Recently, another human clinical trial of TE blood vessels was recently presented at the American Heart Association meeting. In this approach strong TE blood vessels (L'Heureux, 2006) were used in haemodialysis patients. The grafts were used as an A-V shunt between the humeral artery and axillary vein in two dialysis patients. Follow-up showed no failures up to six and a half months. The utilization of TE grafts in these patients could not only serve as a trial for the use in CABG, but might also represent a large clinical application area for TE blood vessels.

Even though promising results are reported in clinical trials, the stage at which autologous tissue-engineered vascular replacements are available off the shelf, clinically applicable to all surgical centers and cost-effective for surgical use, is still far away.

In conclusion, the small diameter TE blood vessels presented in this thesis showed good tissue development and are strong enough justifying further research including animal models. Prior to implantation in these models, matters on the elasticity and compliance

of the vessels have to be addressed through more elaborated mechanical testing protocols. In addition, the constructs have to be seeded with endothelial cells to provide a functional endothelium.

# References

- Ameer GA, Mahmood TA, Langer R. A biodegradable composite scaffold for cell transplantation. *J Orthop Res.* 2002 Jan;20(1):16-9.
- Andel CJ van, Pistecky PV, Borst C. Mechanical properties of porcine and human arteries: implications for coronary anastomotic connectors. *Ann Thorac Surg.* 2003 Jul;76(1):58-64; discussion 64-5.
- Baguneid MS, Seifalian AM, Salacinski HJ, Murray D, Hamilton G, Walker MG. Tissue engineering of blood vessels. *Br J Surg.* 2006 Mar;93(3):282-90.
- Berger K, Sauvage LR, Rao AM, Wood SJ. Healing of arterial prostheses in man: its incompleteness. *Ann Surg.* 1972 Jan;175(1):118-27.
- Berglund JD, Mohseni MM, Nerem RM, Sambanis A. A biological hybrid model for collagen-based tissue engineered vascular constructs. *Biomaterials.* 2003 Mar;24(7):1241-54.
- Berglund JD, Nerem RM, Sambanis A. Incorporation of intact elastin scaffolds in tissue-engineered collagen-based vascular grafts. *Tissue Eng.* 2004 Sep-Oct;10(9-10):1526-35.
- Berglund JD, Nerem RM, Sambanis A. Viscoelastic testing methodologies for tissue engineered blood vessels. *J Biomech Eng.* 2005 Dec;127(7):1176-84.
- Billiar K.L., T.Q. Tran, N. Bachrach Effect of longitudinal stretch on the compliance of a collagen vascular graft BED-Vol. 50, 2001 Bioengineering Conference ASME 2001
- Boccafoschi F, Habermehl J, Vesentini S, Mantovani D. Biological performances of collagen-based scaffolds for vascular tissue engineering. *Biomaterials.* 2005 Dec;26(35):7410-7.
- Bolgen N, Menceloglu YZ, Acatay K, Vargel I, Piskin E. In vitro and in vivo degradation of non-woven materials made of poly(epsilon-caprolactone) nanofibers prepared by electrospinning under different conditions. *J Biomater Sci Polym Ed.* 2005;16(12):1537-55.
- Bordenave L, Fernandez P, Remy-Zolghadri M, Villars S, Daculsi R, Midy D. In vitro endothelialized ePTFE prostheses: clinical update 20 years after the first realization. *Clin Hemorheol Microcirc.* 2005;33(3):227-34.
- Boron W.F., E.L. Boulpaep Medical physiology Saunders, 2003
- Canver CC. Conduit options in coronary artery bypass surgery. *Chest.* 1995 Oct;108(4):1150-5.
- Carmines DV, McElhaney JH, Stack R. A piece-wise non-linear elastic stress expression of human and pig coronary arteries tested in vitro. *J Biomech.* 1991;24(10):899-906.
- Cesarone CF, Bolognesi C, Santi L. Improved microfluorometric DNA determination in biological material using 33258 Hoechst. *Anal Biochem.* 1979 Nov 15;100(1):188-97.
- Clerin V, Nichol JW, Petko M, Myung RJ, Gaynor JW, Gooch KJ. Tissue engineering of arteries by directed remodeling of intact arterial segments. *Tissue Eng.* 2003 Jun;9(3):461-72.
- Cummings CL, Gawlitta D, Nerem RM, Stegemann JP. Properties of engineered vascular constructs made from collagen, fibrin, and collagen-fibrin mixtures. *Biomaterials.* 2004 Aug;25(17):3699-706.
- Deitzel JM, Kleinmeyer J, Harris D, Beck Tan NC  
The effect of processing variables on the morphology of electrospun nanofibers and textiles, *Polymer*, 42, 261, 2001

- Doriot PA, Dorsaz PA, Dorsaz L, De Benedetti E, Chatelain P, Delafontaine P. In-vivo measurements of wall shear stress in human coronary arteries. *Coron Artery Dis.* 2000 Sep;11(6):495-502.
- Driessen NJ, Wilson W, Bouten CV, Baaijens FP. A computational model for collagen fibre remodelling in the arterial wall. *J Theor Biol.* 2004 Jan 7;226(1):53-64.
- Edelman ER. Vascular tissue engineering: designer arteries. *Circ Res.* 1999 Dec 3-17;85(12):1115-7.
- Engbers-Buijtenhuijs P, Buttafoco L, Poot AA, Dijkstra PJ, de Vos RA, Sterk LM, Geelkerken RH, Vermes I, Feijen J. Biological characterisation of vascular grafts cultured in a bioreactor. *Biomaterials.* 2006 Apr;27(11):2390-2397. Epub 2005 Dec 15.
- Farndale RW, Buttle DJ, Barrett AJ. Improved quantitation and discrimination of sulphated glycosaminoglycans by use of dimethylmethylene blue. *Biochim Biophys Acta.* 1986 Sep 4;883(2):173-7.
- Frazza EJ, Schmitt EE. 1971. A new absorbable suture. *J Biomed Mater Res Symp* 1: 43-58
- Gao J, Niklason L, Langer R. Surface hydrolysis of poly(glycolic acid) meshes increases the seeding density of vascular smooth muscle cells. *J Biomed Mater Res.* 1998 Dec 5;42(3):417-24.
- Goldsborough MA, Miller MH, Gibson J, Creighton-Kelly S, Custer CA, Wallop JM, Greene PS. Prevalence of leg wound complications after coronary artery bypass grafting: determination of risk factors. *Am J Crit Care.* 1999 May;8(3):149-53.
- Hamid SA, Daly C, Campbell S. Visualization of live endothelial cells ex vivo and in vitro. *Microvasc Res.* 2003 Sep;66(2):159-63.
- Han HC, Ku DN, Vito RP. Arterial wall adaptation under elevated longitudinal stretch in organ culture. *Ann Biomed Eng.* 2003 Apr;31(4):403-11.
- Harris L. D., Kim, B. S., and Mooney, D. J.: Open pore biodegradable matrices formed with gas forming. *J. Biomed. Mater. Res.*, 42, 396–402 (1998)
- He H, Matsuda T. Arterial replacement with compliant hierarchic hybrid vascular graft: biomechanical adaptation and failure. *Tissue Eng.* 2002 Apr;8(2):213-24.
- Hertzer NR. Regeneration of endothelium in knitted and velour dacron vascular grafts in dogs. *J Cardiovasc Surg (Torino).* 1981 May-Jun;22(3):223-30.
- Hoerstrup SP, Zund G, Lachat M, Schoeberlein A, Uhlschmid G, Vogt P, Turina M. Tissue engineering: a new approach in cardiovascular surgery--seeding of human fibroblasts on resorbable mesh. *Swiss Surg.* 1998;Suppl 2:23-5
- Hoerstrup SP, Zund G, Ye Q, Schoeberlein A, Schmid AC, Turina MI. Tissue engineering of a bioprosthetic heart valve: stimulation of extracellular matrix assessed by hydroxyproline assay. *ASAIO J.* 1999 Sep-Oct;45(5):397-402.
- Hoerstrup SP, Sodian R, Daebritz S, Wang J, Bacha EA, Martin DP, Moran AM, Guleserian KJ, Sperling JS, Kaushal S, Vacanti JP, Schoen FJ, Mayer JE Jr. Functional living trileaflet heart valves grown in vitro. *Circulation.* 2000 Nov 7;102(19 Suppl 3):III44-9.
- Hoerstrup SP, Zund G, Sodian R, Schnell AM, Grunenfelder J, Turina MI. Tissue engineering of small caliber vascular grafts. *Eur J Cardiothorac Surg.* 2001 Jul;20(1):164-9.
- Hoerstrup SP, Kadner A, Melnitchouk S, Trojan A, Eid K, Tracy J, Sodian R, Visjager JF, Kolb SA, Grunenfelder J, Zund G, Turina MI. Tissue engineering of functional trileaflet heart valves from human marrow stromal cells. *Circulation.* 2002 Sep 24;106(12 Suppl 1):I143-50.



- Holzapfel GA, Sommer G, Regitnig P. Anisotropic mechanical properties of tissue components in human atherosclerotic plaques. *J Biomech Eng.* 2004 Oct;126(5):657-65.
- Holzapfel GA, Sommer G, Gasser CT, Regitnig P. Determination of layer-specific mechanical properties of human coronary arteries with nonatherosclerotic intimal thickening and related constitutive modeling. *Am J Physiol Heart Circ Physiol.* 2005 Nov;289(5):H2048-58. Epub 2005 Jul 8.
- Holzapfel GA. Determination of material models for arterial walls from uniaxial extension tests and histological structure. *J Theor Biol.* 2006 Jan 21;238(2):290-302. Epub 2005 Jul 25.
- Holthofer H, Virtanen I, Kariniemi AL, Hormia M, Linder E, Miettinen A. Ulex europaeus I lectin as a marker for vascular endothelium in human tissues. *Lab Invest.* 1982 Jul;47(1):60-6.
- Huszar G, Maiocco J, Naftolin F. Monitoring of collagen and collagen fragments in chromatography of protein mixtures. *Anal Biochem.* 1980 Jul 1;105(2):424-9.
- Isenberg BC, Tranquillo RT. Long-term cyclic distention enhances the mechanical properties of collagen-based media-equivalents. *Ann Biomed Eng.* 2003 Sep;31(8):937-49.
- Isenberg BC, Williams C, Tranquillo RT. Small-diameter artificial arteries engineered in vitro. *Circ Res.* 2006 Jan 6;98(1):25-35.
- Jackson ZS, Gotlieb AI, Langille BL. Wall tissue remodeling regulates longitudinal tension in arteries. *Circ Res.* 2002 May 3;90(8):918-25.
- Jeong SI, Kim SH, Kim YH, Jung Y, Kwon JH, Kim BS, Lee YM. Manufacture of elastic biodegradable PLCL scaffolds for mechano-active vascular tissue engineering. *J Biomater Sci Polym Ed.* 2004;15(5):645-60.
- Jeremias A, Spies C, Herity NA, Pomerantsev E, Yock PG, Fitzgerald PJ, Yeung AC. Coronary artery compliance and adaptive vessel remodelling in patients with stable and unstable coronary artery disease. *Heart.* 2000 Sep;84(3):314-9.
- Jockenhoevel S, Zund G, Hoerstrup SP, Schnell A, Turina M. Cardiovascular tissue engineering: a new laminar flow chamber for in vitro improvement of mechanical tissue properties. *ASAIO J.* 2002 Jan-Feb;48(1):8-11.
- Kakisis JD, Liapis CD, Breuer C, Sumpio BE. Artificial blood vessel: the Holy Grail of peripheral vascular surgery. *J Vasc Surg.* 2005 Feb;41(2):349-54.
- Kallenbach K, Leyh RG, Lefik E, Walles T, Wilhelmi M, Cebotari S, Schmiedl A, Haverich A, Mertsching H. Guided tissue regeneration: porcine matrix does not transmit PERV. *Biomaterials.* 2004 Aug;25(17):3613-20.
- Khil MS, Bhattarai SR, Kim HY, Kim SZ, Lee KH. Novel fabricated matrix via electrospinning for tissue engineering. *J Biomed Mater Res B Appl Biomater.* 2005 Jan 15;72(1):117-24.
- Kidoaki S, Kwon IK, Matsuda T. Mesoscopic spatial designs of nano- and microfiber meshes for tissue-engineering matrix and scaffold based on newly devised multilayering and mixing electrospinning techniques. *Biomaterials*, 26, 37, 2005
- Kim BS, Mooney DJ. Engineering smooth muscle tissue with a predefined structure. *J Biomed Mater Res.* 1998 Aug;41(2):322-32.
- Kim BS, Mooney DJ. Engineering smooth muscle tissue with a predefined structure. *J Biomed Mater Res.* 1998 Aug;41(2):322-32.
- Kim BS, Mooney DJ. Scaffolds for engineering smooth muscle under cyclic mechanical strain conditions. *J Biomech Eng.* 2000 Jun;122(3):210-5.

- Kwon IK, Kidoaki S, Matsuda T. Electrospun nano- to microfiber fabrics made of biodegradable copolyesters: structural characteristics, mechanical properties and cell adhesion potential. *Biomaterials*, 26, 3929, 2005
- Lally C, Reid AJ, Prendergast PJ. Elastic behavior of porcine coronary artery tissue under uniaxial and equibiaxial tension. *Ann Biomed Eng*. 2004 Oct;32(10):1355-64.
- Leon L, Greisler HP. Vascular grafts. *Expert Rev Cardiovasc Ther*. 2003 Nov;1(4):581-94.
- L'Heureux N, Paquet S, Labbe R, Germain L, Auger FA. In vitro construction of a human blood vessel from cultured vascular cells: a morphologic study. *J Vasc Surg* 1993;17:499-509
- L'Heureux N, Paquet S, Labbe R, Germain L, Auger FA. A completely biological tissue-engineered human blood vessel. *FASEB J*. 1998 Jan;12(1):47-56.
- L'heureux N, Dusserre N, Konig G, Victor B, Keire P, Wight TN, Chronos NA, Kyles AE, Gregory CR, Hoyt G, Robbins RC, McAllister TN. Human tissue-engineered blood vessels for adult arterial revascularization. *Nat Med*. 2006 Mar;12(3):361-5. Epub 2006 Feb 19.
- Lith R. van, Small-diameter vascular tissue engineering using electrospinning-based polymer scaffolds, Master thesis, Eindhoven University of Technology, 2005, BMTE05.24
- Long JL, Tranquillo RT. Elastic fiber production in cardiovascular tissue-equivalents. *Matrix Biol*. 2003 Jun;22(4):339-50.
- Marquez-Zacarias LA, Rey AR, Heine MC, Manrique JJ. A new biologic prosthesis for vascular substitute in mongrel dogs. *Tex Heart Inst J*. 1985 Sep;12(3):269-74.
- Matsuda T. Recent progress of vascular graft engineering in Japan. *Artif Organs*. 2004 Jan;28(1):64-71.
- Matsumura G, Miyagawa-Tomita S, Shin'oka T, Ikada Y, Kurosawa H. First evidence that bone marrow cells contribute to the construction of tissue-engineered vascular autografts in vivo. *Circulation*. 2003 Oct 7;108(14):1729-34. Epub 2003 Sep 8.
- McKee JA, Banik SS, Boyer MJ, Hamad NM, Lawson JH, Niklason LE, Counter CM. Human arteries engineered in vitro. *EMBO Rep*. 2003 Jun;4(6):633-8.
- Meng X, Mavromatis K, Galis ZS. Mechanical stretching of human saphenous vein grafts induces expression and activation of matrix-degrading enzymes associated with vascular tissue injury and repair. *Exp Mol Pathol*. 1999 Aug;66(3):227-37.
- Mironov V, Kasyanov V, McAllister K, Oliver S, Sistino J, Markwald R. Perfusion bioreactor for vascular tissue engineering with capacities for longitudinal stretch. *J Craniofac Surg*. 2003 May;14(3):340-7.
- Mitchell SL, Niklason LE. Requirements for growing tissue-engineered vascular grafts. *Cardiovasc Pathol*. 2003 Mar-Apr;12(2):59-64.
- Mikos A. G., Thorsen, A. J., Czerwonka, L. A., Bao, Y., Langer, R., Winslow, D. N., and Vacanti, J. P.: Preparation and characterization of poly(L-lactic acid) foams. *Polymer*, 35, 1068–1077 (1994).
- Mo XM, Xu CY, Kotaki M, Ramakrishna S. Electrospun P(LLA-CL) nanofiber: a biomimetic extracellular matrix for smooth muscle cell and endothelial cell proliferation. *Biomaterials*, 25, 1883, 2004
- Mol A, Bouten CV, Zund G, Gunter CI, Visjager JF, Turina MI, Baaijens FP, Hoerstrup SP. The relevance of large strains in functional tissue engineering of heart valves. *Thorac Cardiovasc Surg*. 2003 Apr;51(2):78-83.

## References

- Mol A, van Lieshout MI, Dam-de Veen CG, Neuenschwander S, Hoerstrup SP, Baaijens FP, Bouten CV. Fibrin as a cell carrier in cardiovascular tissue engineering applications. *Biomaterials*. 2005 Jun;26(16):3113-21.
- Mol A. Functional tissue engineering of human heart valve leaflets. Thesis Eindhoven University of Technology, Universiteitsdrukkerij TU Eindhoven, 2005b
- Mol A *Circulation* 2006 (in press)
- Mooney D. J., Baldwin, D. F., Suh, N. P., Vacanti, J. P., and Langer, R.: Novel approach to fabricate porous sponges of poly(D,L-lactic-co-glycolic acid) without the use of organic solvents. *Biomaterials*, 17, 1417–1422 (1996).
- Nair LS, Bhattacharyya S, Laurencin CT. Development of novel tissue engineering scaffolds via electrospinning. *Expert Opin Biol Ther*. 2004 May;4(5):659-68.
- Nam Y. S., Yoon, J. J., and Park, T. G.: A novel fabrication method of macroporous biodegradable polymer scaffolds using gas foaming salt as a porogen additive. *J. Biomed. Mater. Res. B: Appl. Biomater.*, 53B, 1–7 (2000)
- Nerem R.M., J.P.Stegemann Functional Tissue Engineering Springer-Verlag 2003
- Neuenschwander S, Hoerstrup SP. Heart valve tissue engineering. *Transpl Immunol*. 2004 Apr;12(3-4):359-65.
- Niklason LE, Gao J, Abbott WM, Hirschi KK, Houser S, Marini R, Langer R. Functional arteries grown in vitro. *Science*. 1999 Apr 16;284(5413):489-93.
- Niklason LE, Abbott W, Gao J, Klagges B, Hirschi KK, Ulubayram K, Conroy N, Jones R, Vasanaawala A, Sanzgiri S, Langer R. Morphologic and mechanical characteristics of engineered bovine arteries. *J Vasc Surg*. 2001 Mar;33(3):628-38.
- Ogle BM, Mooradian DL. Manipulation of remodeling pathways to enhance the mechanical properties of a tissue engineered blood vessel. *J Biomech Eng*. 2002 Dec;124(6):724-33.
- Opitz F, Schenke-Layland K, Richter W, Martin DP, Degenkolbe I, Wahlers T, Stock UA. Tissue engineering of ovine aortic blood vessel substitutes using applied shear stress and enzymatically derived vascular smooth muscle cells. *Ann Biomed Eng*. 2004 Feb;32(2):212-22.
- Ozolanta I, Tetere G, Purinya B, Kasyanov V. Changes in the mechanical properties, biochemical contents and wall structure of the human coronary arteries with age and sex. *Med Eng Phys*. 1998 Oct;20(7):523-33.
- Pandit A, Lu X, Wang C, Kassab GS. Biaxial elastic material properties of porcine coronary media and adventitia. *Am J Physiol Heart Circ Physiol*. 2005 Jun;288(6):H2581-7. Epub 2005 Mar 25.
- Pavlov MP, Mano JF, Neves NM, Reis RL. Fibers and 3D mesh scaffolds from biodegradable starch-based blends: production and characterization. *Macromol Biosci*. 2004 Aug 9;4(8):776-84.
- Pawlowski KJ, Rittgers SE, Schmidt SP, Bowlin GL. Endothelial cell seeding of polymeric vascular grafts. *Front Biosci*. 2004 May 1;9:1412-21.
- Peykar S, Angiolillo DJ, Bass TA, Costa MA. Saphenous vein graft disease. *Minerva Cardioangiol*. 2004 Oct;52(5):379-90.
- Poh M, Boyer M, Solan A, Dahl SL, Pedrotty D, Banik SS, McKee JA, Klinger RY, Counter CM, Niklason LE. Blood vessels engineered from human cells. *Lancet*. 2005 Jun 18-24;365(9477):2122-4.

- Prabhakar V, Grinstaff MW, Alarcon J, Knors C, Solan AK, Niklason LE. Engineering porcine arteries: effects of scaffold modification. *J Biomed Mater Res A*. 2003 Oct 1;67(1):303-11
- Raja SG, Haider Z, Ahmad M, Zaman H. Saphenous vein grafts: to use or not to use? *Heart Lung Circ*. 2004 Dec;13(4):403-9.
- Rahlf G, Urban P, Bohle RM. Morphology of healing in vascular prostheses. *Thorac Cardiovasc Surg*. 1986 Feb;34(1):43-8. Rashid ST, Salacinski HJ, Fuller J, Hamilton G, Seifalian AM. Engineering of bypass conduits to improve patency. *Cell Prolif*. 2004 Oct;37(5):351-66.
- Rashid ST, Salacinski HJ, Fuller BJ, Hamilton G, Seifalian AM Engineering of bypass conduits to improve patency. *Cell Prolif*. 2004 Oct;37(5):351-66.
- Rhim C, Niklason, L.E Tissue engineered vessels: cells to telomeres. *Progress in pediatric cardiology* 21 (2006) 185-191
- Roeder R, Wolfe J, Lianakis N, Hinson T, Geddes LA, Obermiller J. Compliance, elastic modulus, and burst pressure of small-intestine submucosa (SIS), small-diameter vascular grafts. *J Biomed Mater Res*. 1999 Oct;47(1):65-70.
- Ross JJ, Tranquillo RT. ECM gene expression correlates with in vitro tissue growth and development in fibrin gel remodeled by neonatal smooth muscle cells. *Matrix Biol*. 2003 Nov;22(6):477-90.
- Sarraf CE, Harris AB, McCulloch AD, Eastwood M. Heart valve and arterial tissue engineering. *Cell Prolif*. 2003 Oct;36(5):241-54.
- Sauvage R, Berger KE, Wood SJ, Yates SG 2nd, Smith JC, Mansfield PB. Interspecies healing of porous arterial prostheses: observations, 1960 to 1974. *Arch Surg*. 1974 Nov;109(5):698-705.
- Seifalian AM, Tiwari A, Hamilton G, Salacinski HJ. Improving the clinical patency of prosthetic vascular and coronary bypass grafts: the role of seeding and tissue engineering. *Artif Organs*. 2002 Apr;26(4):307-20.
- Schenke-Layland K, Opitz F, Gross M, Doring C, Halbhuber KJ, Schirrmeister F, Wahlers T, Stock UA. Complete dynamic repopulation of decellularized heart valves by application of defined physical signals-an in vitro study. *Cardiovasc Res*. 2003 Dec 1;60(3):497-509.
- Schenke-Layland K, Riemann I, Opitz F, Konig K, Halbhuber KJ, Stock UA. Comparative study of cellular and extracellular matrix composition of native and tissue engineered heart valves. *Matrix Biol*. 2004 May;23(2):113-25.
- Schmidt D Mol A, Neuenschwander S, Breyman C, Gossi M, Zund G, Turina M, Hoerstrup SP. Living patches engineered from human umbilical cord derived fibroblasts and endothelial progenitor cells. *Eur J Cardiothorac Surg*. 2005 May;27(5):795-800.
- Schnell AM, Hoerstrup SP, Zund G, Kolb S, Sodian R, Visjager JF, Grunenfelder J, Suter A, Turina M. Optimal cell source for cardiovascular tissue engineering: venous vs. aortic human myofibroblasts. *Thorac Cardiovasc Surg*. 2001 Aug;49(4):221-5.
- Seifalian AM, Tiwari A, Hamilton G, Salacinski HJ. Improving the clinical patency of prosthetic vascular and coronary bypass grafts: the role of seeding and tissue engineering. *Artif Organs*. 2002 Apr;26(4):307-20.
- Seliktar D, Black RA, Vitro RP, Nerem RM. Dynamic mechanical conditioning of collagen-gel blood vessel constructs induces remodeling in vitro. *Ann Biomed Eng* 2000;28:351-62

- Seliktar D, Nerem RM, Galis ZS. The role of matrix metalloproteinase-2 in the remodeling of cell-seeded vascular constructs subjected to cyclic strain. *Ann Biomed Eng.* 2001 Nov;29(11):923-34.
- Seliktar D, Nerem RM, Galis ZS. Mechanical strain-stimulated remodeling of tissue-engineered blood vessel constructs. *Tissue Eng.* 2003 Aug;9(4):657-66.
- Shieh SJ, Vacanti JP. State-of-the-art tissue engineering: from tissue engineering to organ building. *Surgery.* 2005 Jan;137(1):1-7.
- Shinoka T, Ma PX, Shum-Tim D, Breuer CK, Cusick RA, Zund G, Langer R, Vacanti JP, Mayer JE Jr. Tissue-engineered heart valves. Autologous valve leaflet replacement study in a lamb model. *Circulation.* 1996 Nov 1;94(9 Suppl):II164-8.
- Shin'oka T, Matsumura G, Hibino N, Naito Y, Watanabe M, Konuma T, Sakamoto T, Nagatsu M, Kurosawa H. Midterm clinical result of tissue-engineered vascular autografts seeded with autologous bone marrow cells. *J Thorac Cardiovasc Surg.* 2005 Jun;129(6):1330-8.
- Shum-Tim D, Stock U, Hrkach J, Shinoka T, Lien J, Moses MA, Stamp A, Taylor G, Moran AM, Landis W, Langer R, Vacanti JP, Mayer JE Jr. Tissue engineering of autologous aorta using a new biodegradable polymer. *Ann Thorac Surg.* 1999 Dec;68(6):2298-304; discussion 2305.
- Simionescu DT, Lu Q, Song Y, Lee JS, Rosenbalm TN, Kelley C, Vyavahare NR. Biocompatibility and remodeling potential of pure arterial elastin and collagen scaffolds. *Biomaterials.* 2006 Feb;27(5):702-13. Epub 2005 Jul 26.
- Sodian R, Hoerstrup SP, Sperling JS, Daebritz SH, Martin DP, Schoen FJ, Vacanti JP, Mayer JE Jr. Tissue engineering of heart valves: in vitro experiences. *Ann Thorac Surg.* 2000 Jul;70(1):140-4.
- Sodian R, S. P. Hoerstrup, J. S. Sperling, S. Daebritz, D. P. Martin, A. M. Moran, B. S. Kim, F. J. Schoen, J. P. Vacanti, and J. E. Mayer. Early in vivo experience with tissue-engineered trileaflet heart valves. *Circulation*, 102:III-22-III-29, 2000a. suppl III.
- Solan A, Mitchell S, Moses M, Niklason L. Effect of pulse rate on collagen deposition in the tissue-engineered blood vessel. *Tissue Eng.* 2003 Aug;9(4):579-86.
- Stegemann JP, Nerem RM. Phenotype modulation in vascular tissue engineering using biochemical and mechanical stimulation. *Ann Biomed Eng.* 2003 Apr;31(4):391-402.
- Stitzel J, Liu J, Lee SJ, Komura M, Berry J, Soker S, Lim G, Van Dyke M, Czerw R, Yoo JJ, Atala A. Fabrication of a biological vascular substitute. *Biomaterials.* 2006 Oct;27(7):1088-94. Epub 2005 Aug 29.
- Stoeker W, Gok M, Sipkema P, Niessen HW, Baidoshvili A, Westerhof N, Jansen EK, Wildevuur CR, Eijssman L. Pressure-diameter relationship in the human greater saphenous vein. *Ann Thorac Surg.* 2003 Nov;76(5):1533-8.
- Swartz DD, Russell JA, Andreadis ST. Engineering of fibrin-based functional and implantable small-diameter blood vessels. *Am J Physiol Heart Circ Physiol.* 2005 Mar;288(3):H1451-60. Epub 2004 Oct 14.
- Tajaddini A, Kilpatrick DL, Vince DG. A novel experimental method to estimate stress-strain behavior of intact coronary arteries using intravascular ultrasound (IVUS). *J Biomech Eng.* 2003 Feb;125(1):120-3.
- Teebken OE, Haverich A. Tissue engineering of small diameter vascular grafts. *Eur J Vasc Endovasc Surg.* 2002 Jun;23(6):475-85.

- Teebken OE, Puschmann C, Aper T, Haverich A, Mertsching H. Tissue-engineered bioprosthesis venous valve: a long-term study in sheep. *Eur J Vasc Endovasc Surg*. 2003 Apr;25(4):305-12.
- Vara DS, Salacinski HJ, Kannan RY, Bordenave L, Hamilton G, Seifalian AM. Cardiovascular tissue engineering: state of the art. *Pathol Biol (Paris)*. 2005 Dec;53(10):599-612. Epub 2005 Jan 25.
- Veress AI, Weiss JA, Gullberg GT, Vince DG, Rabbitt RD. Strain measurement in coronary arteries using intravascular ultrasound and deformable images. *J Biomech Eng*. 2002 Dec;124(6):734-41.
- Watanabe M, Shin'oka T, Tohyama S, Hibino N, Konuma T, Matsumura G, Kosaka Y, Ishida T, Imai Y, Yamakawa M, Ikada Y, Morita S. Tissue-engineered vascular autograft: inferior vena cava replacement in a dog model. *Tissue Eng*. 2001 Aug;7(4):429-39.
- Weaver ME, Pantely GA, Bristow JD, Ladley HD. A quantitative study of the anatomy and distribution of coronary arteries in swine in comparison with other animals and man. *Cardiovasc Res*. 1986 Dec;20(12):907-17.
- Whang K., Thomas, C. H., Healy, K. E., and Nuber, G.: A novel method to fabricate bioabsorbable scaffold. *Polymer*, 36, 837-842 (1995).
- Weinberg C, Bell E. A blood vessel model constructed from collagen and cultured vascular cells. *Science* 1986;231:397-400
- Williams C, Wick TM. Perfusion bioreactor for small diameter tissue-engineered arteries. *Tissue Eng*. 2004 May-Jun;10(5-6):930-41.
- Williamson MR, Coombes AG. Gravity spinning of polycaprolactone fibres for applications in tissue engineering. *Biomaterials*. 2004 Feb;25(3):459-65.
- Wilson GJ, Courtman DW, Klement P, Lee JM, Yeger H. Acellular matrix: a biomaterials approach for coronary artery bypass and heart valve replacement. *Ann Thorac Surg* 1995;60(2 suppl):S353-358
- Xu C, Inai R, Kotaki M, Ramakrishna S. Electrospun nanofiber fabrication as synthetic extracellular matrix and its potential for vascular tissue engineering. *Tissue Eng.*, 10, 1160, 2004
- Xu J, Ge H, Zhou X, Yang D, Guo T, He J, Li Q, Hao Z. Tissue-engineered vessel strengthens quickly under physiological deformation: application of a new perfusion bioreactor with machine vision. *J Vasc Res* 2005 Nov-Dec;42(6):503-8.
- Xue L, Greisler HP. Biomaterials in the development and future of vascular grafts. *J Vasc Surg*. 2003 Feb;37(2):472-80.
- Yoshimoto H., Shin, Y.M., Terai, H., and Vacanti, J.P. A biodegradable nanofiber scaffold by electrospinning and its potential for bone tissue engineering. *Biomaterials* 24, 2077, 2003
- Yu A, Dardik H, Wolodiger F, Raccuia J, Kapadia I, Sussman B, Kahn M, Pecoraro JP, Ibrahim IM. Everted cervical vein for carotid patch angioplasty. *J Vasc Surg*. 1990 Nov;12(5):523-6.
- Zhang Z, Wang Z, Liu S, Kodama M. Pore size, tissue ingrowth, and endothelialization of small-diameter microporous polyurethane vascular prostheses. *Biomaterials*. 2004 Jan;25(1):177-87.
- Zhang Y, Ouyang H, Lim CT, Ramakrishna S, Huang ZM. Electrospinning of gelatin fibers and gelatin/PCL composite fibrous scaffolds. *J Biomed Mater Res B Appl Biomater*. 15, 156, 2005

*References*

- Ziegler T, Nerem RM. Tissue engineering a blood vessel, regulation of vascular biology by mechanical stresses. *J Cell Biochem* 1994;56:204-9
- Zilla P., H. P. Greisler Tissue Engineering of vascular prosthetic grafts. Austin: RG Landes, 1999

# Samenvatting

Coronaire arteriën ontspringen vanuit de aortawortel, lopen over en in de wand van het hart, en voorzien de hartspier van bloed. Door de ontwikkeling van een atherosclerotische plaque in de wand van deze bloedvaten kunnen zij stijver en nauwer worden. Het lumen van de coronaire arteriën wordt kleiner naarmate de plaque groter wordt waardoor er steeds minder bloed doorheen kan stromen. Vernauwde of verstopte coronaire arteriën leiden tot pijn op de borst en, in het ergste geval, tot een hartinfarct. Behandelmethoden bestaan uit medicatie, minimaal invasieve interventies zoals angioplastiek en stent-implantaties, en bypass operaties. Tegenwoordig wordt bij een bypass operatie meestal gebruik gemaakt van een borstslagader (arteria mammaria) en/of een ader uit het onderbeen (vena saphena). Het is aangetoond dat deze bypass grafts, zeker wanneer ze bestaan uit aders, niet optimaal functioneren. Daarnaast heeft een grote groep patiënten door bijvoorbeeld ziekte van de vaten, het gebruik in eerdere bypass operaties of de noodzaak voor meerdere bypasses, geen geschikte arteriën of aders. Verschillende alternatieven zijn onderzocht voor gebruik in een bypass operatie. Synthetische grafts, zoals ePTFE en Dacron, functioneren goed bij diameters groter dan 6mm, maar zijn ongeschikt voor kleine diameter (< 4mm) toepassingen, zoals in bypass operaties. Daarom wordt gezocht naar andere alternatieven zoals getissue-engineerde (TE) vaten met een kleine diameter. In vasculaire tissue engineering wordt gebruik gemaakt van cellen, (bio)materialen en noodzakelijke biochemische en mechanische stimuli voor het in-vitro kweken van levende vaten. Patiënt-eigen cellen worden gebruikt in combinatie met een drager-materiaal of scaffold. De vorming van weefsel wordt gestimuleerd door het opleggen van mechanische en/of chemische conditioneringsprotocollen tijdens de in-vitro kweekperiode. In het algemeen moeten de grafts ten minste voldoen aan de volgende criteria: ze moeten een bepaalde sterkte bezitten om mechanische belasting te weerstaan, ze moeten voldoende elastisch zijn opdat zij na mechanische vervorming terugkeren naar hun oorspronkelijke positie ter voorkoming van aneurysma's. Daarnaast moeten de grafts aan de binnenkant voorzien zijn van een confluent laag endotheel cellen ter voorkoming van thrombose en om te zorgen voor optimale functie van het vat.

Het onderzoek beschreven in dit proefschrift richt zich in eerste instantie op de toename van sterkte van TE vaten door blootstelling aan een rekbelasting tijdens de in-vitro kweekperiode. Het doel was het kweken van voldoende sterke vaten op basis van bio-afbreekbare polymeren en menselijke cellen, geïsoleerd uit de vena saphena. Verschillende scaffold concepten werden geëvalueerd met betrekking tot weefselgroei en mechanische eigenschappen. Het uitgangspunt was een polyglycolic acid (PGA) scaffold met een poly-4-hydroxybutyrate (P4HB) coating. Dit materiaal kan eventueel uitgebreid worden met een binnen- of buitenlaag van elektrogenesponnen poly-ε-caprolactone (PCL) om de mechanische eigenschappen zoals sterkte en elasticiteit te verbeteren. Omdat de PGA/P4HB scaffold al met succes werd toegepast in gekweekte hartkleppen, werden de TE vaten in eerste instantie vervaardigd van dit materiaal alleen. Deze constructen werden ingezaaid met een combinatie van humane myofibroblasten en een fibrine gel. Deze gel maakt een efficiënte zaaimethode mogelijk en bevordert de



weefselgroei. Na een initiële kweekperiode werden de constructen zowel statisch als dynamisch gerekt in de lengte (axiaal) en/of omtreksrichting. Hiervoor werden 2 aparte bioreactoren ontwikkeld. In de eerste opstelling konden de constructen zowel statisch als dynamisch worden belast in axiale richting, terwijl in de tweede opstelling statische axiale rek gecombineerd kon worden met dynamische rek in de omtreksrichting. Statische axiale rek werd geïnduceerd door de weefselcompactie in deze richting tegen te gaan. De weefselvorming en de mechanische eigenschappen van de statisch gerekte buisjes in axiale richting waren beter dan die in statische controle-constructen. De verbetering van de mechanische eigenschappen was met name aanwezig in axiale richting. De toegevoegde waarde van dynamische axiale rek was beperkt of zelfs negatief. De mechanische eigenschappen in omtreksrichting, welke het meest belangrijk zijn voor het mechanische gedrag van een bloedvat, verbeterden sterk wanneer de constructen ook werden blootgesteld aan een dynamische rek in omtreksrichting. Na een kweekperiode van 4 weken bleek de combinatie van statische axiale rek en dynamische rek in omtreksrichting te resulteren in de sterkste TE vaten. Deze vaten konden een druk weerstaan van 900mmHg, hetgeen sterk is ten opzichte van vergelijkbare TE bloedvaten die in een zelfde tijdspanne gekweekt zijn, zoals vermeld in literatuur.

In dit proefschrift werden zowel biochemische als mechanische eigenschappen van de TE vaten vergeleken met die van humane en dierlijke bloedvaten, namelijk met de humane vena saphena en arteria mammaria en met coronaire arteriën van een varken. De hoeveelheid DNA en extracellulaire matrix (collageen en glycoaminoglycans (GAGs)) was, tot op zekere hoogte, vergelijkbaar. Het weefsel van de humane en varkens bloedvaten bleek echter beter ontwikkeld en georganiseerd te zijn. De mechanische eigenschappen van de TE vaten, gemeten met behulp van uniaxiale trekproeven, waren in de fysiologisch relevante range opmerkelijk gelijk aan die van de humane arteriën. De maximale treksterkte van de humane vaten was echter veel groter. Het is hierbij van belang om op te merken dat de mechanische eigenschappen van een TE bloedvat ten tijde van implantatie niet gelijk hoeven te zijn aan die van het vat dat vervangen moet worden. Het TE vat bestaat namelijk uit levend weefsel en is daardoor in staat om te groeien, zich te herstellen en zich aan te passen aan lokale omstandigheden.

TE bloedvaten moeten een bepaalde mechanische sterkte hebben, hetgeen het focuspunt van deze studie was, maar ze moeten ook elastisch and compliant zijn. Daarnaast moeten ze een functionele endotheellaag bezitten. Meer uitgebreide mechanische testen zullen moeten aantonen of verdere verbetering van de elasticiteit en compliantie van de TE vaten noodzakelijk is. Experimenten hebben aangetoond dat het zaaien van humane endotheel cellen op de constructen mogelijk is maar meer onderzoek is nodig voor het verkrijgen van een confluenta, functionele endotheellaag. Wanneer bovengenoemde aspecten betreffende de mechanische eigenschappen en de endotheellaag voldoende opgelost zijn, zal in dierproeven de potentie van de TE bloedvaten verder aangetoond moeten worden.

Samenvattend kan gesteld worden dat in de gepresenteerde TE bloedvaten voldoende weefsel ontwikkeling heeft plaatsgevonden en dat ze sterk genoeg zijn voor verder onderzoek in implantatiestudies in proefdieren. Voordat deze studies mogelijk zijn, moeten er echter nog enkele aspecten betreffende elasticiteit, compliantie en functioneel endotheel onderzocht worden.

# Dankwoord

Promoveren is solistisch werk. Dat maakt het extra mooi wanneer het af is. Toch had ik het niet gekund zonder de hulp van anderen. Deze mensen wil ik hier dan ook bedanken. Als eerste geldt dat voor mijn directe begeleiders Luc Snoeckx en Marcel Rutten. Al vormden we misschien een enigszins onlogische combinatie binnen het onderzoeksgebied, uiteindelijk hebben we toch met z'n drieën de eindstreep gehaald. Luc, u heeft mij al zo'n 8 jaar begeleid; beginnend bij mijn stageopdracht, vervolgens bij mijn afstudeeropdracht en nu tijdens mijn promotieonderzoek. Heel erg veel dank hiervoor. Bij het schrijven van mijn proefschrift heeft u aanhoudend bijgedragen tot duidelijkheid en leesbaarheid van het opgeschreven onderzoek, een niet te onderschatten aspect. Marcel, bedankt voor al je begeleiding en je hulp bij mijn opstellingen. Hoewel jouw geruststellende woorden 'het komt goed' bij mij niet altijd werkten heb je natuurlijk toch gelijk gekregen. Daarnaast wil ik Frank Baaijens bedanken, voor het mogelijk maken van het onderzoek maar daarnaast ook voor de begeleiding. Hoewel je in het begin van het traject op een behoorlijke afstand was, heb je mij uiteindelijk in de kritieke fasen de juiste kant opgestuurd. Zonder jouw bijsturing had ik zeker niet de resultaten behaald waar ik nu zo tevreden op terugkijk. Ik ben dan ook heel blij dat ik nog een tijdje mag doorwerken om na vijf jaar moeizaam onderzoek nu te mogen 'oogsten'. Ik wil Rolf bedanken voor zijn enorme hulp in de laatste schrijffase. Je hebt al mijn hoofdstukken herhaaldelijk gelezen en was altijd kritisch. Nadat je had bevestigd dat het al best een goed stuk was, een noodzakelijke opmerking voor mijn gemoedsrust, volgden altijd vruchtbare discussies waar ik veel aan heb gehad. Dank gaat ook uit naar Rob van de Berg, uiteraard voor het bouwen van mijn opstellingen maar vooral voor je hulp tijdens de laatste serie experimenten. Onder grote tijdsdruk moesten er dingen worden veranderd of aangepast en je hielp me altijd zo snel mogelijk. Rob Petterson wil ik bedanken voor al zijn hulp, in de breedste zin van het woord. Jouw geduld en vastberadenheid waren soms hard nodig voor mijn praktische problemen. Het probleem van de luchtbellen in mijn opstelling, dat mij weerhield van goede experimenten, loste jij op door structureel alles te onderzoeken. Naast deze praktische zaken kon ik alle steun van je verwachten als het, door welke reden dan ook, gewoon even niet lukte. Marcel Wijlaars wil ik bedanken voor zijn praktische hulp in het lab, naar mijn gevoel wordt een probleem bij jou aangedragen gegarandeerd opgelost. Het ingenieuze 'gatenkaasbuisje' in het druksysteem werkt nog steeds uitstekend. Patrick en Leo wil ik bedanken voor alle computerhulp, zelfs met domme vragen, die weldegelijk bestaan, kon ik altijd bij jullie binnenlopen. Verder wil ik bedanken de stagiaires en afstudeerders die mij hebben geholpen; Debbie, Jeroen en Robert. Robert, op verschillende gebieden heb je mij op weg geholpen. Het meeste werk zat echter in het electrospinnen van de

scaffolds, zeker niet een heel leuk werkje. Hoewel van onze gezamenlijke inspanningen op dit gebied relatief weinig is terug te vinden in dit proefschrift, wil ik je toch heel hartelijk danken voor je onmisbare bijdragen. Reinout wil ik bedanken voor de uitgevoerde kleuringen. Ook al kwam ik hiermee op het allerlaatste moment, jij maakte snel tijd voor mij. Verder wil ik Joost ter Woorst graag bedanken voor het ‘leveren’ van de humane vaten. Ik vond het heel bijzonder om een kijkje te mogen nemen in de praktijk. Daarnaast wil ik al mijn collega’s bedanken die zowel in het lab als aan de koffietafel voor de nodige gezelligheid en afleiding zorgden. En dan uiteraard mijn kamergenoten Raoul, Bram, Ralf en Marion. Jullie gezelschap en steun heb ik enorm gewaardeerd. Bram en Raoul, vanaf het allereerste begin hebben wij een kamer gedeeld, helaas zitten jullie beiden nu in Engeland zodat kameravondjes niet meer mogelijk zijn. Ik hoop jullie snel weer eens te zien.

Mijn familie wil ik bedanken voor alle belangstelling en steun. Anke, jou hier bedanken in een paar zinnen doet wel erg tekort aan al je hulp en support. Mijn proefschrift heb ik opgedragen aan ons samen, hopelijk blijft ‘de eenvoud van de tweevoud’ altijd voor ons gelden, ondanks het feit dat onze wegen zich meer zullen scheiden. Lieve Boudewijn, als laatste wil ik jou bedanken. Voor al je steun en liefde. Ik kijk uit naar onze toekomst samen.

Maria Stekelenburg  
Eindhoven, mei 2006

# Curriculum Vitae

Maria Stekelenburg werd geboren op 26 februari 1976 in Raamsdonksveer. In 1994 behaalde zij haar VWO diploma aan het Riethil College te Raamsdonksveer. Aansluitend studeerde zij Technische Natuurkunde aan de Technische Universiteit Eindhoven (TUE). Als onderdeel van deze studie heeft zij stage gelopen bij het Bakken Research Center van Medtronic in Maastricht, met als onderwerp Atomic Force Microscopy (AFM). Ook tijdens haar afstudeerwerk heeft zij hier gewerkt met de AFM, nu toegepast om het mechanisch gedrag van cellen te bestuderen. Eind 2000 is zij begonnen met haar promotie onderzoek aan de faculteit Biomedische Technologie (BMT) van de TUE, resulterend in dit proefschrift. Het onderzoek maakte deel uit van het Tissue Engineering onderzoek dat bij de faculteit BMT gedaan wordt. Aansluitend aan het promotie-onderzoek zal zij haar onderzoek naar tissue-engineering van kleindiameter bloedvaten voortzetten aan de TUE als post-doc.